Ph.D.

Study of the role of Phosphorylated Pathway of Serine Biosynthesis in *Arabidopsis* development and its connections with nitrogen and carbon metabolism

Plant Biology Department

Dissertation submitted in partial fulfillment of the requirements for obtaining the degree of Doctor (PhD) in Biotechnology

By

María Flores Tornero

D030-01 Programa oficial de Postgrado en Biotecnología

Supervisor

Dr. Roc Ros Palau

València, 2016

VNIVERSITAT DE VALÈNCIA **Departament de Biologia Vegetal**

D. Roc Ros Palau, Doctor en Biología y Catedrático del Departamento de Biología Vegetal de la Universidad de Valencia

CERTIFICA:

Que la presente memoria titulada:

"***Study of the role of Phosphorylated Pathway of Serine Biosynthesis in Arabidopsis development and its connections with nitrogen and carbon metabolism***"

ha sido realizada por María Flores Tornero bajo mi dirección y constituye su Memoria de Tesis para optar al grado de Doctor en Biotecnología.

Fdo. Roc Ros Palau

Valencia, 22 de Febrero de 2016

FUNDING

This thesis was funded by:

- "VALi+d program" scholarship of the Generalitat Valenciana.
- "Atracció de talent" scholarship of the Universitat de València.
- Proyecto de investigación BFU2009-07020/BFI del Ministerio de Ciencia e Innovación (2010-2012).
- Proyecto de investigación BFU2012-31519 del Ministerio de Economía y Competitividad (2013-2015).
- PROMETEO/2009/075, Generalitat Valenciana (2009-2013).
- PROMETEO II/2014/052, Generalitat Valenciana (2014-2017).

A mis padres, los pilares de mi vida

ACKNOWLEDGEMENTS

“Ser agradecido es de buen nacido” me decían mis padres de pequeña. Y es que ese acto, dar las gracias, puede resultar una acción tan normal y cotidiana como gratificante y trascendente. En estas líneas intento ceñirme más al segundo caso, a la fuerza, al valor y al sentido profundo que tiene el agradecer de corazón todo lo que me dieron, a aquellos que me lo dieron.

La familia dicen que es el primer pilar en el que te apoyas, y por ello, para ellos son mis primeras palabras de agradecimiento. Mis padres, Jesús y Celina, y mi hermano Daniel, personas que por separado me han enseñado tanto, no cabe en unas líneas todo mi agradecimiento por tanto cariño y tanto apoyo desde siempre y para siempre.

Conforme vas andando, van apareciendo personas que de un modo u otro influirán en tu vida haciendo que tomes unos u otros caminos, y por ello llegados a este punto de culminación académica, no puedo evitar echar la vista atrás y acordarme de D.Gregorio Miguel, mi profesor de biología del instituto. Él, parafraseando a Newton, deseó que en esta vida académica me encontrara con gigantes, y lo hizo sin saber que él era el primer gigante a hombros del cual me subía. Gracias a él me encaminé hacia la biología y hoy estoy a punto de doctorarme. Simplemente gracias, Gregorio.

Continuando con la familia, esta vez la académica, no puedo dejar de agradecerles aquello que me han dado. En primer lugar a la doctora Isabel Arrillaga y al doctor Juan Segura, por contagiarme su amor por la fisiología vegetal, mostrándome con su buen hacer desde un primer momento lo interesante y atrayente que puede llegar a ser esta ciencia. Personalidad, buenos consejos y grandes dosis de paciencia, así como empatía, afecto y apoyo es lo que me han transmitido durante estos años. Si importantes son los primeros pasos en un campo, también lo es la continuidad y el desarrollo en él y eso se lo debo al grupo de investigación del doctor Roc Ros, mi director de tesis. A él quisiera agradecerle no solo su esfuerzo, paciencia y diligencia en la supervisión de este trabajo de tantos años, sino que gracias a él he aprendido a mirar a los problemas de frente, haciéndome mucho más fuerte de lo que imaginaba, lo cual consideraré para mí su principal legado. A Jesús le agradezco todo el tiempo que hemos pasado juntos enseñándome a trabajar en la bancada y compartiendo conmigo los secretos de los protocolos. A Sara, mi compañera de equipo, le agradezco que me haya enseñado a reírme dela vida, de lo bueno, de lo malo y hasta de mí misma. A Armand, mi otro “hermano”, le

agradezco todos los momentos en los que me ha enseñado a tirar para adelante cuando flaquean las fuerzas, tanto en la bancada como en el día a día. A Isabel Mendoza, por tantos y tantos momentos de charlas, confidencias, lágrimas y cervezas juntas desde que entré en el laboratorio. Y hablando de charlas, a mi querida Noelia le agradezco su amistad y complicidad durante todo el desarrollo tanto del máster como de la tesis, sintiendo en determinados momentos que sin ella no podría haber continuado. Y cómo no, a toda la banda del laboratorio, a mi Leo, mi Mariam, mi María, y todo el grupo C y D, gracias chic@s por tantas horas de estupenda convivencia y buen rollo dentro y fuera del laboratorio. También forman parte de esta "familia" Ester Pérez Lorences, a quien agradezco toda su ayuda, consejos, cafés y valoraciones sobre cualquier tema que le pongas sobre la mesa; a Charly, Carmen Calvo y Paco Marco, por estar ahí siempre que les he necesitado. Y por su puesto, sería un crimen no mencionar a mis chicas de secretaría, Mª José, Consuelo y Mª Carmen así como Estrella y Carolina, por todo su apoyo, cariño y ayuda que desde el principio me brindaron.

Este trabajo nunca podría haberse realizado de no ser por la labor técnica y humana de distintas secciones del SCSIE. En primer lugar, gracias a Cristina, Silvia y Carlos por su buena gestión del invernadero y por su apoyo tanto técnico como humano durante todos estos años. También a la sección de secuenciación, donde Vicente, Pedro, Mª Teresa y Úrsula, encabezados por Amparo me han ayudado un montón en todo lo relacionado con los ácidos nucleicos. Y cómo no, los de microscopía y cultivos celulares, por tantas y tantas horas enfrente del microscopio en busca de las mejores imágenes.

Y finalmente, y no por ello menos valioso para mí, están los que nunca se cansan de llamar a tu puerta y sacarte de entre los libros y las pipetas, los que celebran contigo tus triunfos y ahogan contigo tus penas, los que por muy fuerte que sople el viento siempre encuentras un lugar a su abrigo, y ellos son sin duda mis amigos. Martuka, Víctor, Jorge, María, Ferran, Cris, Chuma, Liam, Solete, Tomás, Inma, Lesía entre muchos otros, no sabría cómo agradeceros vuestro papel en el desarrollo de esta tesis, y mucho menos, vuestro lugar esencial en mi vida.

Por todo ello, ya sea de un modo u otro, a toda esta gente y a mucha otra que sin querer me habré dejado, agradecerles todo aquello que me dieron, que me dan y me seguirán dando, y que siempre llevaré conmigo allá donde vaya.

INDEX

LIST OF ABBREVIATIONS

1-3BisPGAP	1,3-Bisphosphoglycerate
2-PGA	2-phosphoglycerate
3-PGA	3-phosphoglycerate
35S	Promoter of the Cauliflower Mosaic Virus
35S:PSP1	*PSP1* cDNA is fused to the *GFP* gene under the control of the *35S* promoter
35S:TPT-GFP	*TPT* cDNA is fused to the *GFP* gene under the control of the *35S* promoter
35S:TPT-His	*TPT* cDNA is fused to 6 His under the control of the *35S* promoter
ABRC	Arabidopsis Biological Resource Center
Alcohol DH	Alcohol dehydrogenase
amiRNA	Artificial microRNA
APS	Adenosine 5'-phosphosulfate
APS	Ammonium persulfate
ATP	Adenosine 5'-triphosphate
ATPS	Sulfate adenosyltransferase
BSA	Bovine Serum Albumin
CBB	Calvin-Benson-Bassham cycle
cDNA	DNA copy
CS	Citrate synthase
Cys	Cysteine
DAP	Days After Pollination
DDM	N-Dodecyl β-D-maltoside
DH5α	*Escherichia coli* strain
DNA	Deoxyribonucleic acid
DNAse	Deoxyribonuclease
DR5:GFP	DR5 promoter (Auxin reporter) driving GFP expression
DTT	1,4-Dithiothreitol
EDTA	Ethylenediaminotetraacetic acid
EGTA	Ethylene glycol-bis(2-aminoethylether)-*N,N,N′,N′*-tetraacetic acid
ENO	Enolase
ER	Endoplasmic reticulum
F	Fumarase
FAME	Fatty acid methyl esters
FAS	Fatty acid synthesis

GAP	Glyceraldehyde 3-phosphate
GABA	γ-Aminobutyric acid
GAPCp1/2	Glyceraldehyde-3-phosphate dehydrogenase plastidial 1 (At1g79530)
GAPCp1:TPT-His	*TPT* cDNA is fused to 6 His under the control of the *35S* promoter
GAPDH	Glyceraldehyde-3-phosphate dehydrogenase
GC/MS	Gas chromatograpy-mass spectrometry
GFP	Green fluorescent protein
Glu	Glutamate
Gluc6P	Glucose 6-phosphate
Gly	Glycine
GOGAT	Glutamate synthetase
GPT	Glucose 6-phosphate/phosphate translocator
GS	Glutamine synthetase
GV3101	*Agrobacterium tumefaciens* strain
His	Histidine
HPLC	High-performance liquid chromatography
HS	Promoter of the heat-shock protein 18.2
HS:PSP1	PSP cDNA is fused to the GFP gene under a heat-shock promoter
LB	Lysogeny Broth medium for bacterial growth
MES	Acid 2-N-Morpholine ethanol sulphonic
Met	Methionine
mRNA	Ribonucleic acid messenger
MS	Murashige and Skoog medium of *Arabidopsis* growth
MSTFA	N-Methyl-N-(trimethylsilyl)trifluoroacetamide
MTT	Methylthiazolyldiphenyl-tetrazolium bromide
NADH	Nicotinamide adenine dinucleotide
NADPH	Nicotinamide adenine dinucleotide phosphate
OAS	O-acetylserine
OASTL	O-acetylserine (thiol) lyase
ORF	Open reading frames
PAPS	Adenosine 3'-phosphate 5'-phosphosulfate
PBS	Phosphate Buffer Saline
PCA	Principal Component analysis
PCD	Programmed cell death
PCR	Polymerase chain reaction
PEP	Phosphoenolpyruvate

PES	Phenazine ethosulfate
PGDH	3-phosphoglycerate dehydrogenase
PGK	Phosphoglycerate kinase
PGM	Phosphoglycerate mutase
Pi	inorganic phosphate
PI	Propidium iodide
PM	Primary metabolism
PMSF	Phenylmethylsulfonyl fluoride
PPSB	Phosphorylated pathway of serine biosynthesis
PPT	Phosphoenolpyruvate/phosphate translocator
ProPSP	Promoter of the gene At1g18640 that encondes PSP1.
PSAT	3-phosphoserine aminotransferase
PSP	3-phosphoserine phosphatase
PVPP	Polyvinyl polypyrrolidone
qRT-PCR	Quantitative Real Time polimerase Chain Reaction
RER	Rough endoplasmic reticulum
RNA	Ribonucleic acid
RNAseq	Ribonucleic acid sequencing technology
RuBisCO	Ribulose-1,5-*bis*phosphate carboxylase/oxygenase
SAT	Serine acetyltransferase
SDS	Sodium dodecylsulphate
Ser	L-serine
SHMT	Ser hydroxymethyltransferase
SM	Secondary metabolism
SOC	Super Optimal broth with Catabolite repression
Suc	Sucrose
TBE	Tris-borate-EDTA buffer
TCAC	Tricarboxylic acid cycle
T-DNA	Transfer DNA
TEMED	Tetramethylethylenediamine
TF	Transcription factors
Tm	Melting temperature
TOP10	*Escherichia coli* strain
TP	Triose phosphate
TPT	Triose phosphate/phosphate translocator
Tris	Tris(hydroxymethyl)aminomethane

WT	Wild-type
XTP	Xylulose 5-phosphate/phosphate translocator

RESUMEN

Estudio del papel de la ruta fosforilativa de biosíntesis de serina en el desarrollo de Arabidopsis y su conexión con el metabolismo del nitrógeno y del carbono

Departamento de Biología Vegetal

Por

María Flores Tornero

Supervisor

Dr. Roc Ros Palau

València, 2016

INTRODUCCION

En plantas se han descrito tres rutas diferentes para la síntesis de serina: la ruta del glicolato, asociada a la fotorrespiración, y dos rutas independientes de ella, la ruta del glicerato y la ruta fosforilativa de biosíntesis de serina (RFBS). Como la ruta del glicolato es la más importante en términos cuantitativos, el papel de la RFBS ha sido poco estudiado hasta hace unos años. Esta tesis doctoral aporta nuevas perspectivas sobre la función de la RFBS tanto en el desarrollo como en el metabolismo de *Arabidopsis*.

La RFBS se abastece de 3-fosfoglicerato (3-PGA) como sustrato, el cual podría ser suministrado por la glicolisis plastidial o citosólica. Se asume que la actividad de estas dos rutas glicolíticas está integrada por medio de un sistema de transportadores, que intercambian los intermediarios glicolíticos a través de la membrana plastidial. Sin embargo, se desconocía si el acervo de 3-PGA del plasto y el citosol podían compensarse mutuamente en células no fotosintéticas. Para resolver esta cuestión, en esta tesis se han utilizado mutantes de las isoformas glicolíticas plastidiales de la gliceraldehído-3-fosfato deshidrogenasa (GAPCp) y se han complementado con el cDNA que codifica el transportador de triosas fosfato (TPT) bajo el control de diferentes promotores.

OBJETIVOS

Esta tesis es parte de un proyecto cuyo principal objetivo es dilucidar el papel y la contribución de la glicolisis plastidial y la RFBS en el metabolismo y desarrollo vegetal. Los objetivos específicos de esta tesis son:

1. Analizar en profundidad el papel de la enzima PSP en el desarrollo embrionario y gametgofítico masculino.
2. Dilucidar las dianas metabólicas y transcriptómicas de la actividad PSP.
3. Corroborar la hipótesis de que la falta de GAPCp en células heterotróficas puede afectar al suministro de 3-PGA al plasto.
4. Demostrar que los niveles de 3-PGA no están en equilibrio entre citosol y plastos de células heterotróficas.

RESULTADOS Y DISCUSION

Los resultados de esta tesis se dividen en dos capítulos que abordan dos aspectos distintos de un mismo tema: por un lado, el origen del suministro de 3-PGA a la RFBS mediante la sobreexpresión de un transportador de triosas fosfato (TPT),(capítulo 1); y por otro, se profundiza en el papel de la RFBS en el metabolismo y desarrollo de Arabidopsis (capítulo 2).

CAPÍTULO 1: La sobreexpresión del transportador de triosas fosfato (TPT) complementa el metabolismo y el desarrollo anormal de los mutantes de la GAPCp.

- **La expresión del TPT es mínima o inexistente a nivel de la raíz.**

Primeramente se realizó un análisis *in silico* de la expresión del gen que codifica para el TPT, dando como resultado una elevada expresión en parte aérea pero total ausencia en raíces. Se confirmó este dato mediante qRT-PCR tanto a nivel de plántula como a nivel de planta adulta.

- **Las plantas sobreexpresoras de TPT fusionadas a GFP y a colas de Histidina complementan el fenotipo de los mutantes *gapcp1gapcp2* a distintos niveles.**

Con el fin de explorar el efecto de la sobreexpresión del transportador TPT en los mutantes de la *gapcp1gapcp2,* se realizaron construcciones en las que

el promotor 35S dirigía la expresión del gen que codifica para el TPT fusionado en el extremo C-terminal con la secuencia que codifica para la proteína GFP (*35S:TPT-GFP*) o la de una cola de 6 histidinas (*35S:TPT-His*). Se obtuvieron varias líneas transgénicas entre las cuales se escogieron por medio de qRT-PCR aquellas que presentaban mayor expresión del TPT. Se verificó la presencia del TPT por medio de detección de la proteína GFP en el microscopio confocal o por medio de Western Blot con anticuerpos dirigidos contra la cola de histidinas, según la construcción. Al cultivar las líneas seleccionadas en placa, se observó que las plantas mutantes *gapcp1gapcp2* transformadas con *35S:TPT-GFP* presentaban una raíz más larga que los mutantes *gapcp1gapcp2* sin transformar, pero no tan larga como la de la planta silvestre control (WT). En el caso del mutante *gapcp1gapcp2* transformado con *35S:TPT-His* la complementación radicular fue completa y su raíz era similar a la del WT. En ambos casos, el incremento en crecimiento radicular correlacionaba con un aumento en biomasa de la parte aérea. Esto aporta evidencias de que la sobreexpression de TPT es capaz de complementar el fenotipo de raíz corta del mutante *gapcp1gapcp2* pero que probablemente la presencia de la GFP provoca cambios estructurales en la proteína que afectan a sus propiedades de transporte. Por ello, se decidió continuar el resto de experimentos con la construcción que presentaba mejor complementación, en este caso, la *35S:TPT-His*. Por último, se confirmó no solo la presencia sino también la funcionalidad del transportador realizando medidas de actividad del TPT en membranas reconstituidas a partir de extractos de raíz de mutantes que sobreexpresan la *35S:TPT-His*. En este ensayo de actividad se realizó mediante el transporte radiactivo de fosfato inorgánico marcado ($^{32}P_i$) a

través de los TPT sobreexpresados y se vio que, en comparación al WT, la actividad era entre un 20 y un 60% mayor.

- **Análisis metabolómicos confirman la complementación de los desórdenes metabólicos del mutante *gapcp1gapcp2* al sobreexpresar el TPT.**

En trabajos previos se observaron alteraciones metabolómicas sobresalientes en determinados metabolitos en el mutante *gapcp1gapcp2*, los cuales restablecieron los valores normales o se acercaron a los del WT en el mutante *gapcp1gapcp2* transformado con el *35S:TPT-His*. Fue particularmente interesante el restablecimiento de los niveles de serina en la línea complementada, puesto que nuestra hipótesis de partida indicaba que el principal sumidero del 3-PGA plastidial era la RFBS. Así los porcentajes relativos de serina con respecto al total de aminoácidos aumentaron en el mutante *gapcp1gapcp2* sobreexpresor del TPT comparado con el mutante *gapcp1gapcp2* del 7% al 14%.

- **La expresión del TPT bajo el control del promotor *GAPCp* lleva a una completa complementación del mutante *gapcp1gapcp2*.**

Además de alteraciones en el desarrollo radicular, el mutante *gapcp1gapcp2* presenta esterilidad masculina, la cual se pudo recuperar mediante la construcción *GAPCp:TPT-His*. Esto se debe a que la GAPCp se expresa en células específicas, como por ejemplo las células del tapete durante el desarrollo del polen. De esta manera, esta construcción no solo

complementa el desarrollo vegetativo del mutante *gapcp1gapcp2* sino que además recupera la fertilidad.

DICUSIÓN CAPÍTULO 1:

- **Los fenotipos del mutante *gapcp1gapcp2* se pueden complementar por expresión específica del TPT en determinados tipos celulares.**

Se ha visto que la complementación del mutante *gapcp1gapcp2* ha dependido no solo del promotor que dirigía la expresión del gen del TPT sino también de la naturaleza de la proteína a la que iba fusionado. En el caso de la proteína GFP y de la cola de Histidina, se vio que esta última complementaba mejor el fenotipo que la GFP debido a que podría interferir menos en la inserción y estructura del transportador al ser de mucho menor tamaño que la GFP. De esta manera, y como la función de una proteína está íntimamente relacionada con su estructura, el transportador actuaría mejor cuando está fusionado a colas de histidinas que a GFP. Por otro lado, en cuanto al promotor 35S, éste tiene una expresión mínima o inexistente en aquellas células esenciales en el desarrollo de granos de polen. Sin embargo, el promotor GAPCp, el cual sí se expresa en dichas células, es capaz de dirigir la expresión del TPT en este tejido y por ello restablecer la fertilidad en el mutante *gapcp1gapcp2.*

- **El conjunto de 3-PGA de la glicolisis plastidial y la citosólica no se encuentra en equilibrio en células heterotróficas.**

En la literatura se ha supuesto que algunos intermediarios glicolíticos están en equilibrio entre el citosol y los plastos, aunque dicho supuesto no se puede generalizar a todos los tipos de plastos, ya que algunos carecen de determinadas actividades de transporte, lo que afectaría al propuesto equilibrio. En esta tesis se ha aportado evidencias genéticas de que cuando se expresa TPT en las raíces con la construcción apropiada se puede transportar 3-PGA, el cual puede restablecer las alteraciones observadas al restablecer la homeostasis metabólica en el mutante *gapcp1gapcp2*. Esto indica claramente por un lado que existe una deficiencia de 3-PGA en el mutante *gapcp1gapcp2* y, por otro, que las concentraciones de 3-PGA del citosol y de los plastos no están en equilibrio.

CAPÍTULO 2: La ruta fosforilativa de biosíntesis de serina es esencial para el desarrollo del embrión, del gametofito masculino y del crecimiento radicular en *Arabidopsis thaliana.*

- **El mutante homocigoto *psp1* produce letalidad en el embrión.**

En una tesis previa llevada a cabo en nuestro grupo se demostró mediante un análisis de segregación que la mutación del gen de la fosfoserina fosfatasa (*PSP1*), gen único que codifica para la enzima que cataliza el último paso de la RFBS, era letal. Para profundizar en dicha cuestión, se diseccionaron silicuas de heterocigotos *PSP1psp1.1* a distintos estadios de desarrollo. De esta manera, 8 días después de la polinización, se empezó a

observar en dichas silicuas una población de semillas con un desarrollo distinto a las de las semillas control (WT) que estaban distribuidas completamente al azar. Estas semillas anormales presentaban una coloración blanquecina y con el paso de los días empezaban a deshidratarse, quedándose tras 22 días completamente arrugadas y de un color marrón intenso. Un análisis de segregación de 5.064 semillas obtenidas a partir de un heterocigoto *PSP1psp1.1* dio como resultado una relación 1:3 (semillas con fenotipo anormal: semillas normales). El genotipado de las semillas anormales permitió concluir que sus embriones eran mutantes homozigotos *psp1.1psp1.1*. Se realizó un estudio de desarrollo embrionario a distintos estadios de estos mutantes. De dicho estudio se concluyó que los mutantes muestran un retraso en el desarrollo embrionario, dando finalmente embriones albinos detenidos en el estadio de desarrollo llamado "cotiledones curvos incipientes".

- **La falta de actividad de la PSP altera el normal desarrollo del tapete y del polen en Arabidopsis.**

Como el promotor 35S exhibe muy poca expresión en el tapete de Arabidopsis, se pudo realizar un análisis ontogénico seriado del desarrollo de las anteras y del polen en los mutantes estériles *psp1.1psp1.1* transfomados con PSP bajo el control del promotor 35S (*35S:PSP1)*. Para ello se cogieron y clasificaron los capullos florales a distintas etapas de desarrollo y se analizaron por microscopía electrónica de trasmisión. De esta manera se empezó el examen en estadio de tétrada, en el cual no se apreciaban diferencias notables ni en los granos de polen ni en el tapete.

Tampoco se apreciaron grandes diferencias en el estadio de microspora recién liberada de la tétrada. Sin embargo, en el estadio de microspora polarizada se empezaron a ver cambios a nivel de aparición de cuerpos oleosos en los tapetosomas del tapete. A continuación, en el estadío bicelular las diferencias entre WT y mutante empiezan a ser mucho más aparentes, observandose en el mutante un colapso celular y la ausencia de un segundo núcleo. En el caso del tapete, se observan tapetosomas con los cuerpos oleosos en las microsporas del WT, pero no en las del mutante *psp1.1psp1.1 35S:PSP1*. Finalmente en el estadio tricelular, los granos de polen desarrollados con normalidad presentan un fenotipo redondo, rodeado de un depósito oscuro llamado cubierta del polen o trifina, mientras que los granos de polen mutantes están completamente arrugados y presentan una ausencia total de trifina en su cubierta exterior. En esta etapa el tapete ya ha desaparecido por completo tanto en el WT como en el mutante *psp1.1psp1.1 35S:PSP1*.

- **El crecimiento radicular del mutante *psp1.1psp1.1 HS:PSP1*está alterado**

Para los estudios posteriores de caracterización funcional de PSP1, se utilizaron mutantes condicionales en los cuales se expresó PSP1 en *psp1.1psp1.1* bajo el control de un promotor inducible por choque térmico (*HS:PSP1*). Estudios de microscopía en los que se tiñeron las paredes celulares con ioduro de propidio demostraron la presencia de un meristemo más corto en el mutante *psp1.1psp1.1 HS:PSP1* en comparación al WT. Además, el número de células epidérmicas en el mutante en esta zona era

muy inferior al del WT. En cuanto a la zona de elongación, se observó que la longitud de dichas células está también alterada.

- **Estudios "-omicos" en el mutante *psp1.1psp1.1 HS PSP:PSP1.***

En esta tesis se han realizado estudios metabolómicos y transcriptómicos del mutante *psp1.1psp1.1 HS:PSP1*. Para poder realizarlos los experimentos y conocer la idoneidad del tiempo de recogida del material, se realizó un experimento de "time-course" en la cual se recogió material a distintos tiempos tras el choque térmico. Se determinó por qRT-PCR que la mayor expresión de *PSP1* en el mutante condicional tras su inducción se alcanza una hora tras el choque. Sin embargo, como la PSP1 ha de ser traducida antes de poder ejercer ningún efecto a nivel transcriptómico, se determinó que 4 horas tras el choque térmico sería suficiente para observar cambios a nivel transcripcional. Así mismo, por Western blot se determinó que 8 horas tras el choque era el momento en el que más proteína PSP1 se acumulaba. De esta manera se fijaron como tiempos de recogida para la transcriptómica 4 horas y para la metabolómica 8 horas tras la inducción.

- **Perfil metabólico del *psp1.1psp1.1 HS:PSP1* bajo distintas condiciones.**

Para explorar la actividad de la RFBS, se recogió material de *psp1.1psp1.1 HS:PSP1* bajo distintas condiciones: material recogido en presencia de luz a concentraciones de CO_2 ambientales, material recogido en presencia de luz con alta concentración de CO_2 (12500 ppms), y también material recogido al final del periodo oscuro. Para cada condición se recogió material tras 8

horas de inducción de la PSP por choque y material sin inducir, además de un lote de material tratado con 0.1 mM de serina en condiciones de luz. Tras procesar el material para la extracción de metabolitos, derivatizado y analizado en el cromatógrafo de gases acoplado al espectrofotómetro de masas, se obtuvieron lo datos brutos que serían procesados por el programa TagFinder. Una vez procesados los datos, se realizó un análisis de componentes principales (PCA) para observar el comportamiento de las distintas muestras. Según este análisis, en las partes aéreas bajo condiciones de luz, cuando las plantas mutantes y las WT crecen con 0.1 mM de serina, ambas se agrupan en un mismo cuadrante, lo que indica que su perfil metabólico es similar. Sin embargo, cuando crecen sin serina se agrupan en distintos cuadrantes. Ello sugiere que la serina producida por la RFBS es el metabolito clave cuya ausencia afecta al metabolismo de *psp1.1psp1.1 HS:PSP1*. El PCA de las muestras recogidas en oscuridad y elevado CO_2 muestra que también se localizan en cuadrantes distintos, y que la inducción de estas muestras no revierte las diferencias entre el mutante y el WT. Sin embargo, las muestras del mutante bajo estas condiciones (oscuridad y elevado CO_2), inducidas y sin inducir no se solapan completamente, sino que tienden a localizarse en distintos cuadrantes, especialmente en el caso de la parte aérea en oscuridad.

En el caso de las raíces, cuando las plantas han crecido con serina en el medio, colocalizan en el mismo cuadrante que el WT, lo que de nuevo sugiere que la falta de serina en algunos tipos celulares debido a la ausencia de actividad de la RFBS podría ser la causa principal de los desórdenes metabólicos observados en el mutante *psp1.1psp1.1 HS:PSP1*. A pesar de que la inducción del PSP no revierte completamente las diferencias entre el

WT y las líneas mutantes en las condiciones ensayadas, las muestras inducidas y no inducida no se solapan y se localizan en cuadrantes de PCA distintos, sobre todo en el caso de la oscuridad, lo que indica que esta condición es la más afectada por la falta de actividad RFBS.

Aunque se había sugerido que la ruta RFBS no debía ser muy relevante en parte aérea, se observó que, en ausencia de serina en el medio, los niveles del 90% de los metabolitos detectados en este órgano en los mutantes presentaban alteraciones con respecto al WT. Como tendencia general, el mutante *psp1.1psp1.1 HS:PSP1* muestra un incremento en la mayoría de los metabolitos determinados, tanto aminoácidos como ácidos orgánicos y azúcares.

Tras el choque térmico no todos los niveles de metabolitos se vieron afectados. Los más afectados tienen que ver con el metabolismo del carbono concretamente el ciclo de los ácidos tricarboxílicos (TCAC) y la glicolisis, lo cual puede situar al ciclo de Krebs como posible ruta afectada por la actividad de la RFBS.

En el caso de raíces, se observó un incremento notable en aminoácidos, entre ellos glutamina y triptófano, sin embargo no se observó una tendencia parecida a la observada en la parte aérea en cambios de los metabolitos del TCAC o del nivel de azúcares.

Tras la inducción de PSP1, los cambios más importantes están relacionados con la glutamina, los cuales eran significativamente más elevados en todas las condiciones ensayadas y tras el choque revirtieron a niveles normales comparados con el WT. Otro aminoácido relacionado con el metabolismo de la glutamina, el GABA, siguió el mismo patrón descrito por la glutamina.

- **El caso especial de la serina en el mutante *psp1.1psp1.1 HS:PSP1*.**

Los niveles de serina no fueron inferiores en la parte aérea del mutante *psp1.1psp1.1 HS:PSP1* con respecto al WT. Tan solo en raíces y bajo elevadas concentraciones de CO_2 se observó una disminución. Sin embargo, como muchos aminoácidos se incrementan en el mutante, si tenemos en cuenta el porcentaje relativo de serina frente al total de aminoácidos detectados, se encuentran diferencias significativas en muchas de las condiciones ensayadas.

En las partes aéreas, el porcentaje de serina en el mutante *psp1.1psp1.1 HS:PSP1* es significativamente menor que en el WT bajo luz y condiciones elevadas de CO_2. En raíces, las diferencias en el porcentaje de serina entre WT y mutante son mucho más acusadas bajo todas las condiciones ensayadas, pero desaparecen cuando las plantas crecen en presencia de serina. Tras el choque térmico, también se ve que el porcentaje relativo de serina aumenta en todas las condiciones, especialmente en raíces.

- **El contenido de auxinas en las raíces del mutante *psp1.1psp1.1 HS:PSP1* es mayor que en las del WT.**

El análisis de la cromatografía de gases acoplada al espectrómetro de masas reveló unos elevados niveles de triptófano tanto en raíces como en parte aérea del mutante *psp1.1psp1.1 HS:PSP1* comparados con el WT. Debido a que este aminoácido es el precursor de la fitohormona auxina, y junto al fenotipo defectuoso previamente comentado que muestra en la raíz el mutante *psp1.1psp1.1 HS PSP:PSP1,* se decidió hacer medidas de dicha

fitohormona en líneas mutantes *psp1.1psp1.1 HS:PSP1* y WT. Los resultados mostraron que mientras en la parte aérea, las plantas WT muestran más concentración que las mutantes, en la raíz dicha hormona se acumula casi el doble en el mutante *psp1.1psp1.1 HS:PSP1* en comparación con el WT. Además, se realizó un cruce entre líneas silenciadas *amiRNA PSP*, las cuales tienen reducidos niveles de PSP, y las líneas *DR5:GFP*, las cuales expresan la proteína GFP bajo el control de un promotor sensible a auxinas. De esta manera, se pudo detectar una mayor intensidad de GFP en la zona meristemática de las raíces de las líneas mutantes *psp1.1psp1.1 HS:PSP1* que en las raíces WT.

- **Las plantas mutantes** *psp1.1psp1.1 HS:PSP1* **acumulan más almidón que las plantas WT.**

El almidón es un metabolito que da una idea sobre la dinámica del metabolismo del carbono. Durante el día, las plantas almacenan los productos de la fotosíntesis en las hojas en forma de gránulos de almidón. Sin embargo, por la noche este almacén es movilizado y utilizado con distintos fines, como por ejemplo, la respiración o el crecimiento de la planta. Con el fin de explorar el contenido en almidón del mutante *psp1.1psp1.1 HS PSP:PSP1*, se cogieron muestras de la parte aérea antes del amanecer (6 am) y al atardecer, coincidiendo con los momentos de menor y mayor cantidad de almidón almacenado, respectivamente. El resultado fue que los mutantes no sólo tenían más almidón que el WT en ambos puntos de muestreo, sino que además lo mantienen constante durante el día, es decir,

parece que no pueden movilizarlo, lo cual puede ser la causa de su porte enano comparado con las plantas WT.

- **La actividad de algunas enzimas del TCAC se induce en el mutante respecto al WT y tras el choque térmico se igualan.**

En los resultados obtenidos tras el análisis metabolómico, se observó que algunos ácidos orgánicos del TCAC aumentaban en los mutantes. Este es el caso del citrato, succinato, fumarato y malato. Con el fin de corroborar que el TCAC estaba alterado en los mutantes *psp1.1psp1.1 HS:PSP1,* se determinó la actividad de algunas enzimas del TCAC tanto en parte aérea como en raíz, concretamente las actividades de la citrato sintasa y la fumarasa. Esto se realizó antes del choque térmico y a distintos tiempos después del mismo. Como resultado se obtuvo que la actividad de dichas enzimas era significativamente más elevada en el mutante *psp1.1psp1.1 HS:PSP1* que en el WT, pero tras la inducción, los niveles de actividad del mutante comparados al WT se volvían similares y no eran significativamente diferentes.

- **Los niveles de amonio en parte aérea y raíz del mutante *psp1.1psp1.1 HS:PSP1* son más elevados que en el WT.**

Otro resultado interesante que se desprende del perfil metabólico del mutante *psp1.1psp1.1 HS:PSP1* es su elevada cantidad de glutamina comparada con el WT. Tras la inducción los niveles de este metabolito disminuyeron considerablemente en raíces. Una de las posibles razones para explicar este incremento podría estar relacionada con la ruta de asimilación del amonio. Las plantas asimilan amonio en la forma de glutamina a través

de la actividad de la glutamina sintetasa. Con el fin explorar la concentración de amonio que hay dentro de la planta se realizaron medidas tanto a nivel de parte aérea como de raíz y el resultado fue que el mutante doblaba la cantidad de amonio presente en el WT. Además, se testó el efecto que tiene el amonio en el crecimiento radicular, haciendo crecer plantas en medio sin amonio, con exceso de amonio y control. El resultado fue que la raíz de los mutantes *psp1.1psp1.1 HS:PSP1* crece mejor en un medio con nitrato como única fuente de nitrógeno que en un medio con una mezcla de nitrato y amonio.

- **Perfíl transcriptómico del *psp1.1psp1.1 HS:PSP1* en condiciones de oscuridad.**

Con el fin de explorar las diferencias de expresión génica entre el mutante *psp1.1psp1.1 HS:PSP1* y el WT, además de identificar las dianas primarias de la actividad del PSP, se realizó un análisis de RNAseq. Tras tomar en cuenta el importante papel que tiene la RFBS en la oscuridad y los resultados obtenidos en el PCA, se decidió que fuera ésta la condición bajo a la cual se recogerían las muestras. Tras validar la expresión de varios genes mediante qRT-PCR los datos obtenidos por RNAseq, se acotaron aquellos genes cuya expresión era significativamente distinta con respecto al WT y se realizó un análisis de enriquecimiento funcional. De esta manera, se obtuvieron multitud de categorías bajo las cuales se agrupaban los distintos genes. Sin embargo, al comparar los datos de transcriptómica con los de metabolómica, los niveles de auxina detectados y la relación entre la producción de serina y la asimilación de sulfuro y amonio, se decidió acotar el estudio a aquellas categorías funcionales relacionadas con el metabolismo

de auxinas y de triptófano, así como de genes involucrados en la asimilación de amonio y de azufre. Con tal propósito, se identificaron aquellos genes relacionados con dichas categorías, cuyos niveles de expresión estuvieran alterados significativamente en el mutante con respecto al WT. De esta manera, fue posible clasificar los genes en dos grupos, dependiendo del hecho de si las diferencias entre el mutante y el WT persistían tras la inducción o si se eliminaban dichas diferencias tras la inducción de la expresión de la PSP1.

En relación a la parte aérea, pocos genes estaban desregulados en comparación con la parte radicular, y entre ellos no había genes relacionados con las auxinas y tan solo unos cuantos relacionados con el metabolismo del azufre. Sin embargo, en las raíces, el metabolismo de auxinas muestra muchos genes cuya expresión es elevada en el mutante sin inducir y se reduce tras el choque. Si nos fijamos en otras categorías, prácticamente todos los genes relacionados con el metabolismo del azufre y del amonio están reprimidos tras el choque térmico.

Por otro lado está aquel grupo de genes cuyas diferencias en el nivel de expresión respecto al WT persistían tras el choque térmico, los cuales pueden considerarse como genes de respuesta tardía al PSP o simplemente genes de respuesta secundaria. Entre estos genes se identificaron muchos relacionados con las auxinas, con la asimilación de amonio y con el metabolismo del azufre en raíces. Sin embargo en parte aérea pocos genes relacionados se encontraron en dicha categorías.

DICUSIÓN CAPÍTULO 2:

- **La mutación *psp1* presenta letalidad a nivel de embrión.**

Se ha observado que el mutante *psp1.1psp1.1* presenta un retraso en el desarrollo embrionario, el cual empieza en el estadio globular. Se conoce la importancia que tiene en los estadios tardíos del desarrollo embrionario el establecimiento de rutas metabólicas para que el embrión se autoabastezca de determinados metabolitos. Concretamente, los primeros pasos en el desarrollo de proplastidios en los cuales se localiza la PSP1, ocurren en la transición de estadio globular al de corazón. El retraso en el desarrollo embrionario en el estadio globular podría estar relacionado con el establecimiento de la ruta RFBS en el embrión en este punto de su desarrollo.

- **La actividad PSP juega un papel crucial en el desarrollo del tapete y del polen en Arabidopsis.**

Se ha observado que la falta de actividad PSP trae consigo una alteración en el desarrollo del polen. Se ha demostrado también que la PSP se expresa en el tapete y en las microsporas en etapas cruciales del desarrollo. Ya que el tapete es el proveedor de metabolitos, enzimas y precursores de esporopolenina para las microsporas en desarrollo, la falta de expresión de PSP en estas células puede alterar este abastecimiento y producir por consiguiente alteraciones en el desarrollo del polen. Durante el desarrollo del polen, uno de los aspectos observados más interesantes fue que la microspora se detiene en estadio polarizado, sin llegar a producirse la

primera mitosis. Muchos estudios han relacionado a la serina con la regulación del ciclo celular en mamíferos, de forma que la serina podría estar conectando el metabolismo primario con la regulación del ciclo celular también en plantas.

Por otra parte, en el estadio de célula polarizada no se observan cuerpos oleosos en el interior de los tapetosomas de las células del tapete, mientras que en el WT si es posible su observación. El desarrollo normal de los tapetosomas depende de una correcta formación de las endomembranas. Se sabe que los esfingolípidos son componentes importantes de las membranas y que en su síntesis interviene la serina que a su vez reacciona con el palmitoil-CoA por medio de la serina palmitoiltransferasa (SPT). Análisis ultraestructurales revelan que microsporas de mutantes *spt* presentan el mismo fenotipo de colapso celular, detienen su desarrollo en estadio de célula polarizada y no se produce la primera división mitótica, al igual que sucede en el mutante *psp1.1psp1.1 35S:PSP1*. En la presente tesis se hipotetiza que la serina necesitada por la SPT en el tapete y en las microsporas se la suministraría la RFBS, pero como dicha ruta está bloqueada, no se podría aportar suficiente serina para la síntesis de esfingolípidos y ello provocaría las alteraciones en las membranas de los tapetosomas. Debido a que los cuerpos oleosos requieren vesículas membranosas y están relacionados íntimamente con el RE, una alteración de este tipo en su correcto desarrollo podría ser una posible explicación a su ausencia en el mutante *psp1.1psp1.1 35S:PSP1*. Por otro lado, los cuerpos oleosos de los tapetosomas están rodeados de una cubierta de proteínas llamadas oleosinas, siendo la más abundante la GRP17. Esta proteína presenta muchas repeticiones con serina y predominantemente glicinas en su

extremo C-terminal. La serina, precursora de la glicina necesaria para la síntesis de GRP17, podría estar suministrada por la RFBS en las células del tapete. Un estudio de la composición de cuerpos lipídicos demuestra que es precisamente el extremo c-terminal de las oleosinas lo que abunda en la cubierta proteica de los cuerpos oleosos. Por ello, los cuerpos oleosos podrían ser importantes en la formación de la cubierta proteica del polen y podrían ser responsables de la ausencia de ésta en el mutante *psp1.1psp1.1 35S:PSP1*. Finalmente, las células del tapete y las microsporas se desarrollan íntimamente ligadas, y por ello se propone que la ausencia de PSP1 afecta al desarrollo conjunto de ambos tipos celulares.

- **La homeostasis de serina está alterada en el mutante *psp1.1psp1.1 HS:PSP1.***

Los niveles de serina en el mutante *psp1.1psp1.1 HS:PSP1* no son significativamente menores que en el WT en la mayoría de las condiciones ensayadas. Tan solo en raíces bajo condiciones de alta concentración de CO_2 hubo una reducción significativa en su contenido con respecto al WT. Sin embargo, si tenemos en cuenta el porcentaje de serina respecto al total de aminoácidos medidos para cada condición, se pueden contemplar aspectos interesantes. En el WT, el porcentaje de serina es mayor en luz que en las otras condiciones, lo que indica que los requerimientos de serina son mayores durante el día. Los datos obtenidos en *psp1.1psp1.1 HS:PSP1* apoyan la idea de que la RFBS contribuye a la homeostasis de serina en parte aérea, ya que su porcentaje disminuye claramente en el mutante al compararlo con el WT. Bajo condiciones de oscuridad, no se ha podido

detectar diferencias en el porcentaje de serina entre WT y mutante, lo cual no era un resultado esperado. Se podría especular con la idea de que bajo condiciones de oscuridad, se requiere menos serina o que la ruta del glicerato, la cual también sintetiza serina, es más activa por la noche y puede compensar la falta de actividad de la RFBS.

En el caso de las raíces, el porcentaje de serina disminuyó en comparación al WT en todas las condiciones ensayadas, especialmente en oscuridad y bajo elevada concentración de CO_2. Estos resultados, junto con la alteración en el desarrollo radicular del mutante *psp1.1psp1.1 HS:PSP1*, apoyan que la RFBS es la ruta más importante en el aporte de Ser a la raíz, y sobre todo en oscuridad o bajo condiciones en las que la ruta fotorrespiratoria no funciona. El elevado porcentaje de serina en raíces tanto en WT como en el mutante *psp1.1psp1.1 HS:PSP1* bajo condiciones de luz, comparado con oscuridad y alto CO_2, indican que la serina sintetizada en la parte aérea por la ruta del glicolato podría alcanzar las raíces y compensar parcialmente la falta de actividad RFBS.

Un interrogante que necesita ser abordado es por qué las rutas del glicerato o del glicolato no pueden compensar la falta de actividad RFBS en raíces y órganos reproductivos. Se propone que las rutas de biosíntesis de serina participan de forma distinta según el tipo celular, o quizá algunas células carecen de transportadores de serina, como las células del tapete, o no están conectadas a los haces vasculares, como las células meristemáticas. Por ello, la hipótesis más plausible sería que la única fuente de serina para estos tipos celulares sea la generada en su interior por biosíntesis intracelular. Bajo estas circunstancias, nuestros datos apoyan la idea de que el contenido relativo de serina detectado en nuestros datos no refleja el contenido de

serina en estas células específicas. En cualquier caso, los resultados apoyan que las otras rutas de biosíntesis de serina no son de especial relevancia en células del tapete, en el embrión o en los meristemos radiculares, y por ello solo la RFBS sería responsable del aporte de Ser en ellos.

- **Varias rutas metabólicas interaccionan con la RFBS.**

En los mutantes *psp1.1psp1.1 HS:PSP1* se ha visto que tanto el metabolismo central del carbono (TCAC, glicolisis y metabolismo de azúcares) como el metabolismo del nitrógeno están alterados en parte aérea. Sin embargo en raíces están más drásticamente afectados los procesos de asimilación del amonio.

En parte aérea el TCAC en el mutante *psp1.1psp1.1 HS:PSP1* se mostró particularmente alterado, como así lo indican las medidas de actividad realizadas. Tanto las actividades del TCAC como los niveles de los metabolitos se revirtieron o se aproximaron a los niveles WT tras la inducción. Pensamos que tras la inducción por choque térmico de la RFBS, gran parte del 3-PGA se usa como sustrato por la RFBS en vez de redirigirse a reacciones posteriores de la glicolisis plastidial y después al TCAC. Bajo condiciones de alto CO_2, el incremento observado en metabolitos del TCAC como citrato, fumarato y malato, resultó mucho más pronunciado que bajo condiciones normales de luz, lo que indicaría que la RFBS es mucho más activa cuando la ruta del glicolato está inhibida.

En raíces, y bajo condiciones de oscuridad, algunos metabolitos del TCAC se incrementaron en el mutante *psp1.1psp1.1 HS:PSP1*, pero sus niveles no revirtieron tanto como en parte aérea tras la inducción por choque térmico. Para explicar esto se barajan varias opciones: i) puesto que la respiración es

mucho más intensa en condiciones heterotróficas que autotróficas, el consumo de 3-PGA para el funcionamiento de la RFBS es relativamente reducido en comparación con el utilizado para la actividad respiratoria en estas condiciones de heterotrofia; ii) como la fotosíntesis no está activa en condiciones de oscuridad, el aporte de 3-PGA en los plastos no fotosintéticos para el funcionamiento de la RFBS es reducido en comparación con el aporte en plastos fotosintéticamente activos. Ambas opciones pueden implicar que la función de "conmutador" de la RFBS entre el metabolismo del nitrógeno y del carbono sea menos efectiva en condiciones de heterotrofía que en condiciones de auxotrofía.

Los niveles de aminoácidos en el mutante *psp1.1psp1.1 HS:PSP1* se mostraron claramente alterados bajo todas la condiciones ensayadas, tanto en parte aérea como en raíces. Los cambios más importantes en raíces están relacionados con la glutamina y el GABA. Ambos incrementaron en el mutante y se redujeron significativamente tras la inducción. Otros aminoácidos ricos en nitrógeno, como la asparagina, disminuyeron drásticamente en las raíces del mutante, lo cual indicaría que la asimilación del amonio podría estar alterada en el mutante *psp1.1psp1.1 HS:PSP1*. En previos trabajos se ha documentado que el silenciamiento de la PGDH, enzima que cataliza la primera reacción de la RFBS, produce un incremento en los niveles de glutamina y amonio en parte aérea, lo que sugiere que la actividad de la PSAT es necesaria para generar 2-oxoglutarato para la fijación de amonio. La PSAT, es la segunda enzima de la ruta RFBS y produce 2-oxoglutarato en su actividad, el cual es presumiblemente usado para la asimilación de amonio por el ciclo GS/GOGAT. En el presente trabajo aportamos más evidencias de que la RFBS es necesaria para que el

ciclo GS/GOGAT funcione correctamente. Los elevados niveles de amonio detectados en el mutante *psp1.1psp1.1 HS:PSP1,* junto a su fenotipo de hipersensiblidad en el crecimiento radicular, indican que la ruta GS/GOGAT se ha bloqueado en una de sus reacciones, lo que explicaría una acumulación de precursores como la glutamina y el amonio. A nivel transcriptómico, se ha descrito una relación entre la concentración de amonio y la inducción de isoenzimas de la glutamina sintetasa. Los resultados transcriptómicos del presente trabajo muestran una inducción de los genes que codifican para la glutamina sintasa y la GOGAT.

Se postula que la inactivación de la PSP en el mutante *psp1.1psp1.1 HS:PSP1,* afectaría a la actividad de la PSAT, la cual reduciría la disponibilidad de 2-oxoglutarato en el plasto dando por consiguiente una acumulación de amonio, glutamina y GABA. Ello afectaría el desarrollo normal de la planta, especialmente el de raíz.

GABA podría jugar un papel esencial como sumidero de glutamato cuando la GS/GOGAT está reprimida. Glutamato se puede convertir en GABA por la reacción de la glutamato descarboxilasa (GAD). La expresión elevad de GAD en parte aérea y su represión tras la inducción apoyan esta idea.

En los resultados de transcriptómica los mutantes *psp1.1psp1.1 HS:PSP1* mostraron un incremento no solo en la expresión de algunos genes que codifican trasportadores de sulfato sino también enzimas de asimilación de sulfato y serina acetiltransferasas, lo que apoya la idea de que el mutante se comporta como si estuviera bajo condiciones de escasez de azufre. Los niveles de o-acetil serina también son bastante elevados tanto en parte aéra como en raíces en todas las condiciones. Se sabe que las concentraciones de

OAS en hojas y raíces incrementan bajo condiciones de falta de azufre, y por ello este metabolito induce la expresión de genes involucrados en la toma y asimilación de azufre, tal y como se observa en los resultados de transcriptómica.

- **Papel de la RFBS en el desarrollo radicular.**

Los resultados indican que las raíces primarias del mutante *psp1.1psp1.1 HS:PSP1* muestran un meristemo más pequeño y con menor número de células que el WT, además de unas células más cortas en la zona de elongación. Este resultado sugiere que la PSP es necesaria no solo para la división celular, como ya se ha visto en mamíferos, sino también para la elongación del meristemo radicular primario. Como se ha comentado previamente, la RFBS podría ser la única fuente de serina para las células meristemáticas no conectadas a la vasculatura general de la planta.

También se ha comprobado que elevados niveles de amonio en el tejido radicular inhibe el crecimiento de éste al reducir la longitud del meristemo y la zona de elongación. La raíz del mutante *psp1.1psp1.1 HS:PSP1* crece mejor en un medio sin amonio. Estos resultados indican que como mínimo, la toxicidad del amonio como resultado de la falta de la actividad de la RFBS podría, en parte afectar al crecimiento radicular en el mutante.

Otro factor que podría tener relevancia en la inhibición del crecimiento radicular es la excesiva concentración de la fitohormona auxina en este tejido. Además, muchos genes relacionados con el metabolismo de auxinas han sido detectados como genes desregulados en el mutante.

Teniendo en cuenta todos estos resultados, el fenotipo de inhibición de la raíz encontrado en el mutante *psp1.1psp1.1 HS:PSP1* podría ser el resultado de varios factores: falta de serina en el meristemo, toxicidad del amonio y elevadas concentraciones de axina el meristemo radicular. Como el mutante *psp1.1psp1.1 HS:PSP1* crecido en condiciones de medio sin amonio tiene un efecto limitado en el crecimiento radicular, el papel de la serina y/o la auxina podría ser más relevante, pero serán necesarios más experimentos para dilucidar su implicación.

CONCLUSIONES

Con el fin de estudiar en profundidad la RFBS en Arabidopsis, se estudió la PSP1, que es la última enzima de la ruta. La ausencia de actividad de la PSP1 produce un retraso en el desarrollo embrionario, dando como resultado embriones albinos abortados detenidos en el estadio temprano de cotiledones curvos. Por otro lado, el mutante *psp1psp1* transformado con una construcción que expresan PSP1 bajo el control del promotor 35S *(psp1.1psp1.1 35S:PSP1*), el cual se expresa poco en el tapete, mostraron un fenotipo de esterilidad. El desarrollo de microsporas en *psp1.1psp1.1 35S:PSP1* se paralizaba en el estadio de célula polarizada, acompañado de un desarrollo retardado e irregular del tapete. La expresión del PSP1 en el tapete en estadios puntuales del desarrollo de las microsporas sugiere que la actividad del PSP1 en esta capa celular es esencial para el desarrollo del polen. La RFBS también afecta al desarrollo radicular, reduciendo la división celular en el meristemo y la longitud celular en la zona de

elongación. Un abordaje metabolómico y transcriptómico pone de relieve que la RFBS juega un papel esencial en el metabolismo vegetal actuando como un "commutador" entre el metabolismo del carbono y del nitrógeno, además de conectar la glicolisis y el TCAC con la biosíntesis de aminoácidos y las rutas de asimilación de sulfato y amonio.

ABSTRACT

In plants three different serine biosynthesis pathways have been described: the glycolate pathway associated with photorespiration, and two nonphotorespiratory pathways, the glycerate pathway and the phosphorylated pathway of serine biosynthesis (PPSB). As the glycolate pathway is the most important, at least in quantitative terms, the role of the PPSB has been neglected until quite recently. This thesis provides insights into the role of the PPSB in *Arabidopsis* development and metabolism.

The PPSB uses 3-phosphoglycerate (3-PGA) as a precursor which can be supplied through the plastidial or the cytosolic glycolysis. It is assumed that the activity of these two glycolytic pathways is integrated through transport systems, which exchange glycolytic intermediates across plastidial membranes. It was unknown whether plastidial and cytosolic pools of 3-PGA can equilibrate in nonphotosynthetic cells. To solve this matter, we employed mutants of the plastidial glycolytic isoforms of glyceraldehyde-3-phosphate dehydrogenase (GAPCp), which express the Triose Phosphate Translocator (*TPT*) under the control of different promoters. *TPT* expression under the control of the *35S* promoter complemented the vegetative developmental defects and metabolic disorders of GAPCp double mutants (*gapcp1gapcp2*). However, *TPT* expression under the control of the *35S*, which is poorly expressed in the tapetum, hardly complemented *gapcp1gapcp2* male sterility. Full vegetative and reproductive complementation of *gapcp1gapcp2* was rescued only by transforming this mutant with a construct that carried the *TPT* under the control of the *GAPCp1* native promoter. A negative anatomical correlation was found between *TPT* and *GAPCp* expression, which suggests that the translocator is

inactive in heterotrophic cells where GAPCp is functionally significant. Our results indicated that the main function of GAPCp is to supply 3-PGA for anabolic pathways in heterotrophic cells. They also suggest a 3-PGA deficiency in the plastids of *gapcp1gapcp2* and that 3-PGA pools between cytosol and plastid do not equilibrate in heterotrophic cells.

In order to study the PPSB in *Arabidopsis* in depth, PSP1, the last enzyme of the pathway, was targeted. Lack of PSP1 activity delayed embryo development and led to aborted embryos, classified as early curled cotyledons. On the other hand, *psp1.1psp1.1* mutants expressing *PSP1* under the control of the *35S* promoter (*psp1.1psp1.1 35S:PSP1)*, which is poorly expressed in the anther tapetum, displayed a male sterile phenotype. Microspore development in *psp1.1psp1.1 35S:PSP1* was arrested in the polarized stage. The tapetum of *psp1.1psp1.1 35S:PSP1* also displayed delayed and irregular development. The *PSP1* expression in the tapetum in critical microspore development stages suggests that PSP1 activity in this cell layer is essential for pollen development. PPSB also affects primary root development, by reducing cell division in the meristem and cell length in the elongation zone. A transcriptomics and metabolomics study showed that the PPSB plays a crucial role in plant metabolism by acting as a metabolic switch between carbon and nitrogen metabolism, and connecting glycolysis and the Krebs cycle with the biosynthesis of amino acids, and with sulfate and ammonium assimilation pathways.

RESUM

A les plantes s'ha descrit tres rutes diferents per a la síntesi de serina: la ruta del glicolat, associada amb la fotorrespiració, i dos rutes independents d'aquesta, la ruta del glicerat i la ruta fosforilativa de biosíntesi de serina (PPSB). Tot i que la ruta del glicolat és si més no la més important en termes quantitatius, el paper de la PPSB ha sigut ignorat fins fa pocs anys. Aquesta tesi doctoral aporta noves perspectives sobre la funció de la PPSB, tant al desenvolupament com al metabolisme d'*Arabidopsis*.

La PPSB s'abastix de 3-fosfoglicert (3-PGA) com a substrat, el qual pot ser subministrat per la glicòlisi plastidial o citosòlica. S'assumeix que l'activitat d'aquestes dues rutes està integrada mitjançant un sistema de transport, el qual intercanvia els intermediaris glicolítics a través de la membrana plastidial. Tanmateix, es desconeixía si el conjunt de 3-PGA del plàstid i el citosol podien compensarse mutuament en cèl·lules no fotosintétiques. Per a resoldre aquesta qüestió, s'ha fet servir mutatns de les isoformes glicolítiques plastidials de la gliceraldehid-3-fosfat deshidrogenasa (GAPCp) que expressen el transportador de trioses fosfat (TPT) sota el control de diferents promotors. Sota el control del promotor *35S*, el gen *TPT* va complementar els defectes tant fenotípics com metabolòmics que presentaven els dobles mutants GAPCp (*gapcp1gapcp2*). Tot i així, l'expressió del gen *TPT* sota el control del *35S*, el qual s'expressa mínimament al tapet, no va poder complementar el fenotíp d'esterilitat masculina. La complementació total del *gapcp1gapcp2*, tant vegetativa com reproductiva, es va obtindre mitjançant la transformació del *gapcp1gapcp2* amb el *TPT* sota el control del promotor *GAPCp1*. A més a més, es va

observar una correlació negativa a nivel anatòmic entre l'expressió de *TPT* i la de *GAPCp*, la qual cosa suggereix que el TPT està innactiu en cèl·lules heterotròfiques on la GAPCp n'és funcionalment significativa. Els resultats obtinguts indiquen que la funció principal de la GAPCp és aportar 3-PGA per a rutes anabòliques en teixits heterotròfics. També, aquestos resultats apunten a una deficiència de 3-PGA als plàstids de *gapcp1gapcp2*, com a conseqüència de que els conjunts de 3-PGA entre citosol i plàstid no es troben en equilibri en cèl·lules heterotròfiques. Amb la finalitat d'estudiar en profunditat la PPSB en *Arabidopsis*, PSP1, el darrer enzim de la ruta, fou l'objectiu d'aquet estudi. L'absència d'activitat de la PSP1 produeix un retard en el desenvolupament embrionari, produint com a conseqüència embrions albins abortats a l'etapa primerenca de cotilèdons curvs. Per altra banda, *psp1.1psp1* que expressa *PSP1* sota el control del promotor *35S* (*psp1.1psp1.1 35S:PSP1*), el qual al seu torn s'expressa poc en tapet, va mostrar un fenotip d'esterilitat. El desenvolupament de micròspores en *psp1.1psp1.1 35S:PSP1* es paralitzaba a l'etapa de cèl·lula polaritzada, acompanyat d'un desenvolupament retardat i irregular del tapet. L'expressió de *PSP1* en el tapet en determinades etapes del desenvolupament de les micròspores suggerix que la activitat del PSP1 en aquesta capa cel·lular és esencial per al desenvolupament normal del pol·len. La PPSB també afecta al desenvolupamnet radicular, reduïnt la divisió cel·lular al mersitem i la longitut cel·lular a la zona d'elongació. Un estudi metabolòmic i transcriptòmic de la PSP1 fa palessa que la PPSB juga un paper esencial al metabolisme vegetal i servix com a "commutador" entre el metabolisme del carboni i del nitrogen, a més de connectar la glicòlisi i el cicle de Krebs amb la biosíntesi d'aminoàcids i les rutes d'assimilació de sulfat i amoni.

1. **INTRODUCTION**

1.1 Plant biology and *Arabidopsis thaliana*

Plant biology is concerned about the life processes of plants, and at the beginning it focused especially on crop plants. Our ancestors discovered that when collecting seeds from vigorous plants and cultivating them under appropriate conditions of water availability and sun light, it is possible to obtain the same vigorous plants. With the passing of centuries of agricultural practice, humanity learnt how to cross plant species to obtain improved varieties and began to draw knowledge about incipient plant breeding (ISAA, 2010).

Nowadays the study of plant biology has extended to many different groups of plants, of which higher green terrestrial plants are the most attractive. During the history of plant biology, many plants have been considered promising candidates to be model plants, like petunia and snapdragon, or particularly those relevant to agriculture, like maize, tomato, pea, rice and barley. However, just one, *Arabidopsis thaliana*, has been chosen by the plant science community as the most suitable model for studying processes that are common to all plants (Meinke et al., 1998).

Arabidopsis thaliana, called *Pilosella siliquosa* at the beginning by Johannes Thal, was discovered in the Harz mountains in the sixteenth century. Later in 1753, Carl Linnaeus renamed this plant as *Arabis thaliana* in honor of Thal but it was not until 1842 that Gustav Heynhold created the new genus *Arabidopsis* and placed that plant in that genus (Meyerowitz, 2001).

Its common name is thale cress or mouse-ear cress, a small weed in the Brassicaceae or Cruciferae family. Its important features like short generation time, small size and prolific seed production through self-pollination, make it a suitable plant model (Koornneef et al., 2010).

In 1943 Friedrich Laibach took advantage of these specific features and founded experimental *Arabidopsis* research by initiating experiments to treat *Arabidopsis* with X-rays. It was not until the early 1980s, when the modern era of *Arabidopsis* research began its most active period thanks to the release of a detailed genetic map, that the transformation protocols were created and, in 1996 the Arabidopsis Genome Initiative dedicated to coordinating large-scale sequencing efforts was established (Koornneef et al., 2010).

1.1.1 Biology and genetics of *Arabidopsis thaliana*

Arabidopsis thaliana has a broad natural distribution throughout Europe, Asia and North America with more than 700 ecotypes available for experimental analysis. A good example of such are Columbia and Landsberg, two of the standard ecotypes for genetic and molecular studies. Its life cycle is completed in just 6 weeks. Seedlings develop into rosette plants by bolting starts about 3 weeks after planting, and the resulting inflorescence forms a linear progression of flowers and siliques for several weeks before onset of senescence. Mature plants reach 15-20 cm in height, and often produce several hundred siliques with more than 5,000 seeds. Flowers of 2 mm are composed of an outer whorl of four green sepals and an inner whorl of four white petals, six stamens and a central gynoecium that forms the silique. Fortunately, flowers can be easily crossed by

applying pollen to the stigma surface. The slender fruits produced are the siliques that contain seeds of 0.5 mm in the maturity stage of development (Koornneef et al., 2010). *Arabidopsis* plants can also be grown in petri plates or maintained in pots located either in a greenhouse or under fluorescent light in the laboratory.

Given its biological particularities as regard short generation time, small size and large number of offspring, *Arabidopsis* presents many advantages for genome analysis. Its nuclear genome is 125 Mb large and is distributed into five chromosomes, which encode approximately 26,000 genes (Borevitz et al., 2004). Apart from the nuclear genome, plastids and mitochondria also present their own genome (Table 1.1), which is not very large and encodes subunits of the photosystem, the electron transport chain (plastid genome) and essential subunits of the respiratory chain (mitochondria).

Table 1.1. Features of the genes encoded by the three genomes in *Arabidopsis*. nt, nucleotid. Source: Arabidopsis Genome Initiative (2000).

	Nucleus/cytoplasm	Plastid	Mitochondria
Genome size	125 Mb	154 kb	367 kb
Genome equivalent/cell	2	560	26
Duplication	60%	17%	10%
Number of protein genes	25.498	79	58
Gene order	Variable, but syntenic	Conserved	Variable
Density (Kb per protein gene)	4.5	1.2	6.25
Average coding length	1,900 nt	900 nt	860 nt
Genes with introns	79%	18.4%	12%
Genes/pseudogenes	1/0.03	1/0	1/0.2-0.5
Transposons (% of total genome size)	14%	0%	4%

1.1.2 *Arabidopsis* embryogenesis

Starting from a zygote, embryogenesis produces not only the first tissue precursors, but also the first stem cells. By the end of embryogenesis the zygote has transformed into a mature embryo, which invariably comprises the same basic tissue types of any postembryonic plant. Embryogenesis in this plant follows a simple, highly regular predictable pattern of cell division (ten Hove et al., 2015). The development stages are described in Figure 1.1. Basically, the main stages are zygotic, globular, transition, heart, torpedo and mature stage.

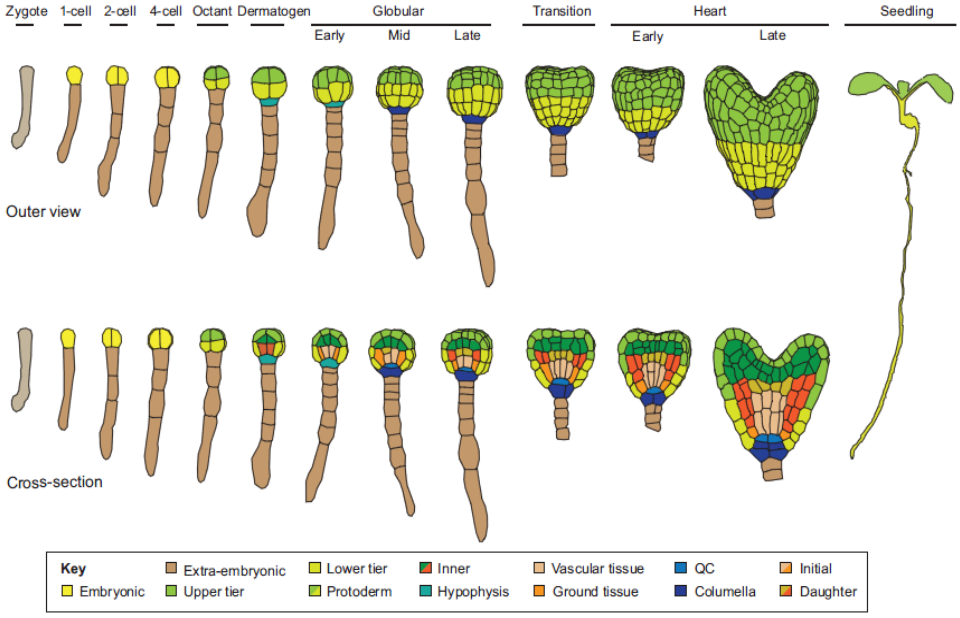

Figure 1.1. *Arabidopsis* embryo development. Surface view and longitudinal cross-sections of a developing *Arabidopsis* embryo. Cells are coloured according to their lineage, as indicated in the key. Based on data from Yoshida et al. (2014). Source: ten Hove et al. (2015).

A collection of 800 genes, which gives a loss-of function phenotype in Arabidopsis embryos, has been identified and characterized. The Arabidopsis genes that are required for viability under normal conditions and cannot be passed to subsequent generations when disrupted, are often considered essential in embryo development (Tzafrir et al., 2004).

1.1.3 The Development of mature pollen grains

This process is essential for successful reproduction of higher plants (Figure 1.2; Backues et al., 2010). In the first stage of pollen development, microsporocytes are surrounded by a layer of β-1,3-glucan called callose (Dong et al., 2005; Regan et al., 1990). Then they undergo two meiotic divisions and produce a tetrad, a structure of four microspores surrounded by callose. After the release of microspores by the dissolution of the callose wall, the nucleus of the microspore, which is located in the centre of the cell, migrates to the periphery, and gives the appearance of a polarised and vacuolated microspore. In the next step, the nucleus of the microspore undergoes a first mitosis, which leads to a vegetative cell and a generative cell, and reaches the so-called bicellular stage. Finally in the tricellular stage, the generative cell undergoes a second mitosis and produces two sperm cells (Bedinger, 1992).

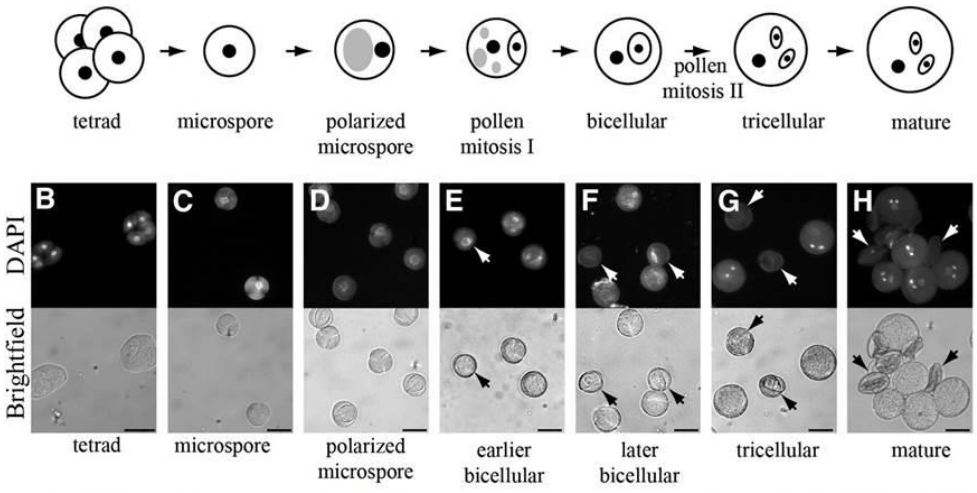

Figure 1.2. Diagram of pollen sac development. Black dots indicate nuclei, gray ovals indicate vacuoles, and black lines indicate cell boundaries. Source: Backues (2010).

Proper development of microspores depends, in turn, on the normal development of the tapetum, the layer of cells adjacent to the locule of the anther, which plays a crucial role in microsporogenesis by providing metabolites, enzymes, nutrients and sporopollenin precursors (Feng et al., 2010; Liu et al., 2013a). Premature or delayed differentiation, and disintegration of the tapetum results in male sterility (Liu et al., 2013a; Kawanabe et al., 2006).

The mature pollen wall has three different layers: the pollen coat, the exine and the intine (Jiang et al., 2013). The pollen coat, also known as pollenkitt or tryphine, fills the interstices of the pollen wall surface in the final stage of its development, and is composed mainly of proteins and lipids (Ishiguro et al., 2010). These compounds are present in two predominant storage organelles: the elaioplasts and tapetosomes of tapetal cells (Ting et al., 1998). In the final development stage, tapetal cells undergo programmed cell death (PCD) and release storage materials, which will become the coat

of mature pollen (Hsieh et al., 2007). The next pollen wall layer is the exine, which presents a kind of roof called tectum, some prominent columns known as bacula, and a foot layer termed the nexine (Vizcay-Barrena et al., 2006). This layer is composed of sporopollenin secreted by tapetal cells (Liu et al., 2013a). A thin band of wall material located immediately below the nexine is the intine, formed mainly by the cellulose and pectin secreted by the microspore in the ring-vacuolated stage (Vizcay-Barrena et al., 2006; Yamamoto et al., 2003). The study of the molecular mechanisms involved in male gametophyte development has identified several mutations that affect the pollen wall structure and composition to result in male sterility. For example, the recessive and conditional male-sterile *Arabidopsis* mutant, *flaky pollen1-1* (*fkp1-1*), whose pollen grains lack functional pollen coats, has been characterised (Ishiguro et al., 2010). The double mutant *long-chain acyl-CoA synthetases* (*lacs1 lacs4*) also encounters problems during the production of pollen coat lipids (Jessen et al., 2011). However, the vast majority of the mutations related with the microspore pollen wall are also related with exine alterations (Dong et al., 2005; Guan et al., 2008; Ariizumi et al., 2004; Paxson-Sowders et al., 2001). Aberrations in this layer appear in the *kaonashi* (*kns1*) mutants, whose microspores present disorders in callose wall formation, defective tecta formation or densely distributed bacula (Suzuki et al., 2008).

In some cases the male sterility phenotype is not related with alterations in the exine or the pollen coat, such as the chromosomal high-mobility group proteins (*hmg1hmg2*) double mutant. This double mutant exhibits shrunken pollen grains with a perfectly normal pollen wall whose inside is hollow and less packed than in the wild-type (WT)(Suzuki et al., 2009). Finally there

are many reports where male sterility is associated with not only disturbances in microspore development, but also with tapetal development and degeneration. Such is the case of the *male sterility1* mutant (*ms1*) in which tapetum PCD is altered, which leads to abnormal pollen development (Vizcay-Barrena et al., 2006; Yang et al., 2007; Ito et al., 2007). Another interesting case is the *dysfunctional tapetum1* mutant (*dyt1*), which exhibits defective tapetum development (Zhang et al., 2006).

Recently, a mutation has been identified, which is essential for not only male gametophyte development, but also for embryo and root growth in *Arabidopsis* (Cascales-Miñana et al., 2013). This mutation is related with a pathway of serine biosynthesis, the so-called phosphorylated pathway of serine biosynthesis (PPSB), which will be introduced later.

1.2 Plant metabolism

Plant metabolism is understood as the entire multitude of interrelated biochemical reactions that take place in cells. Plant metabolism can be divided into primary and secondary metabolism. As its name indicates, primary metabolism (PM) is essential for survival and is not only ubiquitously present in all plant cells from all species, but also occurs in the cells of animals, fungi and bacteria. It provides building blocks of sugars, amino acids, nucleotides, lipids and energy sources, and its metabolic pathways include processes like photosynthesis, respiration, mineral acquisition or glycolysis (Arabidopsis Genome Initiative, 2000).

Apart from producing primary metabolites, plants also have a secondary metabolism (SM) that produces a vast range of metabolites, many generated

exclusively by specific plant species or taxa. These metabolites are not essential for plant survival, but play a key role in maintaining plant fitness as they function in the protection of plants against microbial (fungi and bacteria) and viral infections, herbivory, ultraviolet radiation, attraction of pollinators, allelopathy and signaling. They are divided into four groups: phenolic compounds, terpenoids, alkaloids and glucosinolates.

Both primary and secondary metabolisms are coordinated through transcription factors (TF) that regulate the simultaneous expression of their genes. In recent years, it became apparent that many TFs also coordinate the transcriptional activation of SM genes with the expression of the genes in the upstream pathways of PM, which serve as precursors for the synthesis of specific metabolites (Aharoni et al., 2011). In addition to transcriptional regulation, metabolism is controlled at two levels: by mechanisms that modulate the activities of the enzymes that catalyze the reactions of a metabolic pathway or by the compartmentation of that pathway into different organelles, such mitochondria, vacuoles or plastids.

1.2.1 Plastids

One of the most remarkable features in plant cells is the presence of plastids. These organelles arise as a result of an endosymbiotic event in which a primitive eukaryotic host engulfed an early photosynthetic cyanobacterium (Wise, 2006). All plastids are surrounded by a double envelope whose composition reflects their bacterial origin: the outer membrane, made of galactolipids and β-barrel proteins, which acts as a barrier to movement of proteins, and the inner membrane, a peptidoglycan barrier to small metabolites (Facchinelli et al., 2011).

Once the engulfment of the cyanobacterium has taken place, the events that occur at the interface between the endosymbiont and the host are of crucial importance for plastid establishment. In order to take advantage of the metabolic entity that has been adquired, the host cell inserts protein translocators into the inner envelope. Thus, translocators become essential for the coordination of the flux of the precursors and products between the plastid and other cellular compartments (Facchinelli et al., 2011). There are many types of translocators depending on the substance they translocate, but only plastidic phosphate translocators are referred to herein.

1.2.1.1 Plastidic phosphate transclocators

This family of transporters is encoded in the nuclear genome and has a plastidial location signal at the N-terminal position (Flugge, 1999). This family has different members that catalyze the exchange of phosphorylated C3-,C5- and C6-compounds for inorganic phosphate (Pi). This equilibrated exchange guarantees a balance in the phosphate content of the stroma and the cytosol, and ensures constant phosphate provision to sustain adenosine 5'-triphosphate (ATP) synthesis (Weber et al., 2005). One of the members of this family is glucose 6-phosphate/phosphate translocator, or GPT, which is expressed in non-green tissues and mediates the import of glucose 6-phosphate (Glc6P), as well as triose phosphates (TPs) and 3-PGA (Facchinelli et al., 2011).

Other members of this family are: i) the xylulose 5-phosphate/phosphate translocator, or XTP, which is able to transport Pi, TP, 3-PGA and xylulose 5-P (Xul 5-P); ii) phosphoenolpyruvate/phosphate translocator, or PPT, which mediates the import of cytosolic phosphoenolpyruvate (PEP) to the

plastid stroma in exchange for Pi. However, the first copy of deoxyribonucleic acid (cDNA) to encode a plastid envelope metabolite transporter was the triose phosphate/phosphate translocator or TPT (Flugge, 1999; Flugge et al., 1989), the transporter in charge of export TP (dihydroxyacetone phosphate and glyceraldehyde 3-phosphate) and 3-PGA as substrates in the counter exchange of Pi via a strict 1:1 mechanism (Facchinelli et al., 2011). TPT shows the highest 3-PGA transport specificity of all the plastidial transporters studied (Fischer et al., 2002).

This translocator is formed by 400-450 amino acids, with a 5-8 hydrophobic transmembrane α-helix. According to microarrays experiments, TPT is abundantly expressed in leaves, but poorly expressed in roots. (http://bar.utoronto.ca/efp/cgi-bin/efpWeb.cgi; (Winter et al., 2007).

Although the function of TPT in photosynthetic cells has been convingcingly demonstrated, its activity in heterotrophic organs, such as roots, has been questioned.

1.2.1.2 Types of plastids

Their classification into different types is based on their internal structure and origin. All plastids are derived initially from small undifferentiated plastids termed proplastids, found in dividing cells in meristems (Wise, 2006). However during cell differentiation, proplastids differentiate into several types according to the type of cell in which they reside, their storage components and their internal structures to perform different functions in plant cells (Table 1.2; Pyke, 2010).

Table 1.2. Summary of plastids forms and functions. Source: Wise (2006).

Plastid type	Functions(s)	Distinctive features
Muroplast	Photosynthesis	Walled chloroplast found in Glaucocystophytic algae; wall similar to that found in prokaryotes
Rhodoplast	Photosynthesis	Red chloroplast of the Rhodophytes; photosynthetically competent at depths up to 268m
Proplastid		
Germinal	Source of other plastids	Found in egg, meristematic and embryonic cells; source of all other plastids in the plant
Nodule	N2 assimilation	Site of the glutamate synthetase (GOGAT) cycle in nitrogen-fixing root nodules
Etioplast	Transitionary stage	Develops in dark-grown tissue; site of gibberellin synthesis; converts into chloroplast in light
Leukoplasts		
Amyloplast	Starch synthesis and storage	Also functions in gravisensing
Elaioplast	Oil synnthesis and storage	Supplies lipids and oils to excine upon pollen grain maturation
Proteinoplast	Protein synthesis and storage?	May not be a functional subcategory; most protein stored in rought endoplasmic reticulum (RER)-derived seed storage bodies
Chromoplast	Fruit and flower coloration	Rich in carotenoids; used to attract pollinators and seed/fruit-dispersing animals
Gerontoplast	Catabolism	Controls the dismantling of the photosynthetic apparatus during senescence
S-type plastid	Unknown-starch storage?	Found in phloem sieve tubes, relevant in systematics of many plant taxa
P-type plastid	Unknown-defense?	Found in phloem sieve tubes; systematically relevant; rupture upon damage to sieve tube cell
Kleptoplast	Photosynthesis	Stolen from algal cells by sea slugs; functionally active for lifetime of slug (up to nine months)
Apicoplast	Unknown	Found in parasitic worms that cause malaria; drugs that target apicoplast reduce infectivity
Chloroplast		
algal	Photosynthesis	Probably serves many of the same functions as tracheophyte chloroplasts
C3	Photosynthesis	Also functions in fatty acid, lipid, amino acid and protein synthesis, N and S assimilation
C4	Photosynthesis	Dimorphic chloroplasts provide a CO2-rich, O2-poor environment for enhanced Rubisco activity
Sun/shade	Photosynthesis	Dimorphic forms develop under different light conditions in order to optimize photosynthesis
Guard Cell	Stomatal functioning	Senses light and CO2; signals and metabolically drives opening and closing of stomata

By far the best studied of these plastid differentiation pathways is the biogenesis of chloroplasts during leaf mesophyll cell differentiation (Pyke, 2010).

Plastids have retained a semi-autonomous character as their own genome continues to be formed by a circular DNA with a few genes that code for a small number of polypeptides, the expression of which needs to be directed by the nucleus (López-Juez, 2007). However, their essential proteins are encoded in the nucleus, translated in the cytosol, imported into the organelle and targeted to one of its suborganellar compartments. Plastids also need to grow and multiply to keep pace with their 'host' cells, and their number increases by binary fission. The coordination between the nucleus and plastid is ensured because plastids 'report' on their physiological status to the nucleus of the cell by retrograde signaling (López-Juez, 2007).

1.2.1.2.1 Chloroplasts

The chloroplast is the most-widely studied photosynthetic organelle of algal and plant cells (Wise, 2006). Chloroplasts are rich in photosynthetic pigment chlorophyll and look like lens-shaped organelles of about 5-10 μm in diameter. Their protein-rich, semigel aqueous interior, called stroma, contains the enzymes of the Calvin-Benson cycle. The stroma may contain plastoglobuli, which are lipid/protein particles whose number and size increase during senescence (Wise, 2006). The chloroplast also contains the photochemical apparatus within a distinctive internal membrane organization of thylakoid discs (Neuhaus et al., 2000b).

The main function of chloroplasts is to supply the cell with fixed carbon and energy as a result of photosynthetic carbon assimilation. Carbon dioxide assimilation is done in the stroma through a cycle of reactions known as the Calvin-Benson-Bassham (CBB) cycle, or reductive pentose phosphate cycle, discovered in 1950 by Melvin Calvin, Andrew Benson and James Bassham at the University of California, Berkeley (Raines, 2003). This cycle can be divided into three stages: carboxylation, reduction and regeneration.

In the carboxylation step, the most abundant protein on the planet, Ribulose-1,5-*bis*phosphate carboxylase/oxygenase (RuBisCO), catalyzes the combination of three molecules of CO_2 with three molecules of five-carbon compound ribulose 1,5-biphosphate to obtain six molecules of 3-PGA. Then in the reduction step, these six molecules are reduced to three-carbon sugars, the TPs, glyceraldehyde 3-phosphate (GAP) and dihydroxyacetone phosphate (DHAP), through the consumption of six ATP and reductant in the form of six nicotinamide adenin phosphate (NADPH). Finally in the regeneration step, five molecules of these TPs are required for the regeneration of three molecules of ribulose 1,5 biphosphate with the consumption of three ATP to maintain the supply of substrate in the carboxylation stage. One out of six molecules of TP can be exported out of the chloroplast for the synthesis of sucrose through the activity of a TPT, located in the inner envelope of the chloroplast (Raines, 2003).

However, chloroplasts do not only carry out photosynthesis, but are central hubs in plant metabolism (Neuhaus et al., 2000a). For instance, they manufacture fatty acids, aromatic and nonaromatic amino acids for protein synthesis, plant secondary metabolites, purine and pyrimidine bases, isoprenoids and tetrapyrroles, like haem and chlorophylls, and even possess

a plastidial glycolytic pathway, which runs in parallel to the cytosolic one (López-Juez, 2007).

1.2.2 Glycolysis

A major challenge of studying plant metabolism is to understand how metabolic networks are interconnected. To this end, gaining knowledge concerning the spatial and temporal organization of metabolism both within cells and among different cell types is necessary to achieve such a goal.

One of the processes of great importance in primary metabolism is the respiratory pathway, that provides energy and building blocks for anabolism (Fernie et al., 2004). The respiratory pathway includes the glycolysis, the tricarboxylic acid cycle (TCAC) or Krebs cycle and the mitochondrial electron transport chain. Concretely, glycolysis is widely present in all living cells of nearly every kind and description -prokaryotic and eukaryotic- and was the first major biochemical pathway to be well characterized (Givan, 2007). Plant glycolysis is a complex process that occurs in both the cytosol and plastids (Figure 1.3; Muñoz-Bertomeu et al., 2009). It consists in the oxidation of a hexose to produce an organic acid (pyruvate), releasing a small amount of ATP and reducing power as nicotinamide adenine dinucleotide (NADH) as described in the following equation:

$$\text{glucose} + 2\ \text{ADP} + 2\ \text{Pi} + 2\ \text{NAD}^{+} \rightarrow 2\ \text{pyruvate} + 2\ \text{ATP} + 2\ \text{NADH}.$$

In addition to oxidizing hexoses to generate ATP, reducing power and pyruvate, glycolysis is the predominant pathway that "fuels" the TCAC in

mitochondria, and is a major source of precursors for secondary metabolism, amino acid, and fatty acid biosynthesis (Plaxton, 1996).

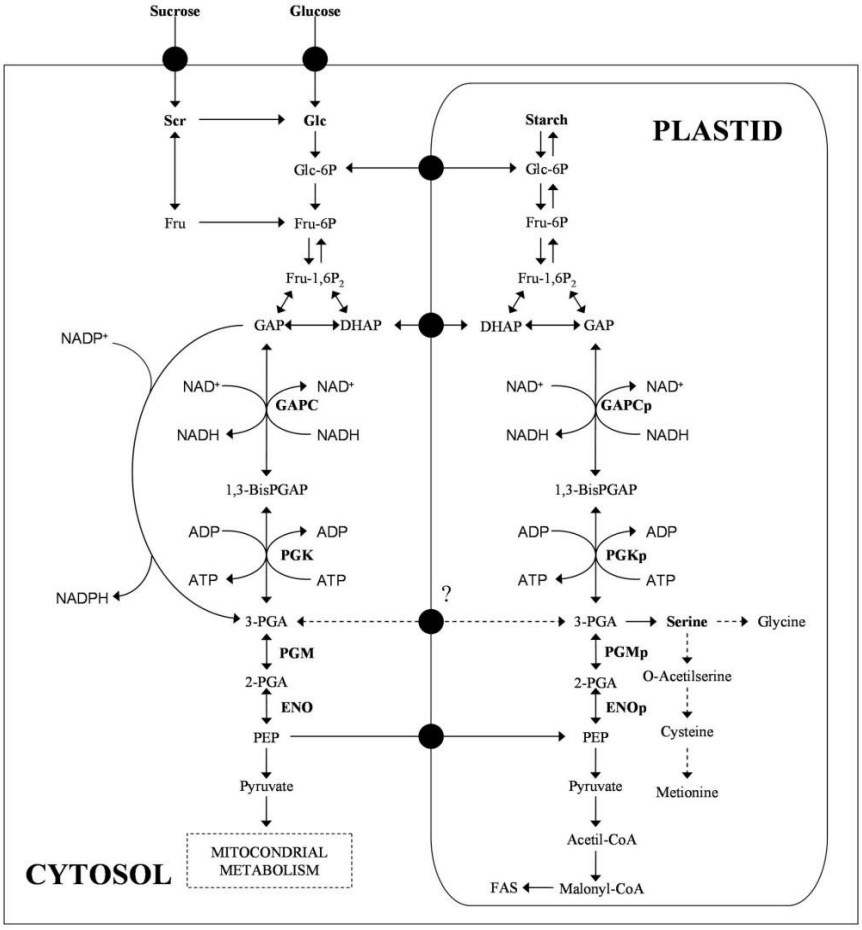

Figure 1.3. Schematic representation of glycolysis in a plant cell. Emphasis is given to the plastidic and cytosolic glycolytic reactions catalyzed by GAPDH (GAPC, cytosolic isoform; GAPCp, plastidial isoform) and phosphoglycerate kinase (PGK, cytosolic isoform; PGKp, plastidial isoform). 1-3BisPGAP, 1,3-Bisphosphoglycerate; DHAP, dihydroxyacetone phosphate; ENO, enolase; FAS, fatty acid synthesis; 2-PGA, 2-phosphoglycerate; PGM, phosphoglycerate mutase. Broken lines indicate several enzymatic reactions. Source: (Munoz-Bertomeu,J. 2009).

It is assumed that the cytosolic and plastid glycolytic pathways participate in the generation of specific products. However, the relative contribution and the degree of integration of both pathways in different cell types, such as photosynthetic or heterotrophic cells, is not well-known. Cytosolic and plastidic glycolytic intermediates have been suggested to be fully equilibrated in both compartments through the highly selective transporters present in the inner plastid membrane (Weber et al., 2005). Because of this, it is difficult to define the role of each glycolytic enzyme and pathway in the primary metabolism of plant cells using only biochemical approaches. Direct molecular or genetic evidence corroborating the *in vivo* contribution of glycolytic enzymes to specific functions is generally lacking. Thus in order to understand glycolytic networks, it remains necessary to (i) identify all the functionally important glycolytic isoforms, (ii) define in which cell types they are active, and (iii) to determine whether or not specific glycolytic intermediates are in equilibrium between the cytosol and plastids.

1.2.2.1 Glycolytic enzymes

In recent years, important advances have been made in the characterization of plastidial glycolytic enzymes (Andre et al., 2007; Baud et al., 2007; Chen et al., 2010). For example, it has been demonstrated that pyruvate kinase plays an important role in seed oil biosynthesis (Andre et al., 2007; Baud et al., 2007; Chen et al., 2010), while triose-phosphate isomerase, is essential for the post-embryonic transition from heterotrophic to autotrophic growth (Chen et al., 2010). However, mutants in plastidial enolase (ENO) and phosphoglycerate mutase (PGM) do not show evident phenotypic alterations

and it has therefore been postulated that they do not play a major role in plant metabolism (Andriotis et al., 2010; Prabhakar et al., 2010). The presence of a complete plastidial pathway, at least in some cell types, has even been questioned (Andriotis et al., 2010; Prabhakar et al., 2010; Van der Straeten et al., 1991). When taken together, these studies underline that the functions of plastidial glycolytic enzymes are very much cell type specific.

1.2.2.1.1 The glyceraldehyde-3-phosphate dehydrogenase

The glyceraldehyde-3-phosphate dehydrogenase (GAPDH) reversibly converts GAP into 1,3-bisPGAP coupled with the reduction of NAD^+ to NADH (Figure 1.3). Four genes coding for glycolytic phosphorylating GAPDHs, two that code for cytosolic (*GAPC1* and *GAPC2*), and two for plastidial (*GAPCp1* and *GAPCp2*) isoforms, have been identified and functionally characterized in Arabidopsis (Muñoz-Bertomeu et al., 2009; Guo et al., 2012). The double knock-out mutants of GAPCps isoforms (*gapcp1gapcp2*) display a drastic developmental phenotype while cytosolic knock-out mutants grow normally under non stress conditions (Guo et al., 2012). In addition, an antisense approach in potato concluded that diminished GAPC activities did not produce major changes in either whole-plant or tuber morphology and that the enzyme plays a minor role in the regulation of metabolism (Hajirezaei et al., 2006). These results demonstrate that, in spite of their low gene expression level as compared to cytosolic isoforms, plastidial GAPCps play an important role in plant function. *Arabidopsis gapcp1gapcp2* mutant displays a phenotype of arrested root development, dwarfism, and male sterility, alongside modifications in the

sugar and amino acid balance (Muñoz-Bertomeu et al., 2009; Muñoz-Bertomeu et al., 2010; Anoman et al., 2015).

It has additionally been demonstrated that *gapcp1gapcp2* roots display an L-Serine (Ser) deficiency and that supplementation of L-Ser to the growth medium rescues root growth in the mutants (Muñoz-Bertomeu et al., 2009). We previously hypothesized that lack of GAPCps in roots could affect the supply of 3-PGA to the PPSB. Functional characterization of the PPSB corroborated that it is indeed essential for *Arabidopsis* root development (Cascales-Miñana et al., 2013; Benstein et al., 2013). These results were unexpected and are controversial since they suggest that 3-PGA pools are not in equilibrium between the cytosol and plastids, at least not in heterotrophic cells. Theoretically, the plastidic glycolytic enzymatic reactions between the TPs pool (GAP and DHAP) and PEP are reversible (Figure 1.3, Buchanan et al., 2002). Thus the PEP transported from the cytosol could be converted into 3-PGA through the reactions catalyzed by the ENO and PGM (Figure 1.3). In addition, several members of the plastid phosphate translocator family could equilibrate the 3-PGA pools between the cytosol and plastids (Flügge, 1999; Fischer et al., 2002; Fischer, 2011; Knappe et al., 2003). Accordingly, it could be assumed that the cytosolic and plastidial glycolytic pathways are connected by metabolite exchange (Weber et al., 2007). In order to test the hypothesis that lack of GAPCps in roots could affect the supply of 3-PGA to plastids, we overexpressed the TPT in *gapcp1gapcp2* roots. We provide genetic evidence that TPT expression in *gapcp1gapcp2* root plastids complements phenotypic and metabolic alterations of the mutant. These results suggest that the

endogenous TPT is inactive in heterotrophic plastids, and that the main source of 3-PGA in these plastids is provided by the reactions catalyzed by the enzymes GAPCp and phosphoglycerate kinase (PGKp). They also suggest that other phosphate transporters typically expressed in heterotrophic cells do not have the capacity to mediate 3-PGA transport.

1.2.3 The importance of serine in plants

The amino acid L-Ser is essential for the synthesis of proteins and other biomolecules required for cell proliferation, including nucleotides and Ser-derived lipids such as phosphatidyl Ser and sphingolipids. Besides its participation in metabolism, additional nonmetabolic functions for Ser have been described in mammals and plants. In mammals, the *de novo* synthesis of L-Ser is essential in the development and function of the central nervous system (Yoshida et al., 2004). Furthermore, L-Ser is the precursor of D-Ser, a well-documented neuromodulator (Mothet et al., 2000). Similarly, in plants, D-Ser has recently been attributed a signaling role in male gametophyte-pistil communication (Michard et al., 2011).

1.2.3.1 Biosynthetic pathways of serine

Ser biosynthesis in plants proceeds via different pathways (Figure 1.4). One is the glycolate pathway, which takes place in mitochondria and is associated with photorespiration (Tolbert, 1980; Tolbert, 1997; Douce et al., 2001; Maurino et al., 2010; Bauwe et al., 2010). Additionally, alternative nonphotorespiratory mechanisms of Ser biosynthesis have been postulated. In quantitative terms, Ser production through the glycolate pathway is considered to be the most important, at least in photosynthetic cells (Tolbert,

1980; Douce et al., 2001). In this pathway, two glycine (Gly) molecules are converted into one molecule of Ser in a reaction catalyzed by two enzymes, the Gly decarboxylase complex and the Ser hydroxymethyltransferase (SHMT) (Figure 1.4). Since the glycolate pathway is associated with photorespiration, it should be active mainly in green tissues during daylight hours. It therefore follows that alternative pathways of Ser biosynthesis may be required in the dark and/or in nonphotosynthetic organs. However, the biological significance of the coexistence of several Ser biosynthetic pathways in plants is still not understood.

A nonphotorespiratory pathway, the so-called Glycerate pathway, synthesizes Ser by the dephosphorylation of 3-PGA (Figure 1.4 Kleczkowski, et al., 1988). This pathway includes a reversed sequence of reactions from a portion of the oxidative photosynthetic carbon cycle linking 3-PGA to Ser (3-PGA to Glycerate to hydroxypyruvate to Ser), with these reactions catalyzed by enzymes such as 3-PGA phosphatase, glycerate dehydrogenase, Alanine-hydroxypyruvate aminotransferase, and Gly hydroxypyruvate aminotransferase. The existence of enzymatic activities of this pathway in plants has been demonstrated (Kleczkowski et al., 1988). However, the extent to which this pathway could be functional in plants is as yet unknown, and genes coding for the specific enzymes of the pathway have not been cloned and/or characterized.

But there is still a second nonphotorespiratory pathway, the PPSB, which synthesizes Ser via phosphoserine from 3-PGA as a precursor (Handford et al, 1958).

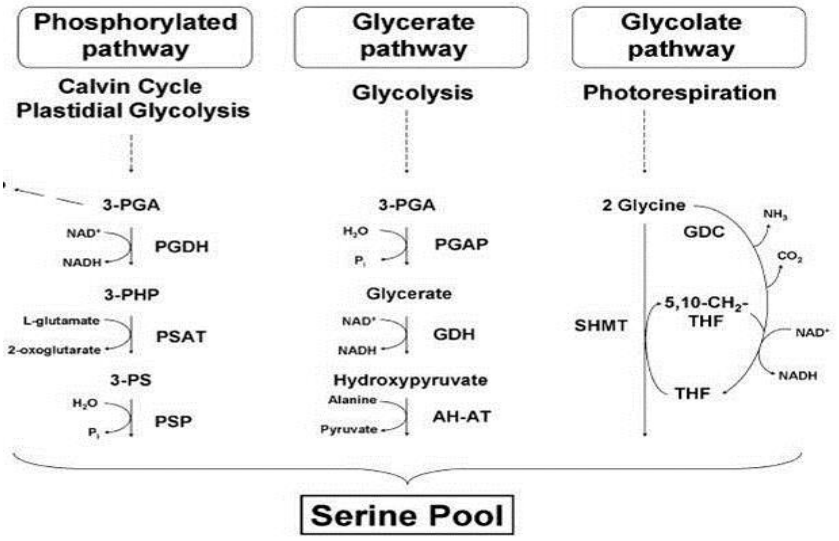

Figure 1.4. Schematic representation of Ser biosynthesis in plants. The enzymes participating in each Ser biosynthetic pathway are listed separately. Photorespiratory pathway (glycolate pathway): GDC, Gly decarboxylase; SHMT, Ser hydroxymethyltransferase. Glycerate pathway: PGAP, 3-phosphoglycerate phosphatase; GDH, glycerate dehydrogenase; AH-AT, Ala-hydroxypyruvate aminotransferase. Phosphorylated pathway: PSAT, 3-phosphoserine aminotransferase; PSP, 3-phosphoserine phosphatase. Abbreviations used for metabolites are as follows: 3-PHP, 3-phosphohydroxypyruvate; 3-PS, 3-phosphoserine; THF, tetrahydrofolate; 5,10-CH2-THF, 5,10-methylene-tetrahydrofolate. Source: (Cascales-Miñana et al,.2013).

Synthesis of amino acids takes place mainly in mature roots and source leaves, which export nitrogen through the phloem-xylem system to supply sinks, such as flowers and seeds (Lam et al., 1996). Specifically, Ser is easily transported through the phloem (Riens et al., 1991). This would imply that the Ser synthesized in photosynthetic cells through the photorespiratory pathway could be supplied to nonphotosynthetic organs. Similarly, Ser synthesized through nonphotorespiratory mechanisms in roots could contribute to the amino acid supply to sinks such as seeds and flowers. However, the relevance of each Ser biosynthetic pathway in different organs and under different environmental conditions remains to be defined.

1.2.3.1.1 Phosphorylated pathway of Ser biosynthesis (PPSB)

Supporting evidence for the PPSB in plants derives from the isolation and characterization of the enzyme activities of this route (Slaughter et al., 1968). This pathway, which is conserved in mammals and plants, defines a branch point for 3-PGA from glycolysis and involves three enzymes catalyzing sequential reactions: 3-phosphoglycerate dehydrogenase (PGDH), 3-phosphoserine aminotransferase (PSAT) and 3-phosphoserine phosphatase (PSP) (Figure 1.4). In humans, the PPSB plays a crucial role in cell proliferation control. This pathway can divert a substantial fraction of the glycolytic flux (carbon metabolism) into Ser biosynthesis (nitrogen metabolism) and can contribute to cell proliferation and oncogenesis (Bachelor et al., 2011; Locasale et al., 2011; Pollari et al., 2011; Possemato, 2011). For instance, an enhanced PPSB results in an increased cell proliferation rate, which is associated with certain breast cancers (Locasale et al., 2011; Possemato, 2011). By contrast, downregulation of the PPSB causes a restriction in tumor cell proliferation (Possemato, 2011). Unlike in mammals, the functional significance of the PPSB in plants has not been started to be elucidated till very recently. Some genes of the pathway were cloned and the enzymes that they encode were biochemically characterized in *Arabidopsis thaliana* years ago (Ho et al., 1998; Ho et al., 1999a; Ho et al., 1999b; Ho et al., 2001). But only recently the genetic evidence for the physiological functions of this pathway was provided (Cascales-Miñana et al., 2013; Toujani et al., 2013; Benstein et al., 2013). Interestingly, the metabolites that are produced in this pathway could be connected to other metabolic pathways that are of paramount importance for the plants, like

sulfur assimilation and ammonia assimilation through the glutamine (Gln) synthetase/Glu synthase (GS/GOGAT) pathway.

1.2.4 Sulfur assimilation

In nature, sulfur is available as both in inorganic and organic forms, but plants assimilate it primarily in the form of anionic sulfate (SO_4^{-2}) (Takahashi, 2010). Briefly, sulfur assimilation occurs as described in Figure 1.5. The transport of sulfate across the plasma membrane occurs with protons at a ratio of SO_4^{-2} 1:3 H^+ (symport) and is driven by a proton gradient maintained by a proton ATPase (Leustek et al., 1999; Droux, 2004). In *Arabidopsis* there are 12 sulfate co-transporter-like genes, divided into four groups (AtSultr1-4)(Droux, 2004). Once sulfate is inside, the high potential needed for sulfate reduction is surmounted by an activation step, catalyzed by sulfate adenosyltransferase (ATPS, a small family of four genes in *Arabidopsis*) to produce adenosine 5'-phosphosulfate (APS) in the presence of ATP. Furthermore, APS is also further phosphorylated to adenosine 3'-phosphate 5'-phosphosulfate (PAPS) by an APS kinase.

Then activated sulfate APS must be reduced to sulfide. Finally the last step is the incorporation of sulfur into the synthesis of the first thiol-containing aminoacid, cysteine (Cys). This final reaction involves two enzymes: the first is serine acetyltransferase (SAT), which catalyzes the synthesis of carbon–nitrogen precursor *O*-acetylserine (OAS) from L-serine and acetyl-CoA. The second enzyme, an *O*-acetylserine (thiol) lyase (OASTL), catalyzes the synthesis of Cys from OAS and H_2S (Droux, 2004). By means of this pathway, plants assimilate sulfate through different steps from the intial uptake until the incorporation of sulfur into Cys, the end product of

the reductive pathway and the starting material for production of methionine (Met), glutathione, and other metabolites that contain reduced sulfur (Leustek et al., 1999).

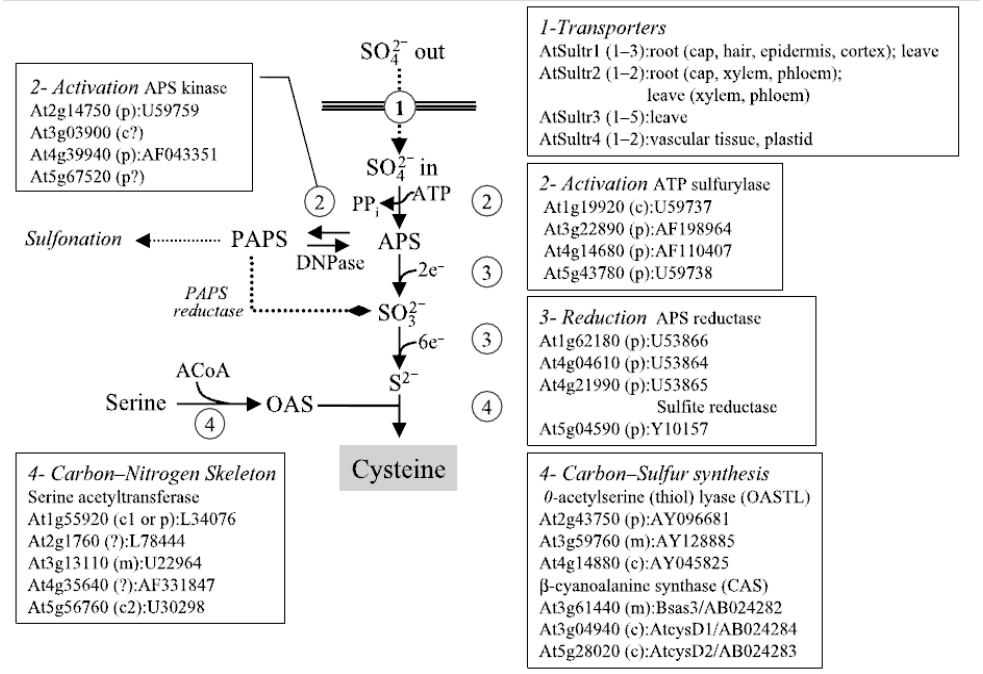

Figure 1.5. The *Arabidopsis* gene family for the sulfate assimilatory pathway and the synthesis of Cys. C,cytosol; m, mitochondria; p, plastid. Source: Droux (2004)

1.2.5 Ammonium assimilation

Some pathways like the nitrate assimilation or the photorespiration generate ammonium (NH_4^+) and the accumulation of this metabolite produces toxicity. The strategy of the plants is basically described as shown in Figure 1.6. NH_4^+ is assimilated into Glu through the action of GS to produce Gln with ATP consumption. When Gln accumulates, GOGAT transfers the amide group of Gln to 2-oxoglutarate to yield two molecules of Glu.

Molecules of 2-oxoglutarate are produced by PSAT of the PPSB, so this pathway provides the GS/GOGAT pathway (GOGAT) with this molecule, which uses 2-oxoglutarate as a co-substrate along with Gln to produce Glu (Lancien et al., 2000).

In that way and in order to avoid its harmful effects, plants convert NH_4^+ into aminoacids by the sequential actions of these two enzymes, the GS and the GOGAT, forming the GS/GOGAT pathway (Masclaux-Daubresse et al., 2006).

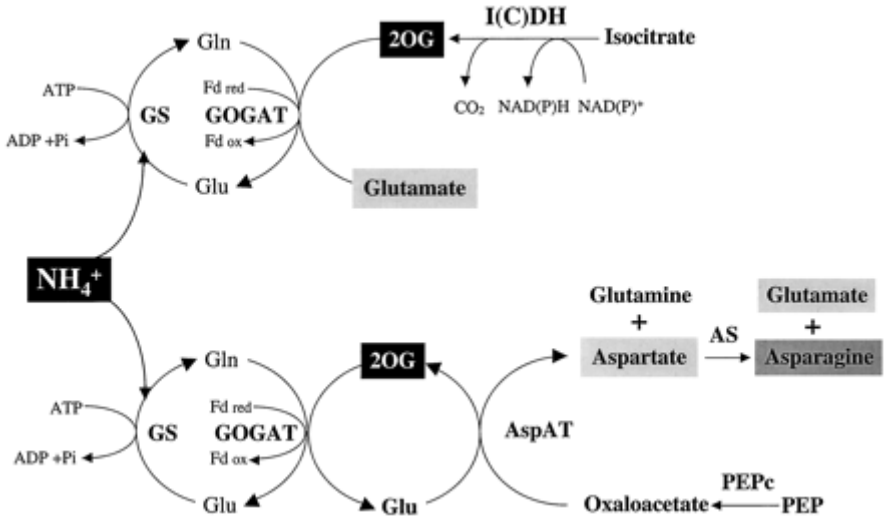

Figure 1.6. Primary amino acid synthesis by the GS/GOGAT cycle in plants. Ammonium is almost exclusively assimilated by the GS/GOGAT pathway. This requires energy, reductant, and C skeletons in the form of 2OG. This organic acid can be synthesized either by an isocitrate dehydrogenase, I(C)DH, or an AspAT. The I(C)DH origin allows for a direct net synthesis of Glu. On the other hand, the AspAT origin produces 2OG at the expense of Glu (no net synthesis) leading to the production of Asp from OAA synthesized via PEPc. The Asp can be used to produce Asn in a reaction carried out by Asn synthase (AS). Source: Lancien, 2000.

2. OBJECTIVES

This thesis is part of a project whose main goal is to unravel the role and contribution of plastidial glycolysis and the PPSB to plant metabolism and development. The specific objectives of this thesis are:

1) An in deep analysis of the role of the PSP enzyme in embryo and pollen development of *Arabidopsis*.

2) To elucidate the metabolic and transcriptomic targets of PSP activity.

3) To corroborate our hypothesis stating that lack of GAPCp in heterotrophic cells could affect the supply of 3-PGA to plastids.

4) To demonstrate that 3-PGA levels are not in equilibrium between the cytosol and the plastid of heterotrophic cells.

3. MATERIALS AND METHODS

3.1 Biological material

3.1.1. Arabidopsis thaliana

This thesis has been developed in the model organism *Arabidopsis thaliana*. Seeds ecotype Columbia-0 were supplied by the European Arabidopsis Stock Centre (Scholl et al., 2000) and by the Arabidopsis Biological Resource Center (ABRC, http://www.biosci.ohio.sate.edu). *gapcp1* (corresponding to *gapcp1.1* allele, SAIL_390_G10) and *gapcp2* (corresponding to the *gapcp2.1* allele, SALK_132788) single and double T-DNA mutant isolation and characterization were described by (Muñoz-Bertomeu et al., 2009) TPT mutant (*ape2*) was kindly provided by Dr. Flügge (University of Cologne). Mutants of the phosphoserine phosphatase (*psp1.1.psp1.1*) overexpressing a cDNA coding for the enzyme PSP1 under the control of the *35S* promoter (*psp1.1.psp1.1 35S:PSP1*), (Cascales-Miñana et al., 2013) were used for the siliques, embryo and pollen developmental analysis by transmission electron microscopy and Hoechst staining. For transcriptomic and metabolomic profiling, the line *psp1.1.psp1.1 HS:PSP1* (Cascales-Miñana et al., 2013), which expresses *PSP1* under the control of the heat-shock inducible promoter *HSP18.2* from *Arabidopsis* gene At5g59720 (Matsuhara et al., 2000) was used. For auxin measurements WT lines in which *PSP1* was down-regulated by an artificial microRNA (*amiRNA PSP*)(Cascales-Miñana et al., 2013) was used together with a WT with the construction *DR5:GFP* (courtesy of Dr. Krüger, University of Cologne, Germany) in order to detect the presence of auxins in specific places of the roots.

3.1.2. Bacterial strains

3.1.2.1 *Escherichia coli*

For the maintenance and obtainment of new plasmids it was necessary the use of the following *Escherichia coli* strains:

- **DH5α**: F- Φ80*lac lac*ZYA-*arg*F)U169 *rec*A1 *end*A1 *hsd*R17(rk-, mk+) *pho*A *sup*E44 *thi*-1 *gyr*A96 *rel*A1 λ-.

- **TOP10**: F- *mcr*A Δ(*mrr-hsd*RMS-*mcr*BC) Φ80*lac*ZΔM15 Δ*lac*X74 *rec*A1 *ara*D139 Δ(*ara-leu*) 7697 *gal*U *gal*K *rps*L (StrR) *end*A1 *nup*G λ-.

3.1.2.2 *Agrobacterium tumefaciens*

For the transformation of Arabidopsis it was used the strain *Agrobacterium tumefaciens* GV3101, which is rifampicin resistant. This strain contains the binary plasmid pMP90, which provides gentamicine resistance, and the helper plasmid pSoup, that provides resistance to tetracycline (Koncz C, 1986; Hellens et al., 2000).

3.1.3 Growth media and conditions

3.1.3.1 *Arabidopsis thaliana*

3.1.3.1.1 *Seed sterilization*

Seeds were placed in 1.5 ml vial (Eppendorf) and then washed following two steps of 1 ml of 70% ethanol and 0.05% SDS (SIGMA, Ref. 1667289) for 15 minutes in constant shake. Afterwards, the washing solution was removed and 1 ml 70% ethanol was added. Seeds were placed in constant shaking for 5 minutes. Finally, seeds were taken to a sterile laminar flow hood and placed in a sterile paper to dry. After the evaporation of the alcohol, the seeds were ready for sowing.

3.1.3.1.2 *In vitro growth*

Seeds were sterilized and sown on 0.8% (w/v) agar plates containing one-fifth-strength Murashige and Skoog (MS) medium with Gamborg vitamins buffered with 0.9 g/l MES (adjusted to pH 5.7 with Tris). After a 4 day treatment at 4ºC, seeds were placed in a growth chamber (Sanyo; MLR-351H) at 22ºC with a 16-hours-day/8-hours-night photoperiod at 100 mmol $m^{-2} \cdot s^{-1}$.For the selection of the transgenic plants, half-strength MS plates supplemented with 0.5% sucrose and appropriate selection markers were used. Where indicated, a 37ºC heat-shock (HS) treatment for 45 minutes was applied to the conditional mutant *psp1.1.psp1.1 HS:PSP1* mutants was 45 min at 37ºC. Some plates were supplemented with 0.1 mM Ser, the

optimal concentration of Ser that was previously determined for *gapcp1gapcp2* (Muñoz-Bertomeu et al., 2009).

3.1.3.1.3 *Greenhouse growth*

Seeds were grown in 200 ml plastic pots filled with vermiculite (ASFALTEX) and moist Kekkila substrate (enriched with macronutrients N-P-K 15-10-20, KEKKILÄ IBERIA) in 1:1 rate. Seeds were sown at the density required by the experiment, normally 3 per pot. After sowing, the trays where the pots were placed were watered and covered with transparent plastic to ensure high humidity and to trigger the germination. Trays were placed in a cold chamber (4ºC) and after 4 days they were placed under the greenhouse staging. Three days later, some holes were made in the transparent plastic to improve the acclimatization process. When the seedlings begin to elongate, the whole transparent plastic was completely removed and the trays were placed on the greenhouse staging. The watering was done with deionized water according to the hydric stage of the seedlings. Growth conditions consisted of 16h light, 50-70% relative humidity and an average temperature of 24ºC during the day and 17ºC during the night. When necessary, these conditions were supplied with artificial light from sodium and mercury vapor lamps. Cross pollination between plants was avoided by using transparent plastic sleeves, which isolated each pot from its neighbours. Plants were watered until at least 90% of the siliques had dried completely and then, when the leaves become yellowish, the plants were allowed to dry slowly in the greenhouse staging for maximum viable seed production. Seeds were harvested after the whole plants had dried out and stored in envelops at room temperature. Finally,

after a week, seeds were removed from each envelope with the help of several sieves of different size and placed into 1.5 ml vials (Eppendorf).

3.1.3.2 *E. coli* and *A. tumefaciens*

3.1.3.2.1 LB medium

The media Lysogeny Broth or LB (Bertani, 1951), was used as a standard media for the growth of bacteria strains. This media consists on the 1% (w/v) of triptone (PRONADISA, Ref. 1612.00), 0.5% (w/v) yeast extraction (PRONADISA, Ref. 1702.00) and 1% (w/v) NaCl. The pH was adjusted to 7.0 with NaOH before autoclaving.

3.1.3.2.2 SOC medium

The Super Optimal broth with Catabolite repression or SOC media was used in the *E. coli* transformation. The composition of this media is 2% (w/v) of triptone, 0.5% (w/v) of yeast extract, 10 mM NaCl and 2.5 mM KCl. The pH was adjusted to 7.0 with NaOH. After having sterilized the media by autoclaving, 10 mM $MgCl_2$ and 20 mM glucose steril solutions were added to the media.

3.1.3.2.3 Maintenance of the strains

The strains were grown in two different media, liquid or solid, depending on the final purpose and applied protocol. For the liquid media, *E. coli* was grown in Corning® tubes of 15 ml and *A. tumefaciens* in sterile flasks of 250 ml. These cultures were incubated in an orbital incubator (COMECTA,

Ref. 5312090) at 37ºC or 28ºC respectively, and a constant shake speed between 200-250 rpm.

3.2 Isolation and analysis of nucleic acids

3.2.1 Isolation of nucleic acids

3.2.1.1 Genomic DNA extraction

A small leaf of the rosette was placed into a 1.5 ml vial (Eppendorf) and used as starting material. Then the leaf was grinded at room temperature with the help of a plastic pestle till it was completely homogenized. After that it was incubated with 400 µl of extraction buffer [200 mM Tris-HCl pH 8.0, 250 mM NaCl, 25 mM EDTA pH 8.0 and 0.5% SDS] and was shaken vigorously for 5 seconds. The next step was to centrifuge the samples for 1 minute at 13,000 rpm. The supernatant was transferred into a new tube and then 300 µl of cold isopropanol were added to trigger the DNA precipitation. Two minutes later the samples were placed into the centrifuge at 13,000 rpm for 5 minutes, the supernatant was removed by decantation and the pellet was placed at room temperature to dry. After 1 hour, the pellet was resuspended in 100 µl of water and conserved at 4ºC.

3.2.1.2 Isolation of plasmidic DNA

For that purpose the kit ROCHE APPLIED SCIENCE *High Pure Plasmid Isolation Kit* (Ref. 11754785001) was used. As starting material 4 ml of saturated *E. coli* culture was centrifuge at 3,000 rpm for 20 minutes. After that 250 µl of resuspension buffer (50 mM Tris-HCl, 10 mM EDTA pH

8.0) was added to the pellet. Then, 250 µl of lysis buffer (0.2 M NaOH, 1% SDS) was added in order to break membranes and extract nucleic acids. After shaking, 350 µl of ice-cold-binding buffer (4 M Hydrochlorilguanidine and 0.5 M potassium acetate pH 4.2) were added.
The mixture was incubated on ice for 5 minutes and centrifuged at 13,000 rpm for 10 minutes. The supernatant was charged into specific columns provided in the kit and then centrifuged again to allow the plasmidic DNA to bind to the membrane. Afterwards, two washing steps of 500 µl into the column, the first with buffer 1 (5 M Hydrochlorilguanidine, 20 mM Tris-HCl, pH 6.6) and the second one (20 mM NaCl, 2 mM Tris-HCl pH 7.5) were performed. For the final elution of the plasmidic DNA, 50 µl of elution buffer (10 mM Tris-HCl pH 7.5) were added and centrifuged at 13,000 rpm for 1 minute. The eluted plasmidic DNA was stored at -20ºC until its use.

3.2.1.3 RNA extraction

The extraction method employed was a modification of the MACHEREYNAGEL *Total RNA Isolation kit* (Ref. 740955.50).
The starting material was a frozen aliquot of 100 mg of *Arabidopsis* powder tissue previously grinded in a morter. The first step was to add 350 µl of RA1, together with 3.5 µl β-mercaptoethanol. The sample was vortexed and charged into a specific filter-column provided in the kit to centrifuge it at 13,000 rpm for 1 minute. The flow through was transferred into a new 1.5 ml vial and then 350 µl of ethanol 70% were added. The homogenized sample was charged into a new filter-column with special properties to bind nucleic acids, and then centrifuged at 13,000 rpm for 1 minute. After

centrifugation, 350 µl of Membrane Desalting Buffer were charged into the column and then 95 µl of DNAse solution was added for 15 minutes at room temperature. Finally, two washing steps of 200 µl of RA2 and RA3 were performed into the column containing the RNA. The final elution was performed with 40 µl of RNAase-free water.

3.2.2 Quantification of nucleic acids

When only semi-quantitative measures were needed, 1 µl DNA sample plus 5 µl of loading buffer was charged in an agarose gel and the band intensity was compared with the *Lambda DNA/HindIII Marker* (Biotools, Ref. 31.011). For quantitative measurements nucleic acids were mesured spectrophotometrically (NanoDrop) at λ = 260 nm and the purity was calculated through the relation between the absorbance at 260 and 280 nm.

3.2.3 Analysis of nucleic acids

3.2.3.1 Polymerase chain reaction (PCR)

The DNA amplification reactions were performed in 30-100 µl containing: 10-50 ng DNA template (1 µl of the genomic DNA extraction per reaction), 200 µM each dNTP, 0.5 µM each primer, 1X PCR Buffer, 0.12-1 units of Taq polymerase (BIOTOOLS, Ref.10.047) and MilliQ water. It was done in multi plate 96-well (VWR, Ref. 82006-636) or in microtubes of 200 µl (THERMO SCIENTIFIC, Ref. AB-0266). The reaction was performed in the thermal cycler GeneAmp PCR SYSTEM 9600 (APPLIED

BIOSYSTEMS). The standard parameters were: 5 minutes at 94ºC, followed by 35-45 cycles of 1 minute at 94ºC, 45 seconds about 5°C below the lowest melting temperature (Tm) of the pair of primers (Innis et al., 1990) and an amplification round after each cycle of 1 minute/ Kb at 72ºC

Finally, the process ends with a final step of 10 minutes at 72ºC. Then, the temperature is kept at 4ºC till the samples are removed from the thermal cycler. The primers used in this thesis are listed in the Table S1 (see Appendix).

3.2.3.2 Purification of PCR products

The ROCHE APPLIED SCIENCE *High Pure PCR Product Purification Kit* (Ref.11732668001) was used. The volume of the PCR product was adjusted to 100 µl with MilliQ water. After that, 500 µl of binding buffer [3 M guanidinium thiocyanate, 10 mM Tris-HCl pH 6.6 and 5% ethanol (v/v)(25ºC)] were added to the solution, mixed by pipetting and charged into the specific filter-column provided by the kit. Then, the column was centrifuged at 13,000 rpm for 1 minute and the flowthrough was removed. Two washing-steps of 500 µl with buffer (20 mM NaCl and 2 mM Tris-HCl pH 7.5) were done prior eluting the sample with 50 µl of elution buffer (10 mM Tris-HCl pH 8.5) by centrifugation at 13,000 rpm for 1 minute. The elution was stored at -20ºC until its use.

3.2.3.3 Agarose gel electrophoresis

The products of PCR were separated in gels of 0.5X TBE (90 mM boric acid, 90 mM Tris-HCl pH 8.0 and 2 mM EDTA pH 8), 0.8% low electroendosmosis agarose D-1 (PRONADISA, Ref. 8016) and 0.5 µg/ml ethidium bromide. Loading buffer (100 mM Tris-HCl pH 7.5, 0.0075% bromophenol blue, 60% Glycerol and 60 mM EDTA pH 8) was added to the samples. 100 bp (BIOTOOLS, Ref. 31.006) or 1 kb DNA marker (BIOTOOLS, Ref. 31.005) was used at a 0.2 mg/ml to determine the size of the bands.

3.2.3.4 Purification of DNA in agarose gel

The DNA fragments were removed from the agarose gel with a scalpel and put into a 1.5 ml vial. The DNA from the gel was purified by the MACHEREY-NAGEL *PCR clean-up Gel extraction*, *NucleoSpin® Extract II kit* (Ref. 740609.50). Basically, the NT buffer was added to the vial in a ratio 200 µl of NT:100 mg of agarose gel. The sample was incubated at 50ºC till the gel was completely melted and then, all the solution was charged into a filter column provided by the kit with a membrane that binds the DNA. After a centrifugation step of 13,000 rpm for 1 minute, the flowthrough was removed and the membrane was washed by 2 times with 700 µl of NT3 solution followed by a centrifugation at 13,000 rpm for 1 minute. Finally, the DNA was eluted from the silica membrane with 50 µl of Elution buffer and stored at -20ºC until it was used.

3.2.3.5 DNA digestion by endonucleases

The digestion of DNA by the restriction enzymes was performed following the protocols provided by the TAKARA and ThermoScientific providers. Normally, it was used between 1-5 units for each µg of DNA to digest.

3.2.3.6 DNA ligation

The DNA ligation was performed using 1 U of the T4 DNA Ligase (INVITROGEN, Ref. 15224-041) per each 10 µl of reaction volume. For the ligation of the fragments, it was used between 10-20 ng of insert maintaining a 1:3 molar relationship (vector:insert). The incubation was performed at least 16h at 16ºC.

3.2.3.7 DNA sequencing

All constructions were verified by sequencing in the "Servicio de Secuenciación de DNA y Proteínas del Servicio Central de Soporte para la Investigación Experimental (SCSIE) de la Universidad de Valencia". The comparison between sequences was performed by BLAST (*Basic Local Alignment Search Tool*, http://blast.ncbi.nlm.nih.gov/Blast.cgi).

3.2.4 Gene expression analysis

3.2.4.1 cDNA synthesis

In order to perform the gene expression analysis and the cloning of some constructions, cDNA synthesis was carried out. It was used a *Maxima® First Strand cDNA Synthesis Kit for RT-PCR* (Fermentas, Ref. K1641). Basically, between 0.5 and 3 µg of RNA were mixed with 2 µl of reaction buffer (5X Reaction Mix), 1 µl of the Maxima® Reverse Transcriptase and the final volume was completed till 20 µl using RNAase-free water. The reaction mixture was incubated in a termocycler with the following programme: 10 minutes at 25ºC, 30 minutes at 50ºC and finally 5 minutes at 85ºC. Once the programme was finished, 20 µl of MiliQ water were added to the sample and stored at -80ºC till its use.

3.2.4.2 Quantitative RT PCR (qRT-PCR)

With the aim of quantifying the expression levels of mRNA from the genes of interest, the SYBR® Premix Ex Taq™, Perfect Real Time (TAKARA, Ref. RR041A) was used, following the instructions from the supplier. First of all, 0.4 µl of each primer (forward and reverse) of the gene of interest were mixed with 7.8 µl of water per reaction to obtain the primer mixture. Then, a reaction mixture was prepared with 10 µl of SYBR® Premix Ex Taq™ (2X), and 0.4 µl *ROX Reference Dye* per reaction. Once both mixtures were prepared, 8.6 µl of the primer mixture were deposited in each well of an Applied Biosystems ®, MicroAmp® Fast Optical 96-Well Reaction Plate, Ref 4346907. Then, 1 µl of cDNA was charged in each well

and finally, 10.4 µl of the reaction mixture was applied on each well. The analysis by qRT-PCR was done by the GeneAmp® 5700 *Sequence Detection System* (APPLIED BIOSYSTEMS, Ref. PN 4304472), that detects the emitted fluorescence of the SYBER® GREEN I inserted between the double strand of the DNA. The amplification method was as follow: 10 minutes at 95ºC, followed by 40 cycles of 15 seconds at 95ºC, 30 seconds at a specific primer temperature and 1 minute at 72ºC. After the amplification cycles, a dissociation curve was performed between 72ºC and 95ºC in order to confirm the specificity of the amplified product. The efficiency of the qRT-PCR was calculated through the use of different housekeeping genes as internal controls. These housekeeping genes were selected following the methodological principles described in (Czechowski et al., 2005). The relative abundance of the mRNA was calculated by comparative analysis of the Ct different parameters (Pfaffl, 2001).

3.3 DNA plasmid constructions

3.3.1 Cloning and transforming vectors

The cDNA U11044, which corresponds to *TPT* (At5g46110), was supplied by the ABRC. This cDNA was placed under the control of two different promoters (*35S* and *GAPCp1*) and fused in frame to two different tags (green fluorescent protein (GFP) and 6 Histidine (His) tags) to give constructs *35S:TPT-GFP*, *35S:TPT-His* and *GAPCp:TPT-His*. All PCR-derived constructs were verified by DNA sequencing.

3.3.1.1 Gene construction *35S:TPT-GFP*

The *TPT* cDNA U11044 was PCR-amplified with primers *At5g46110RepCR8* and *At5g46110FopCR8*, and the product was cloned in the *pCR8/GW/TOPO* plasmid (Invitrogen). *TPT* cDNA was subcloned in plasmid *pMDC83* (Curtis et al., 2003) using the Gateway technology with clonase II (Invitrogen). This plasmid allowed us to clone *TPT* in frame with a GFP cDNA at the Ct position (TPT-GFP) to give the *35S:TPT-GFP* construct.

3.3.1.2 Gene construction *35S:TPT-His*

The *TPT* cDNA U11044 was PCR-amplified using primers *At5g46110XhoIF* and *At5g46110XbaIRe3* to introduce *Xho* I and *Xba* I sites. The amplified fragment was cloned between the *Xho* I and *Xba* I sites in a modified *pGreen II* plant transformation vector (Hellens et al., 1993) named *p336* kindly provided by Dr. Jeff Harper (University of Nevada). This vector allowed to obtain the *35S:TPT-His* construct.

3.3.1.3 Gene construction *GAPCp:TPT-His*

A fragment containing *TPT-His* was exchanged with the *GAPCp1* cDNA between the *Xho* I and *Bam* HI sites of a previously obtained construct, where *GAPCp1* was expressed under the control of a 1.5 kb fragment corresponding to the native *GAPCp1* promoter (Muñoz-Bertomeu et al., 2010). This construct was named *GAPCp:TPT-His*.

3.4 Transforming procedures

3.4.1 *E. coli* transformation

The transformation of *E. coli* competent cells was performed following the indications of Mandel et al., (1992). The competent cells maintained at -80ºC were placed on ice for 5 minutes and then from 1 to 10 µl of the transforming plasmid was added. The cells with the plasmid were mixed and placed on ice for 30 minutes. After that, a HS of 42ºC for 90 seconds was applied to the cells, and immediately after that the cells were put back on ice for 2 minutes. Then, 1 ml of SOC media was added and the cells were incubated 1h at 37ºC in smooth shake. Finally, the transformed cells were spread in three petri dishes with solid LB medium and the appropriate antibiotic depending on the plasmid used. In each petri dish a different volume of the transforming cells was spread (25, 100 y 500 µl) by using sterile laboratory glass beads. A fourth petri dish with LB without antibiotic was used as a control to spread on it 100 µl of the transforming cells, just to check the viability of these cells. The resistant colonies obtained 8-12h after the incubation were verified by PCR. The positive colonies were inoculated in 5 ml of LB liquid media plus the appropriate antibiotic. After incubation overnight at 37ºC in smooth shake, the plasmid was extracted and sequenced.

3.4.2 *A. tumefaciens* transformation

The strain that was used was GV3101 pSoup and the method followed was a modification of freezing-unfreezing method (Holsters et al., 1978). An aliquot of 100 µl of competent cells was defrosted and 1 µg of plasmid was added. The mixture was smoothly shaked and placed rapidly in liquid nitrogen. After that, it was incubated for 5 minutes at 37ºC, and after the incubation 1 ml of liquid LB plus gentamicine (25µg/ml) and tetracycline (5µg/ml) was added to the cells. The transforming cells were incubated for 4h at 28ºC at constant shake (250 rpm). Finally, 100 µl of the transforming cells were spread into petri dishes with solid LB plus gentamicine, tetracycline and the appropriate antibiotic depending on the plasmid used. These plates were incubated at 28ºC for 2 or 3 days and after that, the visible colonies were checked as positive ones by PCR colony. The positive colonies were inoculated in 5 ml of LB medium plus gentamicine (25µg/ml), tetracycline (5µg/ml) and the appropriate antibiotic depending on the plasmid used. After one day incubation at 28ºC an aliquot was glycerinated to keep the transforming cells at -80ºC.

3.4.3 *Arabidopsis thaliana* transformation

The method used was the floral dipping (Clough et al., 1998) using *A. tumefaciens*. To perform the transformation, 20 seeds were sown in pots of 15 cm diameter and were grown under greenhouse conditions until the stalk reached 15 cm height. In order to perform the transformation, 1 ml of saturated culture of *A. tumefaciens* with the plasmid of interest (0.2-0.3 of Optical density at 600 nm) was inoculated in 200 ml of liquid LB plus

gentamicine, tetracycline and the appropriate antibiotic. This medium was incubated at 28ºC for 12-16h in constant shaking (200 rpm). After that, it was centrifuged at 4,000 rpm for 20 minutes at 4ºC to obtain the cell pellet which was resuspended in 400 ml of transforming solution (5% (w/v) sucrose, 10 mM $MgCl_2$, 1 g/l MES and 0.02% (v/v) of Silwet® L-77 (Lehle Seeds)). The transformation was carried out by floral dipping, that is, the immersion of the floral buds into the transforming solution for 2 minutes. Then, pots were covered for a day with the help of transparent plastic bags in order to keep the appropriate moisture to *A. tumefaciens* to infect. The next day, the plastic bags were cut in the edges to allow the income of fresh air and 24h later these plastic bags were removed from the top of the pots. These pots were regularly watered as usual and finally, when the siliques were yellowish, the watering procedure was interrupted to allow the siliques to get completely dry to be harvested.

3.5 Selection of transgenic lines

After harvesting the seeds from the transformed Arabidopsis plants, they were sown on petri dishes with ½ MS medium plus sucrose, the appropriate antibiotic from the T-DNA insertion and cefotaxime (100µg/ml) to inhibit the growth of the residual *A. tumefaciens* cells. After 4 days at 4ºC, these petri dishes were transferred into a growth chamber for 8-12 days. The seedlings that were able to grow in the antibiotic media (T_1) were then transferred to pots with soil and carried to greenhouse conditions till the end of their vital cycle. The seeds of these plants (T_2) were sown again in the same ½ MS media described above plus T-DNA selection antibiotic but

without cefotaxime. In these T_2 plants the segregation rate of the T-DNA insertion was calculated by counting the number of resistant plants against the number of sensitives to the antibiotic. Only those plants that adjust this segregation rate to the Mendelian laws of inheritance for just one dominant gene (3 resistant plants: 1 sensitive) were selected for further characterization. The resistant seedlings from the selected lines were transferred to pots filled with soil in the greenhouse until the endo of its vital cycle. The seeds that were harvested from these T_2 lines were the T_3 generation and they were tested in ½ MS media plus the antibiotic of the T-DNA insertion in order to select those lines that were 100% resistant to the antibiotic, that is to say, the homozygous lines for the T-DNA with a single insertion. Finally several plants from these 100% homozygous lines and their respective WT controls were transferred to soil pots in order to obtain more seeds to perform all the experiments.

3.6 Quantification of bioparameters

3.6.1 *In vitro*

For the *in vitro* analysis plants were grown in square petri plates in vertical orientation. Bioparameters that were evaluated were fresh weight of the aerial parts and roots and the root length. The fresh weight was evaluated in 18-22 day-old plants with a OHAUS ANALYTICAL *Standard AS60* scale.

Root length was measured every two days since the radicular emergence until day 10. The root growth rate was the result of the root length per day of growth.

3.6.2 In greenhouse

The plants grown under greenhouse conditions were used to measure the length of the stalk, its fresh weight, the rosette fresh weight and its diameter.

3.7 Starch determination

In order to evaluate differences in the starch content of the samples, three biological replicates of 50 mg of fresh weight of leaf material was harvested at the end of the dark and light periods. The samples were frozen in liquid nitrogen and grinded with a morter. After that, 1 ml of 80% (v/v) ethanol was added to each sample and all of them were shaken for 15 minutes at 80ºC. Then, the samples were centrifuged for 10 minutes at 20,000 g at room temperature. Till this point, the washing process with ethanol was repeated twice in order to clean as much as possible the samples. Once finished, the pellet was washed with 1 ml of ice-cold water by vortexing and then centrifuged for 10 minutes at 20,000 g at 4ºC. The next step was removing the supernatant by pipetting and drying the pellet using a speed-vac for 30 min. At this point the pellet can be stored at 4ºC overnight.

To release all the starch molecules from the samples, the pellet was homogenized in 0.5 ml of 200 mM KOH and incubated for 1h at 95ºC. After that, 88 µl of 1 M acetic acid was added to neutralize the KOH till pH 7.0. Then the samples were centrifuged for 10 min at 20,000 g at room temperature. Finally, 50 µl of amyloglucosidase-solution (BIOPHARM: Ref.10207748035) was added to the 50 µl supernatant and the mixture was incubated for at least 3h (or overnight) at 55ºC. For starch determination, a test solution of 200 µl per sample was made. The composition of the test

solution was 90 µl of a buffer mix (45 mM Tricine/NaOH pH 7.8 and 2.25 of $MgCl_2$ pH 7.8), 20 µl of 2 mM ATP, 5 µl of 0.5 mM $NADP^+$ and 0.4 µl of 1.2 U/ml glucose-6-phosphate dehydrogenase. Then, 80 µl of sample was added and the mixture was incubated for 10 minutes at 30ºC before measuring the absorbance at 340 nm. Once the lecture was stable, the reaction was started with the addition of 0.8 ul of 6 U/ml hexokinase in 6 µl of its buffer and the lecture kept on reading till the level was stable. The amount of starch was quantified using a glucose standard curve.

3.8 Ammonium determination

To determine the amount of ammonium, plant tissue was grinded in a frozen morter with liquid nitrogen. After that, 800 µl of MilliQ water were added to an aliquot of 25 mg of powder tissue and then incubated for 5 minutes at 80ºC. Once finished the incubation, the mixture was centrifuged at 13,000 rpm for 20 minutes and the supernatant was recovered to determine the ammonium content. The determination was based in Berthelot's method and it consisted basically on the sequential addition of 166 µl of Solution A (0.33 M Sodium phenoxide trihidrate), 334 µl of Solution B (0.02% sodium nitroprusside fresh prepared) and 166 µl of Solution C (sodium hypochlorite 1:50) to 166 µl of sample. The absorbance was determined with a spectrophotometer at 635 nm.

3.8.1 Ammonium assay

In order to see the ammonium effect on *psp1.1psp1.1 HS:PSP1* mutants, three media of MS of different amount of ammonium were assayed; control, excess of ammonium and ammonium depleted medium. The composition of each medium is described in the Table 3.1.

Table 3.1. Composition of the media for the ammonium assay.

	Control	NH_4^+-excess	NH_4^+-depleted
Micro Elements	**mg/l**	**mg/l**	**mg/l**
$CoCl_2 \cdot 6H_2O$	0.025	0.025	0.025
$CuSO_4 \cdot 5H_2O$	0.025	0.025	0.025
FeNaEDTA	36.7	36.7	36.7
H_3BO_3	6.2	6.2	6.2
KI	0.83	0.83	0.83
$MnSO_4 \cdot H_2O$	16.9	16.9	16.9
$Na_2MoO_4 \cdot 2H_2O$	0.25	0.25	0.25
$ZnSO_4 \cdot 7H_2O$	8.6	8.6	8.6
Vitamins			
Glycine	2	2	2
myo-inositol	100	100	100
Nicotinic acid	0.5	0.5	0.5
Pyridoxine HCl	0.5	0.5	0.5
Thiamine HCl	0.1	0.1	0.1
Macro Elements	**g/l**	**g/l**	**g/l**
$CaCl_2$	3.32	3.32	3.32
KH_2PO_4	1.7	1.7	1.7
KNO_3	19	-	41.67
$MgSO_4$	1.8	1.8	1.8
NH_4NO_3	16.5	33	-

3.9 Enzymatic activity

To test the activity of the citrate synthase and fumarase, the proteins were extracted with the Stitt buffer (50 mM Hepes/KOH pH 7.4, 1 mM EDTA, 1 mM EGTA, 2 mM Benzamidine, 2 mM E-aminocaproic acid, 0.5 mM PMSF, 10% glycerol and 0.1% Triton x-100)

A. **CITRATE SYNTHASE**: it was assayed on 96-well-microplates using a modification of the method of Stitt et al., (1989). The reaction mixture is described in the Table 3.2.

Table 3.2. Composition of the reaction mixture for the citrate synthase activity determination.

Substance	Final concentration	1 reaction (µl)
Water		30.725
Tricine KOH pH 8.5	100 mM	5
Malate	0.3 mM	0.15
Triton X-100	0.05%	2.5
Malate DH	5U/ml	1
NAD^+	0.25 mM	0.625

As standard, concentrations from 0 to 1 nmol of NADH were used.

For a single reaction (50 µl), 5 µl of sample were added to 40 µl reaction mixture and it was allowed to come to equilibrium. The addition of 5 µl of Acetyl CoA (2mM) started the reaction. Then, the reaction was mixed and incubated at room temperature for 1h. After that, the reaction was stopped with 20 µl of 0.5 M KOH and incubated at 95ºC for 5 minutes. The next step was to neutralise the mixture with 20 µl of 0.5 M HCl in 0.2 M Tricine KOH pH 9.0 and 10 µl of water. Finally, the composition of the determination mixture is described in the Table 3.3.

Table 3.3. Composition of the determination solution for the citrate synthase activity determination.

Substance	Final concentration	1 reaction (µl)
Water		20.84
Tricine KOH pH 9.0	100 mM	14
EDTA	4 mM	1.12
PES	0.1 mM	0.7
MTT	0.6 mM	8.4
Ethanol	500 mM	4.1
Alcohol DH	6 U/ml	0.84

The kinetic was read at 570 nm for 1h.

B. **FUMARASE:** it was assayed on 96-well-microplates using a modification of the method of Stitt et al., (1989). The reaction mixture is described in the Table 3.4.

Table 3.4. Composition of the reaction mixture of the fumarase activity determination.

Substance	Final concentration	1 reaction (µl)
Water		33
Tricine-KOH pH 8.0	100 mM	5
acetyl-CoA	0.2 mM	1
K-P buffer pH 7.5	5 mM	0.25
$MgCl_2$	5 mM	0.25
NAD^+	0.2 mM	0.1
Triton X-100	0.05%	0.25
malate DH	12 U/ml	0.1
citrate synthase	1 U/ml	0.05

As standard, concentrations of NADH from 0 to 1 nmol were used.

For a single reaction, 5 µl of sample were added to 40 µl reaction mixture and the mixture was allowed to come to equilibrium. The addition of 10 mM Fumarate (ref: sigma F1506) started the reaction. Then, the reaction

was mixed and incubated at room temperature for 40 minutes. After that, the reaction was stopped with 20 µl of 0.5 M KOH and incubated at 95ºC for 5 minutes. The next step was to neutralise the mixture with 20 µl of 0.5 M HCl in 0.2 M Tricine KOH pH 9.0 and 10 µl of water. Finally, the determination was made as described in the Table 3.5.

Table 3.5. Composition of the determination solution for the fumarase activity determination.

Substance	Final concentration	1 reaction (µl)
Water		20.84
Tricine KOH pH 9.0	100 mM	14
EDTA	4 mM	1.12
PES	0.1 mM	0.7
MTT	0.6 mM	8.4
Ethanol	500 mM	4.1
Alcohol DH	6 U/ml	0.84

The kinetic was read at 570 nm for 1 h.

3.10 Auxin determination

This determination was done as an external collaboration with Dr. Stephan Krüger from the Universität zu Köln.

3.11 Fatty acid determination

The composition of fatty acids was determined by gas chromatography of the fatty acid methyl esters (FAME) as described by Focks N, (1998) with some modifications. In order to determine the FAMEs, 10 seeds were weighted and placed in a glass tube with screw caps. Then 1 ml 1 N HCl in methanol was added. After that 10 µg/µl of internal control pentadecanoic acid was added and the mixture was incubated at 80ºC for 90 minutes. Then,

the glass tubes were placed at room temperature for 5 minutes to cool down and then 1 ml of 9% NaCl and 1 ml hexane was added. The mixture was vortexed and centrifuged at 1,000 rpm for 4 minutes. Afterwords, the upper phase with the hexane and the FAMEs of interest were placed in a new glass tube. The FAMEs were concentrated under a nitrogen flow, dissolved in 100 µl of hexane and placed in a small vial used in gas chromatography, ready for the analysis.

3.12 Microscopy analysis

3.12.1 Confocal microscopy

A LEICA TCS-SP (Leica Microsystems Heidelberg GmbH, Heidelberg, Alemania) was used to perform the visualization and location of the GFP. This machine is composed of an inverted microscope DMIR2 and a SL spectral confocal unit with two fluorescent detectors and four lasers (458 nm, 488 nm, 514 nm and 534 nm). In order to excite the GFP, the 488 nm laser was used and its emission was detected between 500-520 nm. The chlorofile was excited with the same laser, and its emission was detected between 660-690 nm. To visualize the samples, the organ of interest (roots or aerial part of 9 day-old-plants) was placed into a slide and then, after the deposition of a drop of water, the sample was covered with a tilted coverslip, ready to be visualized.

In order to detect the presence of high amounts of auxin in root tissue, *amirRNA PSP1* plants were crossed with WT plants that carry the construction *DR5:GFP*. In these plants, wherever auxin is, the GFP is

synthesized and could be detected by confocal microscopy. After detection of fluorescence, its intensity was compared to the WT plants and evaluated by ImageJ.

For root length measurements and for counting the number of meristematic cells, seedlings of 9 days-post-germination (dpg) were mounted straight on slides. To improve the whole mount, aerial part of the seedlings was removed by cutting it directly on the slide. A dilution of 10 µg/ml of a propidium iodide (PI) Stock solution (P4864, Sigma Aldrich) were used directly on the roots placed on the slide in order to stain them for 5 minutes of incubation. After that, water was added and a coverslip was placed on the top for confocal microscopy. An Olympus FV100 confocal laser scanning microscope was used. We analysed propidium iodide-stained roots of *Arabidopsis thaliana* by performing optical z-sections through meristematic zones at 20× magnification. PI was excited at 559 nm and the emission was collected at 570 to 670 nm.

3.12.2 Transmission Electron Microscopy

For transmission electron microscopy of anther and pollen, inflorescences containing buds at different developmental stages from WT and *psp1.1psp1.1 35S:PSP1-GFP* plants were collected and classified into different development groups according to (Smyth et al., 1990). Buds from the same group were removed from plants, fixed with 2.5% glutaraldehyde, and postfixed in 1% osmium. Tissue was dehydrated in an ethanol series and infiltrated with LR-White resin. Ultrathin sections (60 nm) were examined with a JEOL_1010 transmission electron microscope at 60 kV

equipped with a MegaView III digital camera with Analysis software. For differential interference contrast microscopy, siliques from heterozygous *PSP1psp1.1* plants were dissected longitudinally at 2, 5, 7, and 10 days after pollination (DAP).

3.12.3 Hoechst stain

For nucleus staining with Hoechst, inflorescences containing buds at different developmental stages from WT and *psp1.1psp1.1 35S:PSP1-GFP*, plants were collected and classified in different groups as described for transmission electron microscopy. Buds from the same group were dissected on a microscope slide, and pollen grains released from anthers were stained with 10 μg/mL Hoechst dye. Samples were observed with Nikon Eclipse E800 compound microscope equipped with an epifluorescence module and a Nikon DXM1200F digital camera with Nikon ACT-1 software.

3.12.4 Differential interference microscopy

Ovules from individual siliques were morphologically classified, cleared in Hoyer's solution (30 g gum Arabic, 200 g chloral hydrate, 20 ml glycerol, all in 50 ml distilled water) and observed with a Nikon ECLIPSE E800 compound microscope equipped with Nomarski differential interference contrast optics and a Nikon DXM1200F digital camera with Nikon ACT-1 software. Bright-field photographs of 15-d-old hand-dissected embryos submerged in water were obtained using a stereoscopic zoom microscope Nikon SMZ 1500 equipped with a DS-Fi1 digital sight camera.

3.13 Western blot analysis

3.13.1 Protein extraction

Samples (leaves, roots or whole seedlings) were grinded in a morter with liquid nitrogen. To 500 mg aliquots, 750 µl of the extraction buffer was added (140 mM NaCl, 8 mM $Na_2HPO_4 \cdot 7H_2O$, 2 mM KH_2PO_4 and 10mM KCl pH 7.4) and 16.5 ul of a protease inhibitor cocktel (Sigma, P9599). The extracts were centrifuged at 14,000 rpm for 20 minutes at 4ºC, and the supernatants were transferred to new vials. The extracted proteins were quantified by the Bradford assay (Bio-Rad, 500-0006) using different concentrations of Bovine serum albumin (BSA) as a standard. All the protein extractions were diluted to the same concentration using the previous extraction buffer. After that, loading buffer 5X Laemmli (7.5% SDS, 0.1M DTT, 10 mM EDTA, 30% sucrose, 0.25 mg/ml bromophenol blue and 0.3 M Tris-HCl pH 6.8) was added and samples were incubated for 10 minutes at 95ºC. Then, samples were ready to use or to store at -80ºC until its use.

3.13.2 SDS-PAGE

For that part of the western blot, 60-120 µg of proteins were used. The acrylamide/bisacrylamide gels (Sigma-Aldrich, 30% Solution, A3699) consisted in two different parts: the stacking gel (upper part, 4% acrylamide), where all the proteins are concentrated, and the running gel (lower part, 8% acrylamide), where the proteins are separated according to its molecular weight. The polymerization of the gels was performed with

ammonium persulfate (APS) and Tetramethylethylenediamine (TEMED). The electrophoresis was performed with a specific buffer (190 mM Glycine, 25 mM Tris and 0.1% (p/v) SDS pH 8.3) under 75V.

3.13.3 Transfer and detection

The proteins were electrotransferred to nitrocellulose membranes AmershamTM HybondTM-ECL (RPN203D, GE Healthcare) for 1h under 100V, using the Mini Trans-Blot® Cell (BioRad) system with the transference buffer (192 mM Glycine, 16.94 mM Tris and 20% methanol) at 4ºC. The efficiency of the transference and the proper charge of proteins was tested in the membranes with the Ponceau solution [0.1% Ponceau S (P3504, Sigma) and 1% acetic acid] and then discoloured with Phosphate Buffer Saline or PBS (80 mM Na_2HPO_4, 20 mM NaH_2PO_4 and 100 mM NaCl pH 7.5).

The immunological detection was performed with the Amersham ECL Advance Western Blotting Detection Kit (GE Healthcare) following the instructions provided by the manufacturer. A washing buffer PBS-Tween [PBS with 0.1% (v/v) of Tween 20] and a blocking solution PBS-T-B [PBS-T with 2% (w/v) of blocking powder (ECL Prime blocking agent, RPN418V)] were prepared. The membranes were incubated for 1h in constant shaking in PBST-B, followed of two washing steps of 30 seconds with the PBS-T solution. After that, the membranes were incubated overnight with the primary antibody at the specific concentration (1:25,000) in constant shaking at 4ºC. The antibodies were diluted in the PBS-T-B

solution. The primary antibody was the anti-GFP (Molecular probes, ref. A-11122).

At the end of the incubation time, the membranes were washed 6 times for 5 minutes at room temperature with the PBS-T solution. Then, the membranes were incubated for 2h with the secondary antibody (*Ac Anti-Rabbit;* RPN2124, GE-Healthcare) at a dilution of 1:25,000. After the incubation time, the membranes were washed again 6 times with the PBS-T and finally they were incubated with the detection agent (ECL SelectTM Western Blotting Detection Reagent, RPN2235, AmershamTM, GE Healthcare) for 5 minutes. The signal was detected by Amersham HyperfilmTM ECL (KNO 70243, GE Healthcare). The film development was performed in a dark room with the developing solution (Anatomix Developer Replenisher, 753269,Fuji Hunt) and fixing solution (X-Fix Fixer & Replenisher, 753277, Fuji Hunt). According to the intensity of the signal, the exposure of the membrane varied between 5 seconds and 1h.

3.14 Transport activity measurements

Plant tissue was ground in liquid nitrogen and proteins extracted in 2 volumes (w/v) of a buffer containing 0.1 M Tricine-KOH pH 8.0, 4 mM EDTA, 4 mM DTT, 6 mM ascorbate; 0.1% (w/v) BSA, 0.1% (w/v) PVPP and 0.2% DDM (v/v). After thawing on ice, the plant extract was centrifuged for 1 min at 500 g at 4ºC, and the supernatant was aliquoted in 50 µl. Reconstitution of crude membrane extracts and transport activity measurements were carried as described by Flugge et al., (1994).

3.15 "-Omics" era: tools for plant biology

With the onset of the so-called 'omics' approaches used in modern biology, plant biologists began to look at plants in an entirely new way. 'Omic' technologies are primarily aimed at the universal detection of genes (genomics), mRNAs (transcriptomics), proteins (proteomics) and metabolites (metabolomics) in a specific biological sample. In this thesis we have chosen transcriptomic and metabolomic approaches to perform a deeper study in the characterization of the gene *PSP1*.

3.15.1 Metabolomic profile

This tool consists of the identification and quantification of all metabolites in a biological sample. The essence of metabolite profiling is the discovery of novel marker metabolites and determination of relative changes of metabolite pool sizes in comparison to a reference sample. The technology provides high analytical precision, comprehensiveness, and sample throughput. However, as the metabolites are extremely diverse and physico-chemically different it is necessary the application of different complementary analytical methods (Weckwerth, 2007).

Most metabolites can be partitioned into polar and nonpolar fractions and, after specific derivatizations, make each fraction volatile and able to be analyzed by gas chromatograpy-mass spectrometry or GC-MS. GC-MS is very popular in the detection of the metabolic profile of biological samples and has a relatively broad coverage of compound classes, including organic

and amino acids, sugars, sugar alcohols, phosphorylated intermediates and lipophilic compounds (Lisec et al., 2006).

It has its major application in clinical diagnosis, but also plant metabolite profiling has also been used to demonstrate gene function by comparison of mutants of *Arabidopsis* to their respective WT ecotypes, facilitating the annotation of genes (Lisec et al., 2006). This, added to the transcript profile of a sample, it proves effective for identifying candidate genes not only for basic understanding of gene function in plants but also for biotechnological purposes.

3.15.1.1 Metabolite extraction

50 mg of fresh weight was used as starting material. The samples were grinded with morter and pestle and collected in a 1.5 ml vial (Eppendorf). It was added to each sample 460 µl of absolute methanol and 20 µl of ribitol as internal standard (0.2 mg/ml en H_2O). Then, the samples were heated at 70ºC during 15 minutes and then centrifuged at 14,000 rpm during 10 minutes at room temperature. The supernatant was transferred to a new 1.5 ml vial and then added 250 µl $CHCl_3$ and 500 µl of MilliQ water. After that, the samples were shaken using a vortex during 15 seconds and then centrifuged at 4,000 rpm for 15 minutes. Then, two aliquots of 150 µl and 300 µl from the polar phase were taken. The samples were desiccated in a speed vac during 3h. Finally, the vials were filled with N_2 and were stored at -80ºC until they were used for metabolite determination.

3.15.1.2 Derivatization

Before beginning the analysis, the samples were derivatized in two following steps: first it was added 40 µl of methoxamine hydrochloride (20 mg/ml in pyridine) and the samples were left at 37ºC for 2 h. After that, 70 µl of a reaction mixture (1 ml MSTFA (N-metil-N-trimethylsilyl acetamide and 20 µl FAMEs were added to each sample. Then the samples were incubated at 37ºC for 30 minutes. Finally, the processed samples were transferred to specific vials and the levels of metabolites were determined by GC/MS using the protocol defined by Lisec et al., (2006).

3.15.2 Transcriptomic profile

Transcriptomics refers to the study of the transcriptome, that is, the complete set of RNA transcripts produced by the genome of a cell under specific circumstances. Comparison of transcriptomes between different cells or between a mutant and its WT ecotype allows the identification of genes that are differentially expressed in distinct cell populations, or in response to different treatments.

Regarding methodology, it uses high-throughput methods, such as microarray analysis or RNAseq.

3.15.2.1 Microarray analysis

During the past years, there has been an increase in DNA sequence information for plants, but the question now is how to deal with all this information. One of the most powerful tools that has been recently

developed to bridge the gap between sequence information and functional genomics is DNA microarray technology (Kehoe et al., 1999). It allows the simultaneous analysis of tens of thousands of genes in a single experiment (Wu et al., 2001).

As a hybridization-based approach, it involves the incubation of fluorescently labelled cDNA with custom-made DNA microarrays. It is basically the amplification by PCR of open reading frames or ORFs from genomic DNA and its deposition on microscope slides at specific locations. Then, the probes of two biological samples are labeled with fluorescent nucleotides, such as Cy3-dCTP and Cy5-dCTP, mixed together and hybridized into a microarray under a coverslip. After some washing steps, the fluorescent signal of each element of the microarray is detected by a dual laser scanning device, so quantitative values for the signals for each probe and the ratio of signals for the two probes can be calculated using various software programs (Kehoe et al., 1999).

Microarrays are high throughput and relatively inexpensive (Aharoni et al., 2001). However, among its drawbacks, there is the reliance upon existing knowledge about genome sequence, high background levels owing to cross-hybridization and a limited dynamic range of detection owing to both background and saturation of signals. Furthermore, comparing expression levels across different experiments requires complicated normalization methods (Wang et al., 2009)

In order to improve these drawbacks, a novel high-throughput DNA sequencing method, the RNA-Seq, has been developed for both mapping and quantifying transcriptomes.

3.15.2.2 RNA-Seq

It is based on developed deep-sequencing technologies and consists of the conversion of a population of RNA into a library of cDNA fragments with adaptors attached to one or both ends. Then each molecule is sequenced in a high-throughput manner to obtain short sequences from one end (single-end sequencing) or both ends (pair-end sequencing) (Wang et al., 2009). After that, the resulting reads could follow two directions: if there is a reference genome or reference transcripts, they could be aligned. However, in the case of not having a reference genome, these reads could be assembled de novo without the genomic sequence to produce a genome-scale transcription map that consists of both the transcriptional structure and/or level of expression for each gene.

In comparison with DNA microarrays, RNA-Seq presents many powerful advantages, like for example, it is not limited to detecting transcripts of existing genomic sequence or it also reveals the precise location of transcription boundaries to a single-base resolution. Furthermore, the level of background signal is very low compared with DNA microarrays because DNA sequences can be unambiguously mapped to unique regions of the genome. Also, in terms of quantification, DNA microarrays lack sensitivity for genes expressed at very low or very high levels, whereas RNA-Seq does not have an upper limit for quantification. And finally, results of RNA-Seq are more reproducible than DNA microarray results (Wang et al., 2009).

Methods such RNA-seq and microarrays have provided a vast amount of genomic and transcriptomic information about plant biology, but at post-transcriptional level there are considerable modifications executed on the

metabolite and on the protein level. Consequently, the analysis of the molecular phenotype demands the step towards post-genomics techniques such as metabolomics.

For the analysis of the gene expression (transcriptomics), WT and *psp1.1psp1.1 HS:PSP1* 21-day-old mutant plants grown *in vitro* were used. The plates with the plants were separated into two different sets: one of the sets was heat-shock (HS) treated at 37ºC for 1h and the other set was keep at 22ºC and used as control. After 4h of HS induction, aerial parts and roots of both sets were harvested in liquid nitrogen and stored at -80ºC.

3.15.2.2.1 RNA extraction

It was carried out as described previously in the section 3.2.1.3.

3.15.2.2.2 Obtainment of a RNA-Seq library

Using as starting material 3-15 µg of RNA, a mRNA enrichment was performed with the *MicroPoly(A) Purist kit* (AMBION). In order to prepare the RNA-Seq library, the kit *SOLID Total RNA-seq* (Life Technologies) was used as follows: the RNA was firstly fragmented using RNaseIII, in order to obtain a distribution of fragments of different sizes, with an average size of 200 nucleotides.

After that, the hybridization and ligation of the adaptor to the fragmented RNAs was performed. The hybridization of the adapters is directional, that is, the binding is different depending on the 3' or 5' end, so in that case, the strand specificity is kept. Then a reverse transcription is performed in order to obtain the cDNA. After that, the cDNA is purified and then charged into an acrylamide gel 10% TBE-Urea 1.0 mM in order to select the fragments

with the most appropriate size. The next step was the amplification of the cDNA in 15 cycles and then the size of the library was determined and quantified.

After the obtainment of the library, an equimolar mixture of it is used to perform an emulsion PCR using the authomatic system of EZ Beads (Life Technologies). Then, the bead enrichment is performed followed by its deposition in the sequencing wells. The sequencing step is done by SOLID 5500XL equipment of 75 nucleotides using the Exact Call Chemistry.

3.15.2.2.3 RNA-Seq data analysis

In order to analyze the data obtained, several programs were used sequentially. First, to filtrate the readings depending on their adaptor the program Cutadapt v1.8 was used. Then, to evaluate the quality of the reads, FastqQC was used. After that, to perform the mapping against a reference, Tophat2 was employed. To visualize and obtain the raw counts it was used Seqmonk v0.29. Finally, DeSeq was used to see the differential expression in the data. In order to validate empirically these data, qRT-PCR of selected genes were performed. The primers used are listed in the Table S2 (see Appendix).

4. RESULTS AND DISCUSSION

4.1 Chapter 1:

Overexpression of the triose phosphate translocator TPT complements the abnormal metabolism and development of plastidial glycolytic glyceraldehyde-3-phosphate dehydrogenase mutants

4.1.1 RESULTS

4.1.1.1 TPT expression is low or absent in root tissue

An *in silico* expression analysis (http:// www.bar.utoronto.ca/efp/cgi-bin/efpWeb.cgi, https://genevestigator.com/gv/) of the Arabidopsis *TPT* gene encoded by At5g46110 revealed an abundant expression in leaves and aerial parts (AP), and a very low expression in root cells. In many root cell types, the *TPT* expression is less than 1% of that in cotyledons and cauline leaves. These data are in agreement with our results, in which *TPT* expression in roots, leaves, shoots, siliques and flowers was assessed by quantitative real time-PCR (qRT-PCR) in mature plants and seedlings (Figure 4.1A and B). In both cases, the expression of *TPT* was low or absent in roots, but high in AP. Given that we have previously suggested that lack of *GAPCp* expression in root plastids lowers the 3-PGA levels required, amongst other things, for the PPSB, we hypothesized that overexpression of a transporter such as the TPT could revert *gapcp1gapcp2* root phenotype.

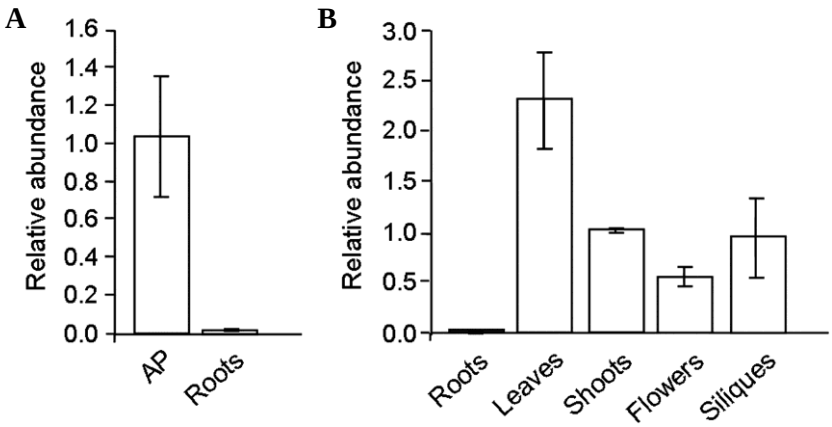

Figure 4.1. Expression analysis of *TPT* in seedlings (A), and mature plants (B). Values represent three biological replicates.

4.1.1.2 Transgenic plants that overexpress *TPT* fused to a GFP and His-tag complement *gapcp1gapcp2* phenotypes to a varying extent

In order to explore the effect of *TPT* overexpression on the phenotype of *gapcp1gapcp2*, we transformed the mutant with constructs in which *TPT* was fused to two different tags at its C-terminus (GFP and His-tag) under the control of the *35S* promoter. Since *gapcp1gapcp2* is sterile, the progeny of heterozygous plants (heterozygous for *GAPCp1* and mutant homozygous for *GAPCp2*) were transformed with the different constructs. Homozygous *gapcp1gapcp2* were identified by PCR genotyping in the segregating population. Five lines overexpressing *TPT-GFP* (*35S:TPT-GFP* lines) and seven overexpressing *TPT-His* (*35S:TPT-His* lines), with different *TPT* expression levels in roots were obtained (Figure 4.2A and C).

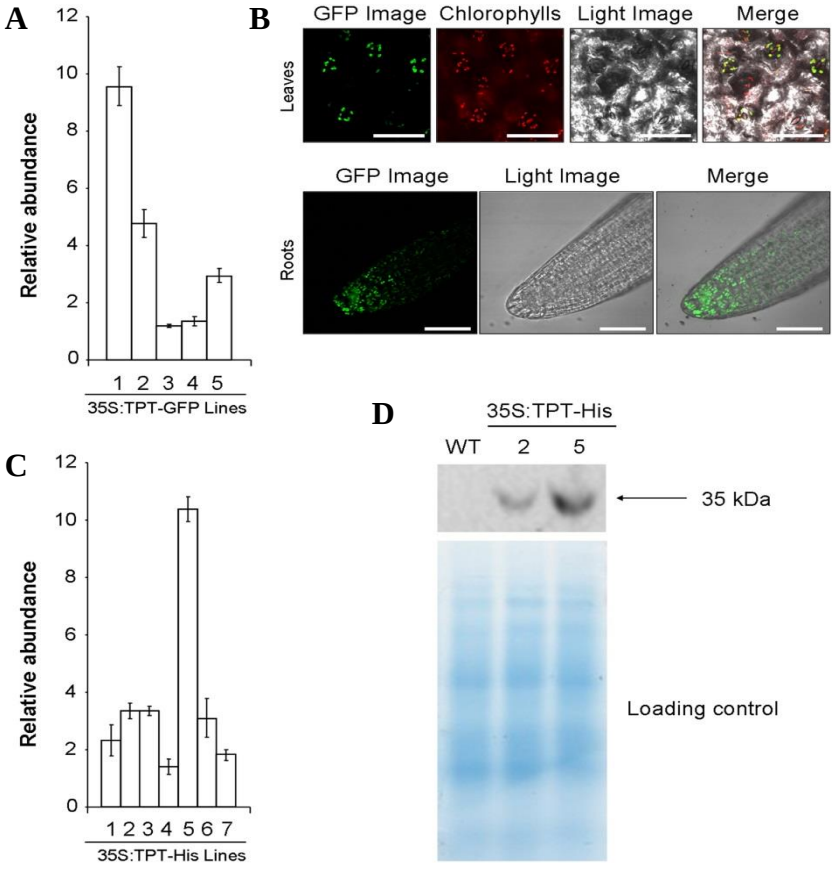

Figure 4.2. Molecular analysis of *gapcp1gapcp2* (*g1g2*) expressing *TPT* under the control of the *35S* promoter. (A) qRT-PCR analysis of *TPT* in the roots of 21-day-old *35S:TPT-GFP* lines as compared to wild-type (WT). (B) Cellular expression of TPT-GFP under the control of *35S* promoter in leaf and root plastids. (C) qRT-PCR analysis of *TPT* in the roots of 21-day-old 35S:TPT-His lines as compared to WT. (D) Immunoblot showing *TPT* expression in the roots of two representative *35S:TPT-His* lines as compared to WT. Protein gel blot analysis was performed using anti-His antibodies. Values are the mean ± SE (n = 3). Scalebar = 50 µm.

Three lines of each construct were selected on the basis of having the highest expression levels and their root growth was compared to that of *gapcp1gapcp2* (Figure 4.3A and B).

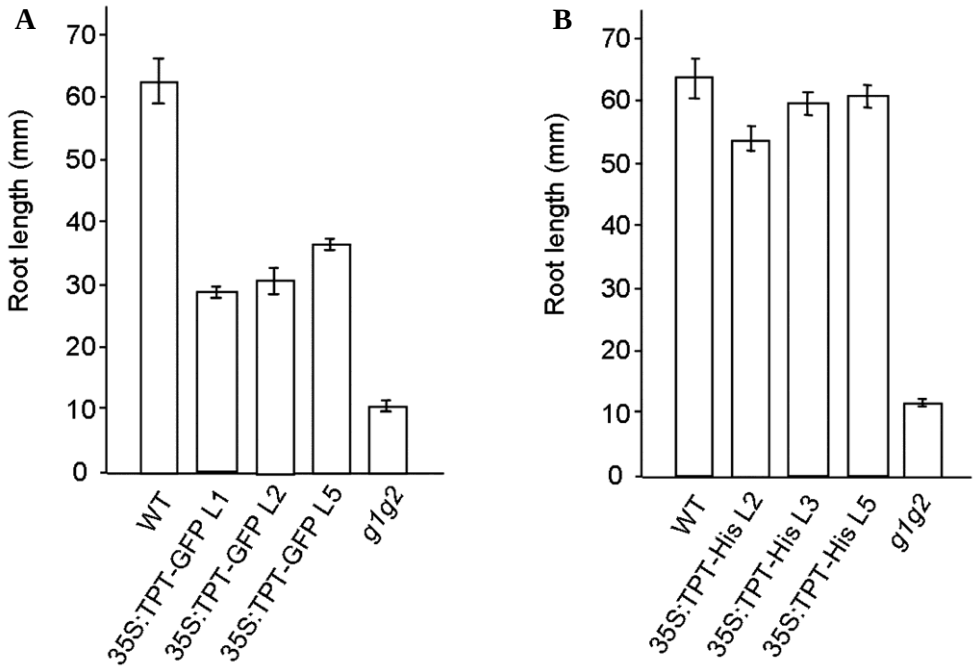

Figure 4.3. Primary root length of *gapcp1gapcp2* (*g1g2*) expressing TPT-GFP (A) or TPT-His (B) under the control of *35S* promoter lines compared to *g1g2* and wild-type plants.Values represente the mean of n = 25 plants.

All selected lines complemented the arrested root growth phenotype of *gapcp1gapcp2* to a variable degree depending on the construct (Figure 4.2A and B).

Further experiments were performed with a seed pool of the best two lines for each construct. TPT-GFP fluorescence confirmed that the protein was localized in the plastids of both roots and aerial part (Figure 4.2B). TPT-His expression in roots was confirmed by Western blot using antibodies against the His-tag of the fused protein (Figure 4.2D).

When grown on plates, the root length of the *35S:TPT-GFP* lines were significantly higher than that of *gapcp1gapcp2*, but were still shorter than that of WT (Figure 4.4A and B). In the *35S:TPT-His* lines, the root phenotype of *gapcp1gapcp2* was almost fully complemented, reaching 90% of the final WT length. In both cases, the increase in root growth correlated with an increase in AP biomass (Figure 4.4C). These findings provide evidence that *TPT* overexpression complements *gapcp1gapcp2* root and aerial part growth inhibition, but to a different extent depending on the construct used. For this reason, we decided to further study the activity of the TPT in *gapcp1gapcp2* roots in the *35S:TPT-His* lines.

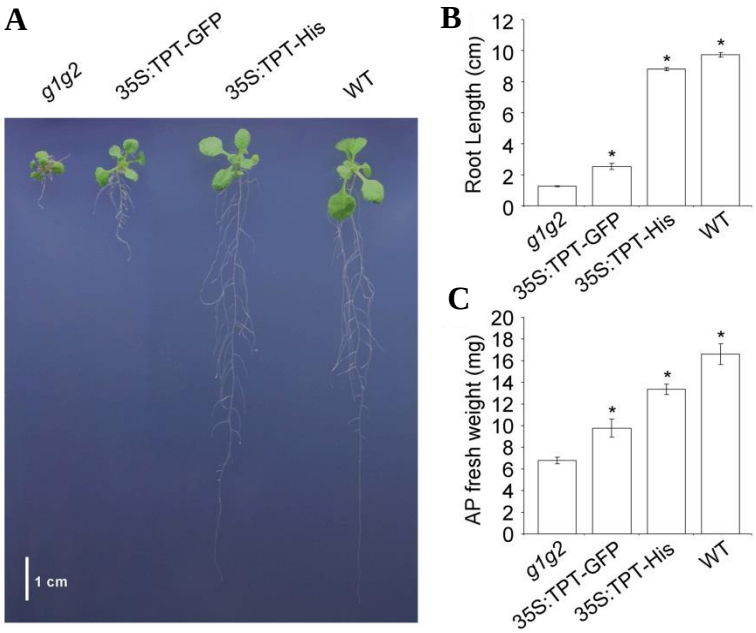

Figure 4.4. Phenotypical analysis of *gapcp1gapcp2* (*g1g2*) expressing TPT-GFP or TPT-His under the control of *35S* promoter (*35S:TPT-GFP*, *35S:TPT-His*). (A) Picture of a representative individual of *g1g2*, *g1g2* expressing TPT-GFP (*35S:TPT-GFP*), *g1g2* expressing TPT-His (*35S:TPT-His*) and wild-type plants (WT) grown on vertical plates for 12 days. In (B) and (C) the root length and fresh weight of the aerial parts (AP) of *g1g2*, *35S:TPT-GFP*, *35S:TPT-His* and WT are shown. Values are the mean ± SE of two independent transgenic lines ($n \geq 30$ plants). * Significantly different as compared to *g1g2* ($P < 0.05$), according to T-student test.

The activity of the TPT transporter, which exchanges 3-PGA with P_i in a strictly coupled antiport system, has been described in AP (Weber et al., 2005). However, in roots, where *TPT* expression is low, the 3-PGA pools of the cytosol and stroma could remain compartmented. According to our initial hypothesis, *TPT* expression in roots could transport 3-PGA from the cytosol to plastids to counteract the deficiency in this organelle caused by lack of GAPCp activity. To test for presence of TPT activity in roots of the overexpression lines, we reconstituted detergent-solubilized root extracts from the different lines into liposomes, followed by radioactive flux-assay transport experiments in which we determined the rate of uptake of $^{32}P_i$ into the proteoliposomes preloaded with 10 mM 3-PGA as an internal counter-exchange substrate. To distinguish between the activity of the glucose phosphate transporter (GPT) and TPT, in addition to Pi, the external medium contained either an excess of G6P or 3-PGA. Pre-loaded proteoliposomes reconstituted with extracts from *35S:TPT-His* lines displayed much higher transport activity which was dependent of 3-PGA when compared with those made of material from WT or from the TPT mutant *ape2* (Figure 4.5A). The transport activity of the *35S:TPT-His* lines was strongly inhibited by the presence of 3-PGA in the external medium but not by G6P (Figure 4.5B), which agrees with the described selectivity properties of the TPT transporter (Fischer et al., 2002). Taken together, these findings strongly indicate a direct correlation between 3-PGA transport by TPT in roots and the complementation of the arrested root phenotype of *gapcp1gapcp2*.

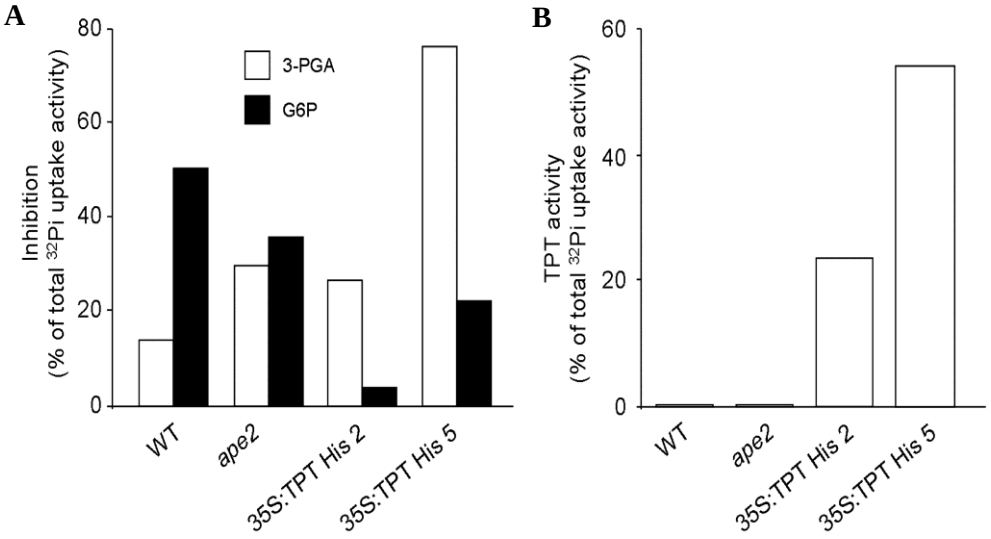

Figure 4.5. TPT activity in reconstituted liposomes from membrane extracts of *gapcp1gapcp2* (*g1g2*) expressing TPT-His under the control of *35S* promoter, TPT mutant (*ape2*) and wild-type plants (WT). (A) Inhibition rate, (B) TPT activity. 3-PGA, 3-phosphoglycerate; G6P, Glucose 6-phosphate.

4.1.1.3. Metabolomic analysis confirmed the complementation of *gapcp1gapcp2* metabolic disorders.

Lack of GAPCp activity leads to a drastic alteration of the plant metabolite profile (Anoman et al., 2015). According to Principal Component Analysis (PCA), the metabolite profile of the aerial part and roots of *35S:TPT-His* lines differs from that of *gapcp1gapcp2*, but is similar to that of WT (Figure 4.6). Thus, in the *35S:TPT-His* AP lines, 76% of metabolites (45 of 59) were significantly different to those of *gapcp1gapcp2*, but only 22% (13 of 59) significantly differed from WT (Table S3, see Appendix). In roots, the relative level of 81% of metabolites analysed in the *35S:TPT-His* lines (39 of 48 metabolites) significantly differed from those of *gapcp1gapcp2* but only 35% of them significantly differed from WT (Table S4, see

Appendix). Accordingly, the Tukey *post hoc* test of the ANOVA of the first principal component grouped the samples from both AP and roots into two different subsets, one including WT and the *35S:TPT-His* lines, and another including *gapcp1gapcp2* (Figure 4.6).

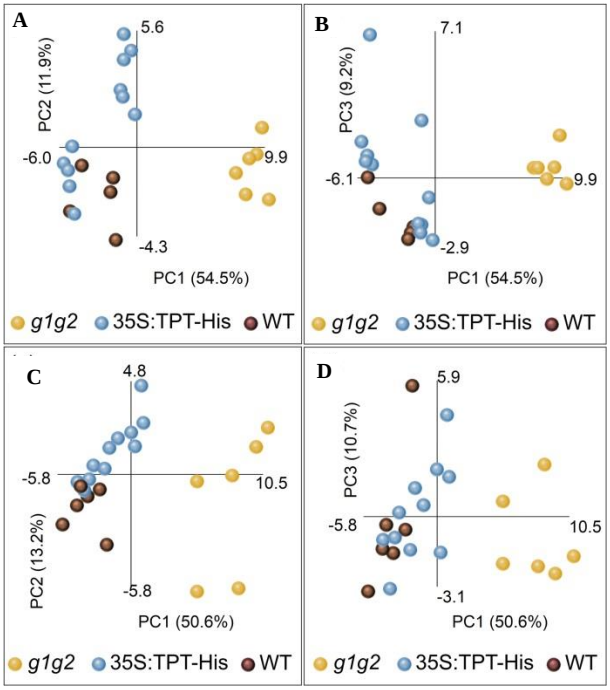

Figure 4.6. Principal component analysis (PCA) of the metabolite profiles of *gapcp1gapcp2* (*g1g2*), *g1g2* expressing TPT-His under the control of *35S* promoter (*35S:TPT-His*) and wild-type plants (WT). Data from the GC-MS analysis were evaluated using the PCA with the three first components accounting for at least 74.5% of total metabolic variance. Values in parentheses give the relative contribution of each component to the total variance observed in the data set. The first principal component was also used for the ANOVA of different lines, with Tukey *post hoc* tests to differentiate between lines. (A) PC1 *vs* PC2 of the metabolites from aerial parts (AP). (B) PC1 *vs* PC3 of the metabolites from AP. (C) PC1 *vs* PC2 of the metabolites from roots. (D) PC1 *vs* PC3 of the metabolites from roots. According to Tukey's test two different subsets are established in both AP and roots: subset 1 (WT and *35S:TPT-His* lines) and subset 2 (*g1g2*).

In a previous study we identified several metabolites modified systematically in the AP and/or roots of *gapcp1gapcp2* under all different

assayed conditions (end of the night, middle of the light period, end of the light period and in the presence of sucrose), which helped narrow down the identification of the most important pathways affected by GAPCp activity (Anoman et al., 2015). Changes in 11 of 12 of these metabolites in the AP, and all of them (11 metabolites) in roots reverted to or approached the WT levels in the complemented *35S:TPT-His* lines (see Apendix, Tables S3 and S4).

Table 4.1. Levels of metabolites in the aerial parts (AP) of *gapcp1gapcp2* (*g1g2*) and *g1g2 35S:TPT-His* (*35S:TPT-His*) lines as compared to wild-type (WT) controls. The chosen metabolites are those that were systematically modified in *g1g2* under all previously assayed conditions when compared to WT (Anoman *et al*., 2015). Metabolites in italics are those that significantly changed more than 20% following GAPCp1 induction in conditional mutants (Anoman *et al*., 2015). Numerical values are relative values normalized to the mean response calculated for WT. Values represent the mean ± SE of 5-6 independent determinations for WT and *g1g2* and 11-12 determinations for the *35S:TPT-His* lines (two different lines). Values that are significantly different from WT according to T-student test are shown in bold, and those that significantly differed from *g1g2* are followed by *, ($P < 0.05$). The full data sets are shown in Table S1.

Metabolites	WT	*g1g2*	*35S:TPT-His*
Citrate	1 ± 0.15	**2.02 ± 0.07**	0.93 ± 0.05*
Fructose	1 ± 0.02	**2.01 ± 0.04**	1.05 ± 0.11*
Fructose-6-P	1 ± 0.02	**0.72 ± 0.02**	0.85 ± 0.06
GABA	1 ± 0.06	**1.27 ± 0.04**	**1.36 ± 0.04**
Galactinol	1 ± 0.06	**2.72 ± 0.10**	0.92 ± 0.05*
Glucose	1 ± 0.03	**1.61 ± 0.11**	0.93 ± 0.10*
Glucose-6-P	1 ± 0.02	**0.73 ± 0.03**	0.97 ± 0.07*
Glutamine	1 ± 0.05	**1.74 ± 0.09**	1.06 ± 0.10*
Glycerate	1 ± 0.08	**3.09 ± 0.38**	**1.25 ± 0.05***
Myo-inositol	1 ± 0.02	**2.14 ± 0.03**	1.24 ± 0.07*
Phosphoric acid	1 ± 0.07	**0.22 ± 0.02**	0.91 ± 0.05*
Trehalose	1 ± 0.02	**2.66 ± 0.05**	1.10 ± 0.03*

Table 4.2. Levels of metabolites in the roots of *gapcp1gapcp2* (*g1g2*) and *g1g2 35S:TPT-His* (*35S:TPT-His*) lines as compared to wild-type (WT) controls. The chosen metabolites are those that were systematically modified in *g1g2* under all previously assayed conditions when compared to WT (Anoman *et al*., 2015). Metabolites in italics are those that significantly changed more than 20% following GAPCp1 induction in conditional mutants (Anoman *et al*., 2015). Numerical values are relative values normalized to the mean response calculated for WT. Values represent the mean ± SE of 5-6 independent determinations for WT and *g1g2* and 11-12 determinations for the 35S:TPT-His lines (two different lines). Values that are significantly different to WT according to T-student test are shown in bold, and those that significantly differed from *g1g2* are followed by *, ($P < 0.05$). The full data sets are shown in Table S2.

Metabolites	WT	*g1g2*	*35S:TPT-His*
Alanine, D, L	1 ± 0.23	**3.41 ± 0.66**	1.74 ± 0.23*
Asparagine	1 ± 0.12	1.11 ± 0.05	0.92 ± 0.05*
Fructose	1 ± 0.04	**4.44 ± 0.09**	1.00 ± 0.05*
GABA	1 ± 0.15	**2.93 ± 0.42**	**1.74 ± 0.20***
Galactinol	1 ± 0.06	**1.71 ± 0.03**	1.25 ± 0.10*
Glutamine	1 ± 0.11	**2.34 ± 0.24**	0.99 ± 0.08*
Glycerate	1 ± 0.05	**5.53 ± 0.26**	**1.65 ± 0.06***
Myo-inositol	1 ± 0.05	**3.86 ± 0.10**	**1.38 ± 0.09***
Raffinose	1 ± 0.25	**2.20 ± 0.19**	1.42 ± 0.14*
Serine	1 ± 0.04	**0.86 ± 0.04**	1.18 ± 0.06*
Trehalose	1 ± 0.10	**2.87 ± 0.06**	1.11 ± 0.04*

We previously demonstrated that many of these metabolites rapidly recovered WT levels following *GAPCp1* induction in conditional mutants (Anoman et al., 2015). Three of them, glutamine, glycerate and galactinol, were altered under all the experimental conditions assayed in both the roots and AP of *gapcp1gapcp2*, displayed the most important changes after *GAPCp1* induction in conditional mutants, and were considered metabolite targets of GAPCp activity (Anoman et al., 2015). Glutamine and galactinol were completely normalized in the AP and roots of *35S:TPT-His* lines as compared to WT while glycerate was reduced by more than 60% and 70% in the AP and root as compared to *gapcp1gapcp2* respectively (Table 4.1 and 4.2). Changes in serine content were also particularly interesting because we postulated that the main sink of the 3-PGA produced by the GAPCp and PGKp would be the plastidial localized PPSB. The level of this amino

acid in the roots of *35S:TPT-His* lines increased in comparison to *gapcp1gapcp2* (Table S4, see Appendix). When looking at the relative level of Ser, in comparison to the total amino acid content, it was 7% in *gapcp1gapcp2*, 14% in *35S:TPT-His* lines and 13% in the WT (Figure 4.7).

Plastidial 3-PGA may also be potentially converted into PEP by PGM and ENO, which can subsequently be converted into acetyl-CoA for fatty acid biosynthesis (Figure 1.3).

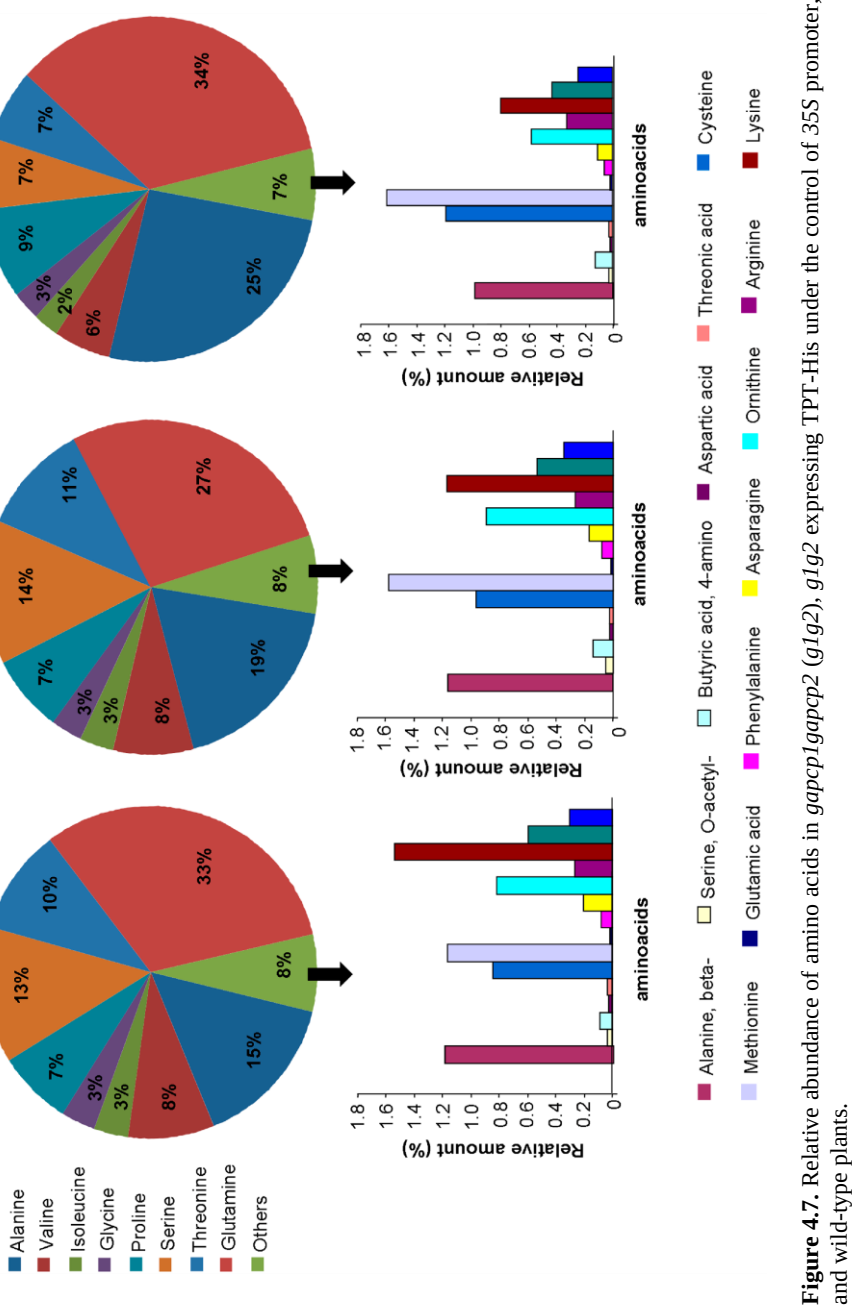

Figure 4.7. Relative abundance of amino acids in *gapcp1gapcp2* (*g1g2*), *g1g2* expressing TPT-His under the control of 35S promoter, and wild-type plants.

4.1.1.4 *TPT* expression under the control of the *GAPCp* promoter leads to a full complementation of the homozygous *gapcp1gapcp2*

The above results demonstrate that *TPT* expression under the control of *35S* suffices to restore the majority of the developmental and metabolic defects associated with *gapcp1gapcp2* vegetative development. Yet, in addition to the growth inhibition of roots and AP, *gapcp1gapcp2* also displays a male sterile phenotype which leads to plants with small siliques with no seeds (Muñoz-Bertomeu et al., 2010). None of the *35S:TPT-GFP* lines were fertile. However, the *35S:TPT-His* lines with the highest *TPT* expression (3 of 7 lines) were fertile (Figure 4.8A).

We demonstrated that *GAPCp* genes have a very low expression level compared to the strong expression of the *35S* promoter. However, the *GAPCp1* promoter is specifically expressed in some cell types, such as the tapetal cell layer during pollen development, where the *35S* is poorly or non-expressed. We transformed *gapcp1gapcp2* with a construct that carried *TPT-His* under the control of the *GAPCp1* promoter *(GAPCp1:TPT-His*) to specifically express *TPT* only in those cell types where GAPCp is required. This construct not only fully complemented all *gapcp1gapcp2* vegetative developmental defects in seedling and adult stages, but also restored fertility in mutant plants (Figure 4.8B-F). A comparison of all the different lines in the seedling and adult stages indicates that in all measured parameters (root length and aerial part fresh weight in seedlings; shoot length, shoot weight and leaf area in the adult stage) the *GAPCp:TPT-His* lines performed similarly or better than the *35S:TPT-His* and the *35S:TPT-GFP* lines (Figure 4.8A-F). The improved growth of transgenic lines followed the order *GAPCp:TPT-His* > *35S:TPT-His* > *35S:TPT-GFP*. These results suggested that TPT was absent in those cell types where GAPCp was functionally significant. A co-expression study using the GENEVESTIGATOR tools (https://genevestigator.com/gv/) showed a

negative correlation (-0.67) at the anatomical level between the expression of *GAPCp1/GAPCp2* and that of *TPT*. *GAPCp1/GAPCp2* also correlated negatively with other genes that code for proteins involved in photosynthesis (data not shown) including the photosynthetic GAPDH subunits GAPA and GAPB with a negative correlation of -0.67 for both genes.

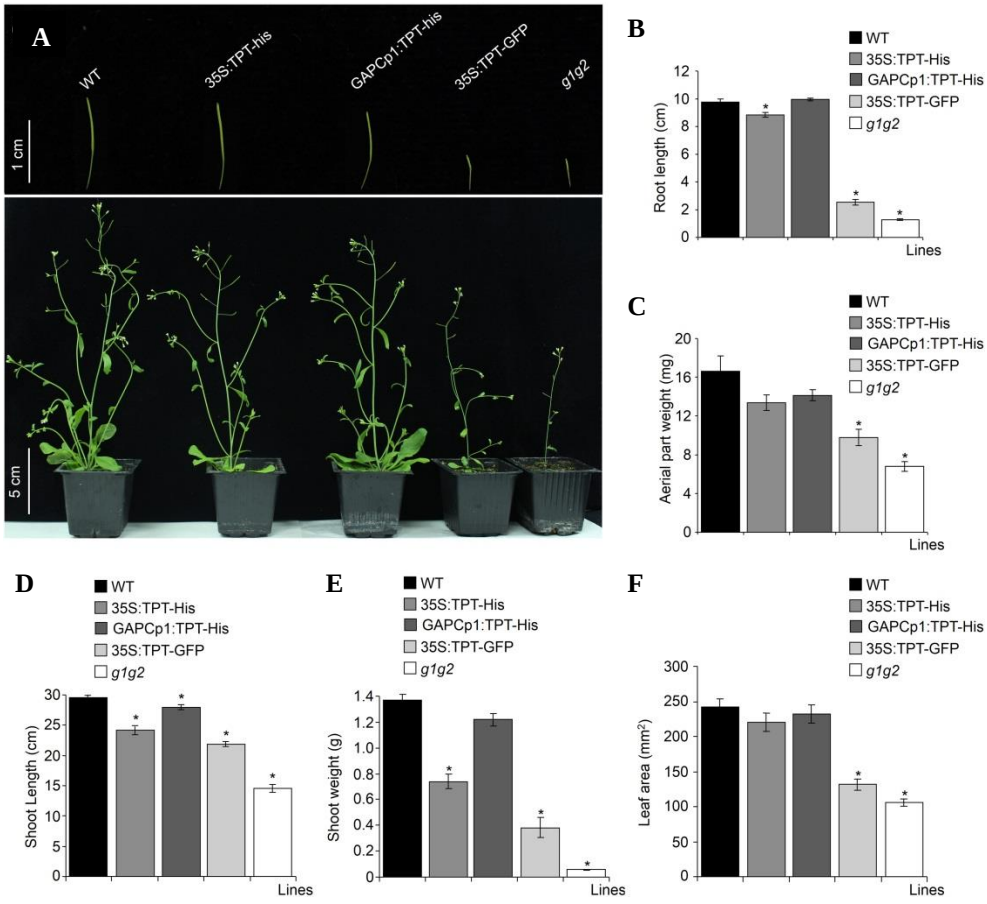

Figure 4.8. Phenotypical characterization of *gapcp1gapcp2* (*g1g2*), *g1g2* expressing TPT-His (*35S:TPT-His*) or *TPT-GFP (35S:TPT-GFP*) under the control of *35S* promoter, *g1g2* expressing *TPT-His* under the control of the *GAPCp1* promoter (*GAPCp1:TPT-His*) and wild-type plants (WT). (A) Primary root length and (B) Aerial part (AP) fresh weight of 12-days-old seedlings grown on vertical plates. (C) Morphology of siliques (top) and adult plants (bottom). In d, e and f shoot length (D), shoot fresh weight (E) and leaf area (F) of 45-days-old adult plants grown in the greenhouse are shown. Values are the mean ± SE of two independent transgenic lines ($n \geq 36$ plants). * Significantly different as compared to WT ($P < 0.05$), according to T-student test.

4.1.2 DISCUSSION

4.1.2.1 *gapcp1gapcp2* phenotypes can be complemented by cell type specific expression of the TPT

We demonstrated that *TPT* expression in *gapcp1gapcp2* roots complements the mutant root developmental arrest to a different extent depending on the promoter driving transgene expression and on the *TPT* fused tag. When *TPT* was expressed under the control of the *35S* promoter, the TPT-His fusion protein complemented the root phenotype more strongly than TPT-GFP. A potential reason for this difference could be a diminished TPT transporter activity as a consequence of fusion to GFP. The TPT transporter needs a specific 3D structure to be inserted into the membrane and to be fully active. Our data suggest that His-tag would affect TPT activity less than GFP-tag.

Like *gapcp1gapcp2*, all the *35S:TPT-GFP* lines and most of the *35S:TPT-His* lines were male-sterile. The low or null expression of the *35S* promoter in cell types essential for male gametophyte development, i.e. the anther tapetum cell layer, where GAPCp activity has been demonstrated to be required (Muñoz-Bertomeu et al., 2010), may explain this phenotype. The results presented herein, are consistent with those of previous studies in which *GAPCp* expression under the control of the *35S* promoter failed to complement the sterile phenotype of *gapcp1gapcp2* (Muñoz-Bertomeu et al., 2010). However, a few of the *35S:TPT-His* lines were fertile. We think that this is probably related to the amount of protein required for complementation since the required protein content of a transporter may be lower than that for an enzyme. *TPT* expression under the control of the *GAPCp* promoter allowed the transporter to be expressed only in those cell types where and when GAPCp is needed in a dose-dependent manner. In

this case, full complementation of root and male sterile phenotypes was achieved, which confirmed that TPT is required to provide the product of GAPCp activity in these specific cell types.

The full complementation of *gapcp1gapcp2* metabolic and developmental phenotypes by *TPT* expression suggests that the main, if not the only, function of GAPCp, along with PGKp, is to supply 3-PGA for anabolic pathways. Other functions have been proposed for GAPCp in combination with PGKp, such as production of NADH or ATP. These functions might not be crucial for several reasons: i) ATP can be produced endogenously in the plastid by other enzymes, such as pyruvate kinase or can be transported from the cytosol through ATP transporters (Reiser et al., 2004); ii) NADH can be provided by the pyruvate dehydrogenase reaction in plastids, and also by import of reducing equivalents generated in the mitochondria or cytosol (Schwender et al., 2003); iii) ATP and NADH levels are not limiting in *gapcp1gapcp2* plastids since the supply of the end product, 3-PGA, overrides its developmental defects. Previous results have indicated that GAPCp activity is not required in photosynthetic cells (Anoman et al., 2015). Our results here demonstrate a negative correlation between the GAPCp and TPT activity, which suggests that the enzyme is only functionally important in heterotrophic cells where TPT is inactive.

4.1.2.2 3-PGA pools are not equilibrated between plastids and cytosol in heterotrophic cells

It is known that plastidic and cytosolic glycolytic pathways interact through highly selective transporters present in the inner plastid membrane (Weber et al., 2005). This fact, along with metabolic flux analysis studies, has led to the suggestion that key glycolytic intermediates are equilibrated between the compartments (Schwender et al., 2003). Although this statement may be true for some plastids, such as the green photosynthetically active chloroplast, it should not be generalized to all plastid types because some may be devoid of certain transport activities, which would impair such equilibration. We have provided genetic evidence, using the *35S:TPT-His* lines, indicating that when *TPT* is expressed in roots, it can transport 3-PGA, and that this transport is able to re-establish metabolic homeostasis in *gapcp1gapcp2*. This clearly indicates that; (i) a 3-PGA deficiency exists inside the plastid in this mutant; (ii) the 3-PGA pools are not equilibrated between heterotrophic plastids and the cytosol. Therefore, the native TPT is not functional in root cells. These results would argue against a function for the TPT translocator in non-green plastids; for instance, as an NADPH reducing equivalent shuttle, or catalyzing Triose-P import into storage plastids during starch synthesis, as proposed in earlier studies (Echeverria et al., 1988; Brautigam et al., 2009). In addition to the triose-3-PGA/Pi translocators several other plastidic phosphate translocators have been identified in *Arabidopsis*, which include the glucose phosphate/Pi translocators, the PEP/Pi translocators or the xylulose phosphate/Pi translocators (Weber et al., 2007; Fischer et al., 1997; Eicks et al., 2002; Kammerer, 1998). Some of them, such as the glucose-phosphate or the

xylulose phosphate translocators, are located in heterotrophic plastid membranes, and their capacity to transport 3-PGA in *in vitro* experiments has been demonstrated (Fischer et al., 2002; Fischer, 2011). Our data indicate that the activity of such transporters in roots does not suffice to compensate for lack of GAPCp activity suggesting that their capacity to transport 3-PGA *in vivo* is limited.

4.1.2.3 Metabolic pathways dependent on GAPCp activity

In addition to the photosynthetic reactions, a huge variety of other metabolic pathways occur in the plastid, including the biosynthesis of fatty acids and amino acids. The 3-PGA transported by TPT to the plastids in the *35S:TPT-His* lines could be directly used for serine biosynthesis through the PPSB or could fuel the downstream reactions of the lower part of the glycolytic pathway catalyzed by PGM and ENO. The complementation of *gapcp1gapcp2* root developmental defects by externally supplied serine (Muñoz-Bertomeu et al., 2009) in a similar way to that obtained when overexpressing the *TPT* transporter, along with the increase in serine content in the roots of the *35S:TPT-His* lines, indicates that the PPSB is probably the main 3-PGA sink in the plastid. However, the seed fatty acid content of *35S:TPT-His* lines was also increased indicating that, at least in the metabolic conditions present in these lines, part of the plastidial 3-PGA is likely converted into the precursor of fatty acids acetyl-CoA (Figure 1.3). Based on available data, a complex partitioning model between the cytosol and plastids of carbon flux from sucrose to fatty acid synthesis has been postulated (Andriotis et al., 2010). The lack of strong phenotypes of

plastidial ENO and PGM (Andriotis et al., 2010) and the strong phenotypes of mutants lacking the plastidial pyruvate kinase (Andre et al., 2007; Baud et al., 2007) led Andriotis et al.(2010) to suggest that, in oilseed embryos, all the 3-PGA made in the plastid may be exported to the cytosol to be converted into PEP, and most or all of it must then move back into the plastids to be converted into pyruvate (Figure 1.3). This suggestion implies that the main source of precursors for fatty acid biosynthesis comes from the cytosol through the PEP transporter. Our data indicate that in *Arabidopsis* seeds, another alternative pathway may occur in which the plastidial 3-PGA could be directly used for fatty acid biosynthesis without the need for a by-pass through the cytosolic glycolytic pathway. This implies that PGM and ENO are able to produce PEP in the plastid, which is then converted into the fatty acid precursor acetyl-CoA. This model is supported by the fact that the double mutant of the PEP translocator and the plastidial ENO is lethal, while both single mutants are viable, and by the rescue of the PEP translocator mutant phenotypes by overexpression of the plastidial ENO (Prabhakar et al., 2010). It may be possible that the plastidial pathway is of lower importance under physiological conditions and that we are only observing the effect of an overexpression effect of the *TPT* transporter. However, our data suggest that the participation of this pathway in the biosynthesis of fatty acids cannot be excluded.

For years, the physiological function and importance of plastidial ENO and PGM in green and non-green plastids have been a matter of debate (Andriotis et al., 2010; Prabhakar et al., 2010; Van der Straeten et al., 1991; Journet et al., 1985; Miernyk et al., 1992). Indeed, it has been suggested that ENO is the only missing enzyme for a complete glycolytic pathway within

plastids (Prabhakar et al., 2010). Since both PGM and ENO are theoretically reversible, PEP imported from the cytosol through the PEP translocator could provide 3-PGA to the plastids of *gapcp1gapcp2*. This does not seem to be the case in *gapcp1gapcp2*, at least not in a sufficient amount to compensate for lack of GAPCp activity in the mutant. However, the increase in the fatty acid content in the *35S:TPT-His* seeds support the notion that the plastidial ENO and PGM are active in the forward glycolytic direction, at least in some cellular types where they could contribute to the biosynthesis of fatty acids in seeds to a certain degree. These results point out to a physiological role of these isoforms, although their quantitative contribution to plant metabolism will need further investigation.

4.2 Chapter 2:

The phosphorylated pathway of serine biosynthesis is essential for embryo development, male gametophyte and for root growth in *Arabidopsis.*

4.2.1 RESULTS

4.2.1.1 The homozygous *psp1* mutation is embryo lethal

In a previous thesis performed in our laboratory we demonstrated that *psp1.1psp1.1* mutants were lethal (Cascales-Miñana et al., 2013). The segregation analysis of reciprocal outcrosses of *PSP1psp1.1* plants indicated that knocking out *psp1.1* triggers an embryo lethal phenotype (Cascales-Miñana et al., 2013). In order to shed light to this embryo lethal phenotype, siliques from heterozygous *PSP1psp1.1* plants were dissected at different developmental stages. From 8 DAP, we observed a population of abnormal seeds, which was randomly distributed along the length of the silique. At 15 DAP mutant seeds were white and started to deflate (Figure 4.9A). At 22 DAP mutant seeds turned dark brown and were completely deflated (Figure 4.9A). Segregation analysis of a population of 5,064 seeds obtained from heterozygous *PSP1psp1.1* plants revealed a 1:4 ratio (20.9% mutant: 79.1% normal seeds; $x^2 = 2.52$; $P > 0.05$). To characterize the nature of the seed nonviability, we examined the embryos in developing siliques of heterozygous *PSP1psp1.1* plants (Figure 4.9B). At 2 DAP all the embryos examined reached a similar developmental stage. However, at 5 DAP some

of the embryos showed delayed development (early globular versus triangular stage). According to microarray databases, *PSP1* expression is maximal at the globular stage (Cascales-Miñana et al., 2013). The developmentally delayed embryos could be assigned to mutant seeds at 7 DAP (heart versus mid torpedo) and 10 DAP (heart versus early cotyledon stage). The terminal aborted embryos (15 DAP) were albino and could be classified as early curled cotyledons (L1) according to the SeedGenes database (http://www.seedgenes.org).

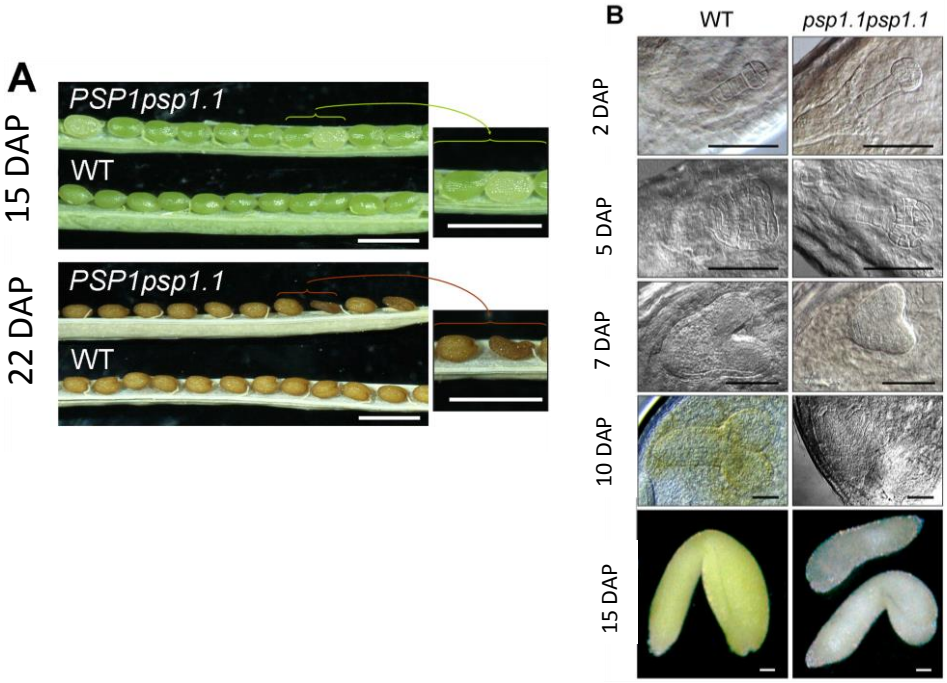

Figure 4.9. *psp1* homozygous mutants die at the embryo stage. (A) Siliques from wild-type (WT) and heterozygous *PSP1psp1.1* plants at 15 and 22 days after pollination (DAP) observed with a binocular microscope. In the *PSP1psp1.1* silique, a population of mutant seeds is observed. The right picture shows a close-up of the mutant seeds. Bars = 1 mm. (B) The micrographs show the embryo development of the wild-type and homozygous *psp1.1/psp1.1* from the same silique at different stages observed with a differential interference contrast microscope (2, 5, 7, and 10 DAP) or with a binocular microscope (15 DAP). Bars = 50 µm.

PCR-based genotyping analysis revealed that the aborted embryos were *psp1.1psp1.1* individuals.

In order to corroborate the phenotype-genotype correlation of the *psp1.1* mutation, *PSP1psp1.1* plants were transformed with a construct carrying the *PSP1* cDNA under the control of either the *PSP1* endogenous promoter (*PSP1:PSP1*) or the *35S* promoter (*35S:PSP1*) (Cascales-Miñana et al., 2013). The embryo-lethal phenotype of *psp1.1psp1.1* individuals was complemented in both cases since homozygous *psp1.1psp1.1* plants were obtained in the segregating population (Cascales-Miñana et al., 2013). However, in the adult stage transgenic *psp1.1psp1.1 35S:PSP1* plants were sterile, producing small siliques with no seeds. A *PSP1* overdose effect was not the cause of the observed sterility phenotype since the WT expressing *35S:PSP1* was fertile (Cascales-Miñana et al., 2013).

4.2.1.2 Lack of phosphoserine phosphatase activity alters pollen and tapetum development in *Arabidopsis*.

As the *35S* promoter exhibits very low expression, or none, in the Arabidopsis tapetum (Muñoz-Bertomeu et al., 2009; Grienenberger et al., 2009), we performed an ontogenic serial analysis of anther and pollen development in *psp1.1psp1.1 35S:PSP1* plants compared with WT. For that purpose, floral buds were classified from stages 7 to 12 according to the landmark events described by (Smyth et al., 1990) and analyzed by transmission electron microscopy.

In the tetrad stage no clear differences were found in the microspores or tapetum cells of WT and *psp1.1psp1.1 35S:PSP1* (Figure 4.10). In both the

mutant and WT, four microspores were present and callose depositions appeared normal and regular (Figure 4.10A and B). In both cases there were small undulations in the membrane of the microspores, which correlated with the future sporopollenin deposition to create the primexine (Figure 4.10C and D). Note that in the *psp1.1psp1.1 35S:PSP1* line, the primexine layer developed slightly more than in the WT in this stage. Regarding tapetal cells, no differences were observed in the structural development of *psp1.1psp1.1 35S:PSP1* compared to WT. They presented two nuclei embedded in a high electron dense cytoplasm filled with organelles (Figure 4.10E and F).

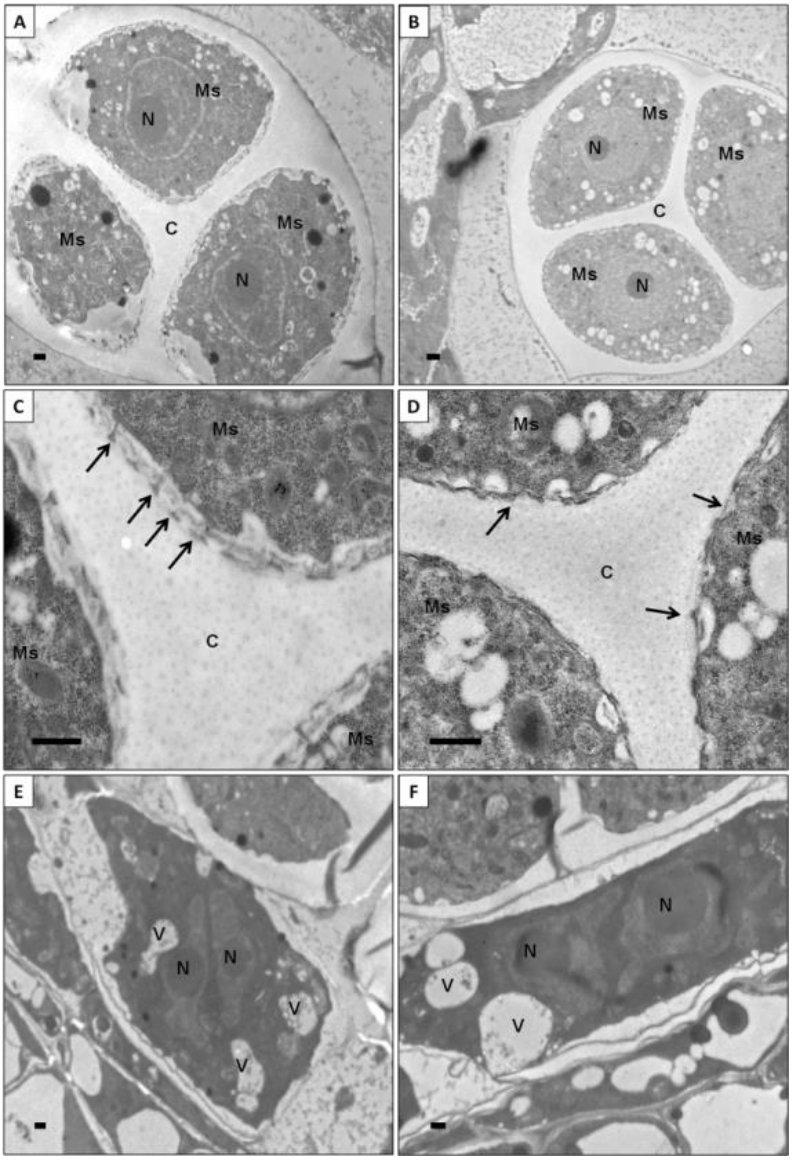

Figure 4.10. Tetrad stage of microspore development. Callose depositions are similar in *psp1.1psp1.1 35S:PSP1* line (A anc C) and wild type (WT)(B and D). It is possible to observe in the microspore surface small undulations where primexine is forming (arrows in C and D). Tapetal cells present no obvious differences in the *psp1.1psp1.1 35S:PSP1* (E) and in the WT (F). C, callose; Ms, microspore; N, nucleus; V,, vesicle. Sacle bar: 500 nm.

After being released from the tetrads, both the WT and *psp1.1psp1.1 35S:PSP1* microspores were round and showed a central nucleus with several organelles surrounding it (Figure 4.11A and B). Homogeneous electron dense sporopollenin depositions, which formed the bacula, the tecta and the nexine of the exine wall, were visible on the surface of the microspore, but no differences in the structure between the *psp1.1psp1.1 35S:PSP1* and WT microspores were seen. The cytoplasmic content of the WT microspore completely filled the space delimited by the microspore wall, while the membrane of the microspore in the *psp1.1psp1.1 35S:PSP1* began to detach from the exine wall, which resulted in a large space between them (Figure 4.11A). In both cases tapetal cells were thick and presented a highly electron dense cytoplasm (Figure 4.11C and D).

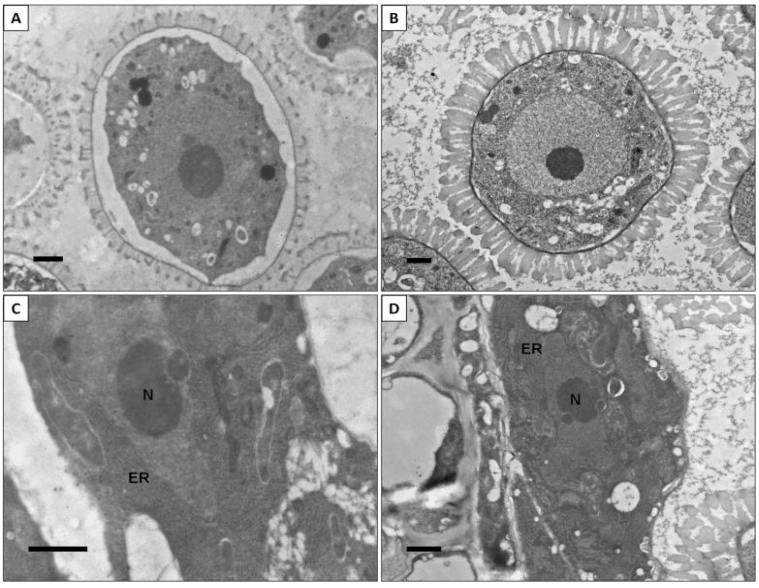

Figure 4.11. Microspores after being released from the tetrad stage. (A) *psp1.1psp1.1 35S:PSP1* microspore with plasma membrane detached from exine wall; (B) Wild-type (WT) microspore. *psp1.1psp1.1 35S:PSP1* tapetal cell (C) and WT (D) are thick, highly active and electron dense. ER, endoplasmic reticulum; N, nucleus. Scale bar: 1 µm.

As shown in Figure 4.12A and B, the microspore began to adopt a trilobular shape in the ring-vacuolated stage and there was no baculum or tectum in those areas where the surface began to constrain. In this stage the sporopollenin formed prominent and highly electron dense bacula and tecta in both the WT and *psp1.1psp1.1 35S:PSP1*. Inside the microspore, all the small vesicles of the cytoplasm that were in the periphery coalesced into a big central vacuole, which displaced the nucleus to the opposite side of the microspore. In the WT, unlike the mutant microspores, many small vesicles were located in the cell periphery, which likely contained material to create the intine layer (Figure 4.12D). In *psp1.1psp1.1 35S:PSP1*, the microspore plasma membrane continued to collapse (Figure 4.12C). Tapetal cells, which still remained thick and active, became less vacuolated in both cases as elaioplasts began to appear in their highly electron dense cytoplasm, these being the first of two densely staining organelles found typically in tapetal cells (Figure 4.12E and F). These elaioplasts were small circular inclusions that are likely to contain steryl esters surrounded by a membrane (Quilichini et al., 2014).

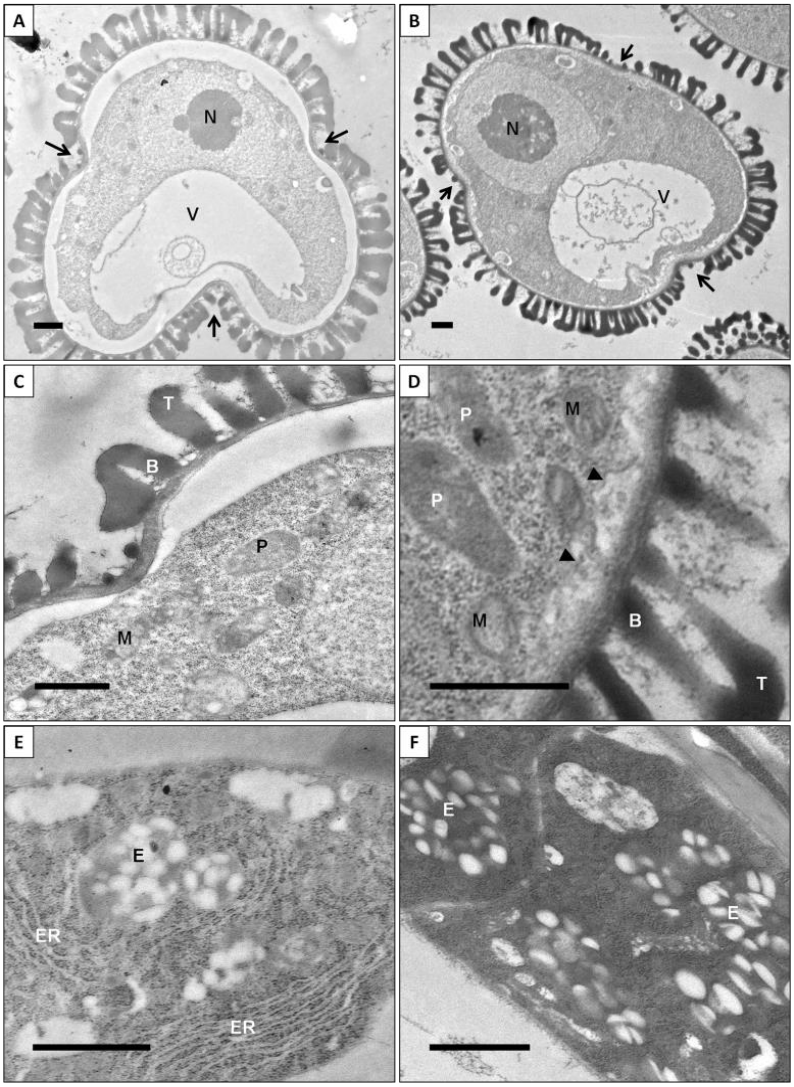

Figure 4.12. Ring vacuolated stage. Microspores of the *psp1.1psp1.1 35S:PSP1* (A and C) and the wild-type (WT)(B and D) present constraining points in the surface (arrows). The nucleus has been displaced to a side by an enormous vacuole (A and B). In the WT (D) it is possible to observe vesicles forming the intine layer (arrow heads). In the tapetal cells of the *psp1.1psp1.1 35S:PSP1* (E) and in the WT (F) elaioplasts begin to appear. B, baculum; E, elaioplast; ER, endoplasmic reticulum; M, mitochondria; N, nucleus; P, plastid; T, tectum; V, vacuole. Scale bar: 1 µm.

After the polarised stage, first mitosis occurred and the differences between the WT and *psp1.1psp1.1 35S:PSP1* microspores became more evident (Figure 4.13A and B). In this stage, the WT microspore was larger and rounder, and the intracellular part changed notably. There were two nuclei: the vegetative cell (the larger one) and the generative cell, surrounded by several small vesicles formed after the disintegration of the bigger vacuole (Figure 4.13B).

Some of these vesicles moved to the membrane surface to release material to finish the formation of the intine (Figure 4.13D). It was also possible to see some highly active organelles, such as the endoplasmic reticulum (ER). However with *psp1.1psp1.1 35S:PSP1*, the microspore was not as round as in the WT, although the exine pattern was normal (Figure 4.13A). The microspore contained a condensed cytoplasm with only one nucleus and a few organelles inside. Furthermore, the large vacuole that displaced the nucleus to the opposite side of the microspore was still present or generated a few other large vacuoles (Figure 4.13A). In tapetal cells, it was possible to see the presence of tapetosomes, where alkanes, flavonoids and oleosines were stored (Figure 4.13E and F)(Quilichini et al., 2014). The cytoplasm of the WT tapetal cells was full of elaioplasts and tapetosomes, which contained oil bodies that accumulate substances to be released into the locule for the formation of the pollen coat (Figure 4.13F). However, elaioplasts were present in *psp1.1psp1.1 35S:PSP1*, but no oil body formation took place inside the tapetosomes (Figure 4.13C).

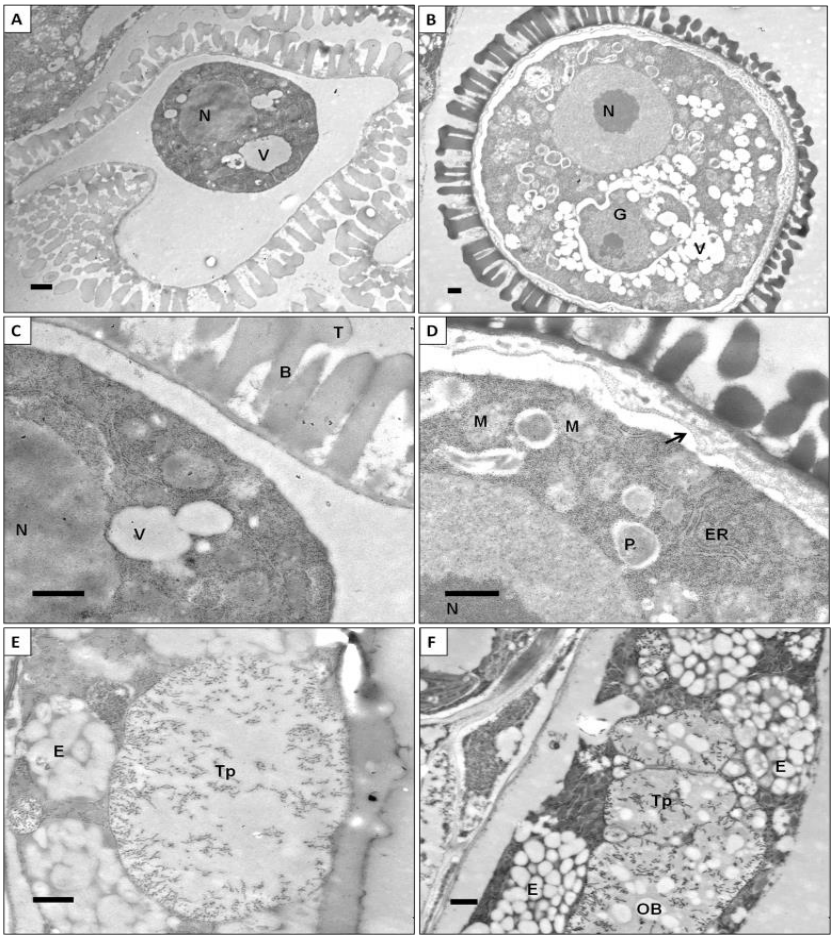

Figure 4.13. Microspores at bicellular stage. In the wild-type (WT) (B) the microspore presents a generative cell surrounded by small vesicles. The *psp1.1psp1.1 35S:PSP1* microspore (A and C) is shrunken, with a detached plasma membrane and no generative cell. In the WT microspore (D) the intine layer is present (arrow), while it is absent in the *psp1.1psp1.1 35S:PSP1* (C). In *psp1.1psp1.1 35S:PSP1* tapetal cells (E) there are tapetosomes without oil bodies, while in the WT microspore (F) the oil bodies are present. B, baculum; E, elaioplast; ER, endoplasmic reticulum; G, generative cell; M, mitochondria; N, nucleus; OB, oil body; P, plastid; T, tectum; Tp, tapetosome; V, vesicle. Scale bar: 500 nm.

In the tricellular stage, the second mitotic division took place and the differences between the WT and *psp1.1psp1.1 35S:PSP1* mutant microspores increased (Figure 4.14A and B). With the WT, the locule of the anther was full of round microspores, in which the spaces between the bacula and tecta in the exine wall were filled completely with the pollen coat to form an electron dense material of various proteins, phenolics and fatty acid derivatives that surrounded the microspore (Figure 4.14D). The different exine and intine layers had completely formed and were distinguishable. The cytoplasm was full of organelles, lipid bodies, starch granules and vesicles (Figure 4.14B). Given the high electron density of the cytoplasm, it was very difficult to see the sperm cells that resulted from the generative cell (Figure 4.14B).

In contrast, the shape of the few *psp1.1psp1.1 35S:PSP1* microspores that remained in the locule of the anther was completely irregular (Figure 4.14A) and the spaces between bacula were absolutely empty and showed no visible pollen coat deposition (Figure 4.14C). The cytoplasm was fully condensed and there were no distinguishable organelles in it. As seen in Figure 4.10A and B, the tapetum had completely disappeared in this development stage.

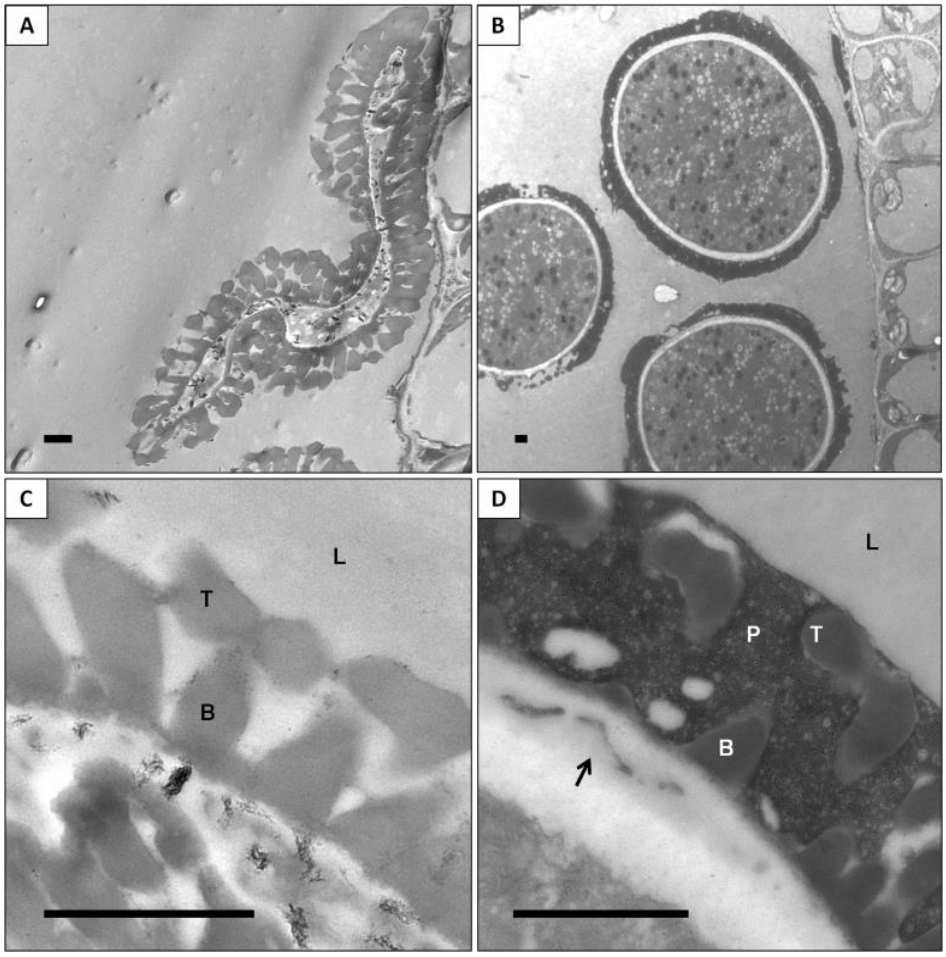

Figure 4.14. Mature microspores in the last stage of development. The *psp1.1psp1.1 35S:PSP1* microspore is completely shrunken (A) and presents a normal exine development but total absence of pollen coat (C). The wild type (WT) microspore is round, full of organelles (B) and the pollen coat is present along with the intine layer (arrow) (D). The tapetum at this stage of development has disappeared. B, baculum; L, locule; P, pollen coat; T, tectum. Scale bar: 1µm.

To confirm which step of gametophyte development was affected by *psp1.1* mutation, we performed Hoechst staining of microspore nuclei from *psp1.1psp1.1 35S: PSP1* plants at different developmental stages (Figure 4.15). For this experiment, the most normally shaped microspores at the last stages of development were selected since most of them were seriously malformed. Nucleus staining corroborated that tetrad and polarized microspore development in *psp1.1psp1.1 35S:PSP1* anthers was normal but in subsequent stages to the polarized microspore stage, development was arrested and no bicellular or tricellular pollen was found. These results indicate that microspores from *psp1.1psp1.1 35S:PSP1* are unable to undergo the double mitosis necessary to reach the mature pollen stage.

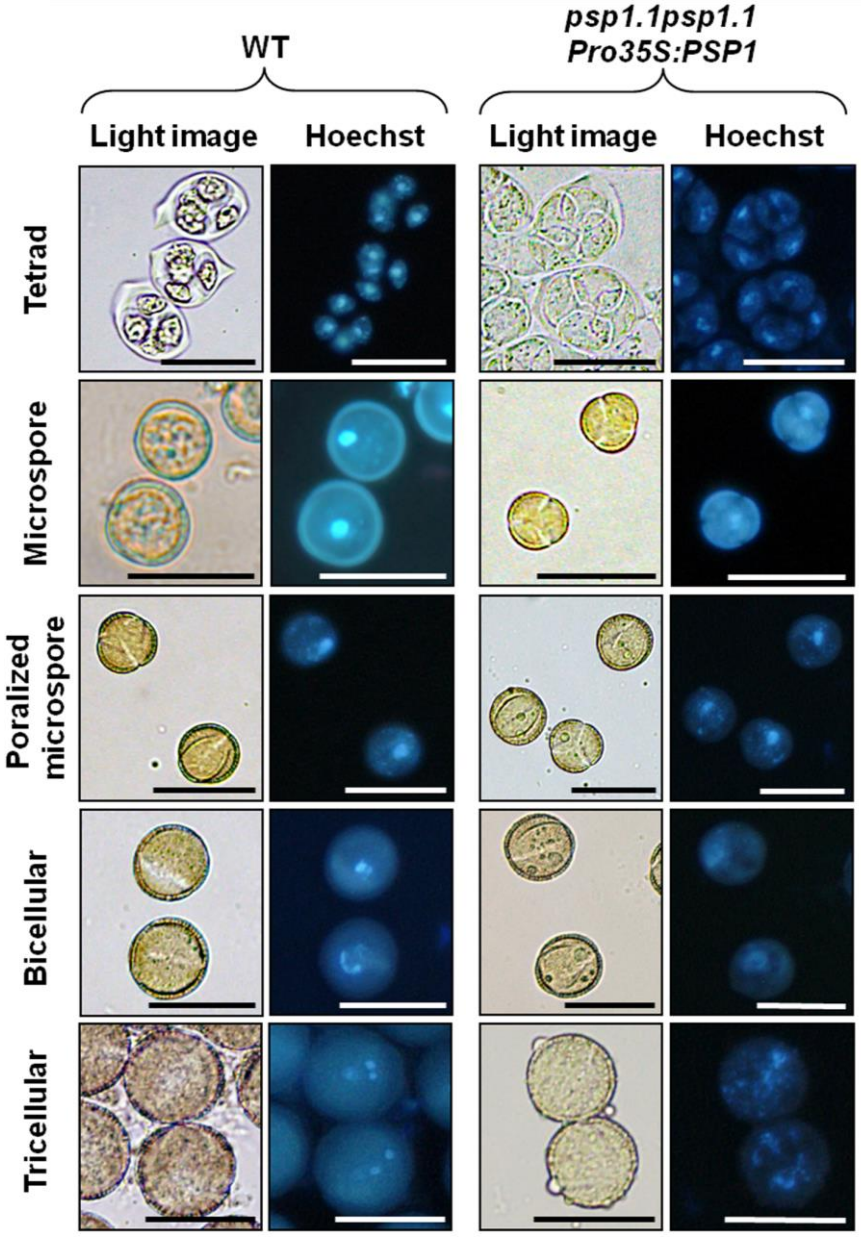

Figure 4.15. Developmental analysis of pollen (from tetrad to tricellular stage) in wild-type and *psp1.1psp1.1 35S:PSP1* plants visualized by Hoecht staining of microspore nucleus. Bars = 25 mm.

4.2.1.3 Primary root growth is impaired in *psp1.1psp1.1 HS:PSP1* mutants

In order to investigate the function of PSP1 in vegetative development, our group obtained conditional *psp1.1psp1.1* mutants (Cascales-Miñana et al., 2013). *PSP1psp1.1* plants were transformed with a construct carrying the *PSP1-GFP* cDNA under the control of the inducible heat-shock promoter *HS18.2* (*HS:PSP1*) (Cascales-Miñana et al., 2013) and homozygous *psp1.1psp1.1* with a single *HS:PSP1* insertion from the segregating T_3 population (*psp1.1psp1.1 HS:PSP1*) were obtained. One of the important features of *psp1.1psp1.1 HS:PSP1* lines is a short root phenotype as compared to the WT. This phenotype was further explored to shed light on the probable cause of its abnormal growth. By using confocal microscopy and propidium iodide as a counterstain, it was possible to analyze the meristematic and differentiated zone of mutant roots compared to the WT (Figure 4.16).

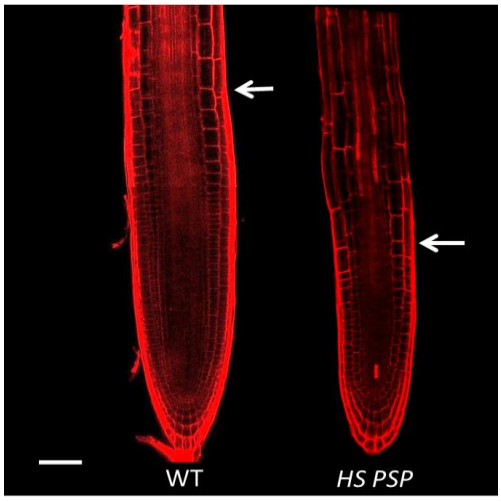

Figure 4.16. Root cellular organisation in the meristem of WT and *psp1.1.psp1.1 HS:PSP* (*HS PSP*) visualised by propidium iodide staining. White arrows indicate the begining of the elongation zone in epidermal cell layers. Scale bar: 50 µm..

As a first approach, the meristematic zone was determined as the root area between the root cap and the first cell, whose size was double compared with the previous cell in the epidermal cell layers. This point is referred to as the "change point". The next 15 cells that started from that point determined the elongation zone. Having determined the study zones, the next step was to calculate the length of the meristematic zone and the number of epidermal cells from the root cap to the change point (Table 4.3).

Table 4.3. Root measurements in WT and *psp1.1psp1.1 HS:PSP1* (HS PSP) lines. In meristems the total length and number of cells were measured. In the elongation zone the total and the individual length of 15 cells were measured. The C1 cell represented the first cell before the change point and C15 the last cell measured. Values are the mean (µm) ± SE; n = 7. Bold values are statistically different from the WT ($p < 0.05$), according to T-student test.

	WT	**HS PSP**
Meristematic zone		
Length	449.92 ± 10.50	**271.50 ± 8.64**
Nº cells	59.00 ± 2.60	**24.28 ± 0.94**
Elongation zone		
Length	63.82 ± 5.20	**41.90 ± 1.43**
C1	1.20 ± 0.16	0.95 ± 0.09
C2	1.53 ± 0.28	1.70 ± 0.23
C3	1.89 ± 0.35	2.16 ± 0.40
C4	2.89 ± 0.64	2.16 ± 0.18
C5	3.09 ± 0.62	3.10 ± 0.33
C6	3.80 ± 0.62	3.18 ± 0.41
C7	4.76 ± 0.69	**2.90 ± 0.19**
C8	4.82 ± 0.55	**2.61 ± 0.24**
C9	5.30 ± 0.62	**3.11 ± 0.31**
C10	5.58 ± 0.46	**3.61 ± 0.14**
C11	5.38 ± 0.49	**3.38 ± 0.15**
C12	4.94 ± 0.35	**3.53 ± 0.32**
C13	5.96 ± 0.27	**3.23 ± 0.23**
C14	6.43 ± 0.25	**3.07 ± 0.14**
C15	6.23 ± 0.30	**3.22 ± 0.24**

The second part was to measure the length of the 15 cells that started from the change point to the elongation zone, and the total length of this part of the root (Table 4.3). As seen in Table 4.3, the WT meristematic zone was 2-fold larger than the mutant meristem. The number of epidermal cells also doubled the WT compared to the mutant. When comparing the elongation zone, once again this area was bigger in the WT compared to the mutant. The fact that the length of the cells was similar at the beginning is interesting. However, the further in the elongation zone, the cells in the mutant greew less than than in the WT. These results indicate that the *psp1.1psp1.1 HS:PSP1* lines display a defect in root cell division and elongation, in which phytohormones, such as auxins, play an important role.

4.2.1.4 "-omic" studies on *psp1.1psp1.1 HS:PSP1*

The conditional expression of genes is a powerful tool in biotechnology in particular, and research in general, as it allows the production of a desired protein in a specific organism within a controlled time frame. As mentioned earlier, six independent conditional *psp1.1psp1.1 HS:PSP1* lines were obtained in a previous work. Based on the induction pattern, three lines, which showed the lowest protein background expression level under non-induced conditions and the highest level of induction after heat-shock treatment, were selected for further analysis.

4.2.1.4.1 PSP1 expression in conditional mutants

Having selected the lines, a time-course experiment was run to decide the best time to pick up samples for both the transcriptomics and metabolomics studies. The relative expression levels were measured by qRT-PCR and showed that the three selected *psp1.1psp1.1 HS:PSP1* lines displayed a peak of *PSP1* mRNA 1h after induction (Figure 4.17).

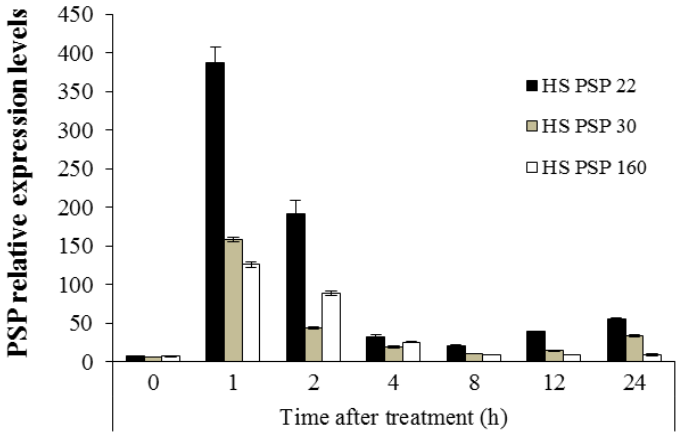

Figure 4.17. Time-course analysis of relative *PSP1* expression in three different *psp1.1.psp1.1 HS:PSP* (*HS PSP*) lines.

In order to evaluate the abundance of the fused PSP1-GFP protein in *psp1.1psp1.1 HS:PSP1* before and after induction, a western blot was performed (Figure 4.18).

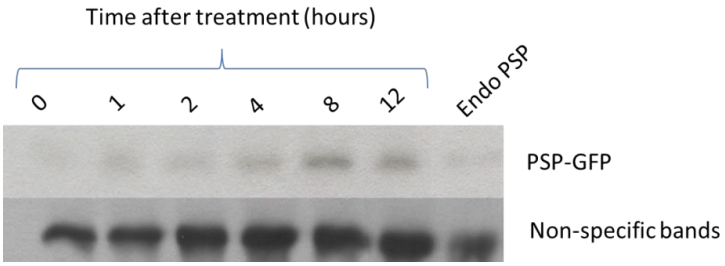

Figure 4.18. Time-course analysis of PSP1 protein expression in a *psp1.1.psp1.1 HS:PSP1* (*HS PSP*) line.

As in the previous experiment, this evaluation was made with whole seedlings of *psp1.1psp1.1 HS:PSP1*. The result showed that the PSP protein reached a peak 8h after induction and was still present 12h after induction. Both results from the abundance of *PSP1* mRNA and the protein after induction of the *psp1.1psp1.1 HS:PSP1* gave us the chance to select the ideal time point to perform the metabolomics and transcriptomic experiments. We assumed that translation was resumed mostly in *Arabidopsis* 1h after heat-shock treatment at 37°C (M. Castellano, personal communication). Since *PSP1* had to be translated to participate in PPSB before having an effect on transcription, we chose 4h after induction to run the transcriptomic experiments and 8h after induction for the metabolomics experiments.

4.2.1.4.2 Metabolic profile of psp1.1psp1.1 HS:PSP1 under several conditions

Since PPSB could perform specific functions under daylight/dark conditions or in heterotrophic organs, for the metabolomics studies aerial parts and roots of the *psp1.1psp1.1 HS:PSP1* and WT lines were sampled under different conditions (light at ambient CO_2, light at high CO_2 levels, end of dark period). For each condition, one group (*psp1.1psp1.1 HS:PSP1* and WT) was heat-shock induced for 1h at 37ºC before sampling, while the other did not receive the heat-shock treatment. Some samples were grown in the presence of 0.1 mM Ser in the growth medium. 8h after induction, the plants grown under the different conditions were harvested and processed to analyze their metabolic profile in both aerial parts and roots.

In order to study the behavior of samples, a PCA of the analyzed metabolite profile was performed (Figure 4.19).

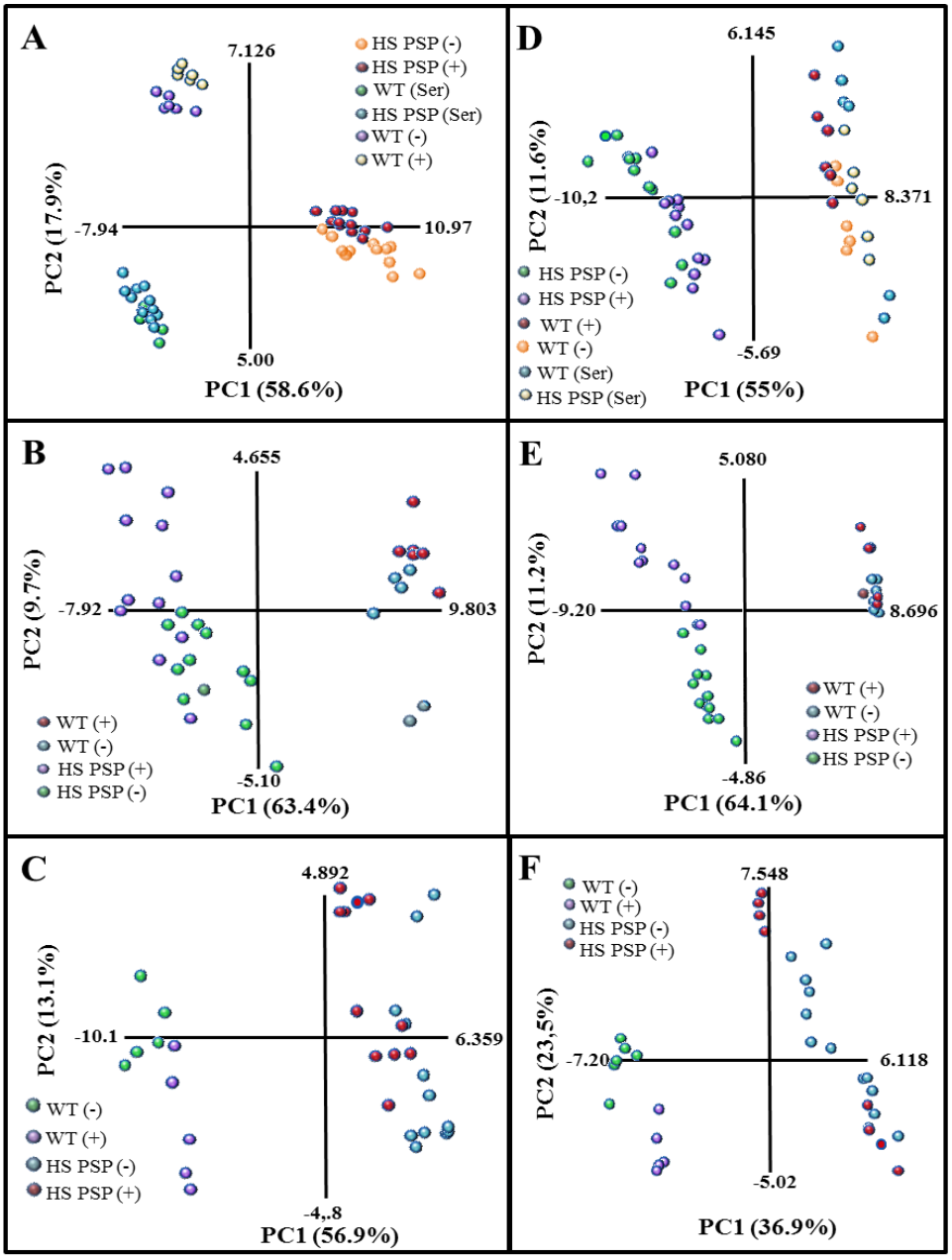

Figure 4.19. Legend in the next page.

Figure 4.19. Principal component analysis (PCA) of the metabolite profile of *psp1.1psp1.1 HS:PSP1* (*HS PSP*) and WT grown under different conditions with (+) or without (-) heat-shock treatment. A, light aerial part with (Ser) and without Ser in the growing medium;; B, darkness aerial part; C, High CO_2 aerial part; D, light roots; E, darkness, roots; F, High CO_2, roots. Data from the GC-MS analysis were evaluated using the PCA with the two first components accounting for at least 60% of total metabolic variance. Values in parentheses give the relative contribution of each component to the total variance observed in the data set.

In the aerial part and under the light conditions at ambient CO_2 (light conditions) the PCA analysis showed that when plants were grown with Ser in the medium, the *psp1.1psp1.1 HS:PSP1* and WT samples were grouped together, but not with that of the WT grown without Ser. However, when plants were grown with no Ser in the growing medium, the WT and *psp1.1psp1.1 HS:PSP1* samples were clearly separated in different quadrants of the of the PCA, which suggests that the Ser provided by PPSB is the main metabolite whose lack affects *psp1.1psp1.1 HS:PSP1* line metabolism. PSP1 induction did not affect the PCA sample distribution in the *psp1.1psp1.1 HS:PSP1* lines, but as shown later, some metabolites were specifically altered. The PCA analysis of the samples collected at the end of the dark period (darkness) and the samples from the plants grown under high CO_2 (CO_2 conditions) indicated that WT and *psp1.1psp1.1 HS:PSP1* were also distributed in the different PCA analysis quadrants (Figure 4.19B). PSP induction did not revert the differences between the WT and mutant lines, but replicates of *psp1.1psp1.1 HS:PSP1* either with or without PSP induction did not completely overlap and tended to localize in the different PCA quadrants, especially in those samples from the darkness conditions (Figure 4.19B).

In the roots of plants grown in the presence of Ser, *psp1.1psp1.1HS:PSP1* samples co-localized with those of WT (Figure 4.19D), which once again

suggests that lack of Ser in some cell types due to the absence of a functional PPSB is the main cause of the metabolic disorders observed in the *psp1.1psp1.1HS:PSP1* lines. Although PSP1 induction did not completely revert the differences between the WT and mutant lines under the different assayed conditions, the replicates of *psp1.1psp1.1 HS:PSP1* either with or without *PSP1* induction did not overlap and clearly localized in different PCA quadrants in the samples taken from the darkness conditions (Figure 4.19E). Thus, the PCA analysis indicated that under darkness conditions *Arabidopsis* could be more affected by lack of PSP1 activity than under light conditions at least in roots.

In aerial parts, although the PCA analysis indicated that when plants were grown in the presence of Ser in the medium, the *psp1.1psp1.1 HS:PSP1* and WT samples are grouped together, many individual metabolites values still significantly differed in both lines. A complet list of all determined metabolites is provided in supplementary tables Tables S5 (aerial parts) and S6 (roots) in the Appendix. In the aerial part, 29% of metabolites (29 of 62) in *psp1.1psp1.1 HS:PSP1* differed significantly in comparison to the WT (Table 4.4). Although significant, these changes were no higher than 50% for most of cases and only fructose varied more than 50%. Despite the assumption that PPSB would play a minor role in aerial parts, when serine was absent from the growth medium, 90% of metabolites (56 of the 62 metabolites determined) significantly changed in *psp1.1psp1.1 HS:PSP1* compared to the WT, and the majority (70%) presented changes over 50%.

Table 4.4. Percentage of metabolites whose levels significantly changed in *psp1.1psp1.1 HS:PSP1* (*HS PSP*) as compared to the wild-type (WT) under light (with or without serine in the growing medium) darkness and high CO_2.

Aerial Part				
	HS PSP (Ser)	*HS PSP* (Light)	*HS PSP* (Darkness)	*HS PSP* (CO_2)
% of change	29	90	83	84
Roots				
	HS PSP (Ser)	*HS PSP* (Light)	*HS PSP* (Darkness)	*HS PSP* (CO_2)
% of change	50	77	87	71

As a general trend, the aerial part of the *psp1.1psp1.1 HS:PSP1* lines displayed an increase in most measured metabolites compared to WT and not only amino acids, but also sugars and organic acids (Table 4.5 and S5). Regarding amino acids, some of them increased under specific growth conditions; e.g glycine under dark conditions and high CO_2 (absence of photorespiration), cysteine under high CO_2 or glutamine which increased under all the conditions assayed but especially under light conditions (Table S5). In quantitative terms the most important increments in amino acids under all the assayed conditions (more than a 2-fold increase) were: arginine, asparagine, GABA, histidine, O-acetyl serine, tryptophan and tyrosine.

Many TCAC (citrate, fumarate, malate and succinate) and glycolytic intermediates (glycerate, several phosphate derivates of glycerate are important intermediates of glycolysis) also increased in the *psp1.1psp1.1 HS:PSP1* lines compared to the WT (Table 4.5 and S5). From all TCAC intermediates measured only 2-oxoglutarate showed a different trend under

CO_2 conditions compared to the other conditions. This metabolite significantly increased in *psp1.1psp1.1 HS:PSP1* lines under light or dark conditions but was reduced in the presence of high CO_2.

The sugars involved in central metabolism, such as sucrose, glucose and fructose, increased in *psp1.1psp1.1 HS:PSP1* lines under all the assayed conditions (Table 4.5 and S5). However, phosphate sugars decreased. This deficiency in sugar phosphates could be related with inorganic phosphate deficiency. Finally the sugars related with the stress conditions or involved in signaling, like galactinol or trehalose, increased substantially in the aerial parts of the *psp1.1psp1.1 HS:PSP1* lines under all the measured conditions compared to the WT.

After PSP1 induction, not all the metabolites responded similarly (Table 4.5). The clearest reversion of the metabolite pattern was related with carbon metabolism: that is, respiration (TCAC, glycolysis) and sugar metabolism (Table S5). The increases observed for the TCAC in citrate, fumarate, malate and succinate in the aerial parts of the *psp1.1psp1.1 HS:PSP1* lines under light and CO_2 conditions were reverted after the induction. Similar changes were observed under the dark conditions, although only succinate and fumarate significantly reduced after PSP1 induction. These results could indicate the TCAC as a pathway affected by PPSB.

Glycerate levels also lowered significantly in aerial parts *psp1.1psp1.1 HS:PSP1* under all the assayed conditions after PSP1 the induction (Table 4.5 and S5). Glucose and fructose levels also reduced in the *psp1.1psp1.1*

HS:PSP1 lines after PSP1 induction. Galactinol or trehalose lowered significantly after PSP1 induction (Table S5).

Table 4.5. Summarized metabolomic profile in aerial part of wild-type (WT) and conditional mutant *psp1.1psp1.1 HS:PSP1 (HS PSP)* under three different conditions (light with or without serine in the medium, darkness and high levels of CO_2), with (+) or without (-) heat shock treatment. Data are normalised and related to the mean of the WT for each condition. Each value represents the mean ± SE (n = 6). Values in bold are significantly different from the WT and that significantly differed from the values of the heat shock treatment are followed by *(P > 0.05).

	Aerial part										
	Light					**Darkness**			**High CO_2**		
		-	+	**serine**			-	+		-	+
Amino acids	WT	HS PSP	HS PSP	WT	HS PSP	WT	HS PSP	HS PSP	WT	HS PSP	HS PSP
Arginine	1 ± 0.05	**2.48 ± 0.07**	2.63 ± 0.07	1 ± 0.03	0.96 ± 0.04	1 ± 0.04	**2.32 ± 0.08***	2.96 ± 0.12	1 ± 0.02	**2.32 ± 0.09***	2.02 ± 0.06
Asparagine	1 ± 0.2	**3.22 ± 0.28**	3.07 ± 0.29	1 ± 0.19	0.87 ± 0.1	1 ± 0.11	**2.32 ± 0.12***	2.81 ± 0.14	1 ± 0.16	**3.82 ± 0.13***	1.98 ± 0.07
Cysteine	1 ± 0.1	1.24 ± 0.08	1.15 ± 0.08	1 ± 0.06	0.93 ± 0.05	1 ± 0.05	1.08 ± 0.05	1.15 ± 0.05	1 ± 0.07	**2.7 ± 0.17***	1.65 ± 0.06
GABA	1 ± 0.08	**2.25 ± 0.14***	1.59 ± 0.13	1 ± 0.06	0.91 ± 0.07	1 ± 0.04	**2.27 ± 0.06***	1.73 ± 0.1	1 ± 0.06	**2.54 ± 0.13***	2.09 ± 0.16
Glutamine	1 ± 0.16	**2.74 ± 0.23**	2.37 ± 0.14	1 ± 0.09	0.98 ± 0.07	1 ± 0.06	**1.44 ± 0.05***	1.42 ± 0.05	1 ± 0.04	**1.27 ± 0.05**	1.12 ± 0.06
Glycine	1 ± 0.04	**0.83 ± 0.03***	1 ± 0.04	1 ± 0.03	**1.28 ± 0.03**	1 ± 0.09	**3.5 ± 0.08***	4.22 ± 0.3	1 ± 0.02	**2.3 ± 0.04***	1.2 ± 0.02
Histidine	1 ± 0.34	**6.02 ± 0.4**	14.12 ± 0.98	1 ± 0.19	0.84 ± 0.16	1 ± 0.26	**3.28 ± 0.14***	4.45 ± 0.22	1 ± 0.04	**5.42 ± 0.13***	3.49 ± 0.07
Serine, O-acetyl-	1 ± 0.02	**2.72 ± 0.09***	2.12 ± 0.04	1 ± 0.03	0.98 ± 0.03	1 ± 0.04	**2.67 ± 0.06**	2.52 ± 0.07	1 ± 0.03	**4.13 ± 0.08***	3.14 ± 0.1
Tryptophan	1 ± 0.07	**5.53 ± 0.43**	5.53 ± 0.3	1 ± 0.11	0.85 ± 0.04	1 ± 0.06	**4.21 ± 0.14**	3.88 ± 0.15	1 ± 0.05	**12.98 ± 0.72***	7.62 ± 0.31
Tyrosine	1 ± 0.15	**5.56 ± 0.48**	5.1 ± 0.44	1 ± 0.04	0.92 ± 0.06	1 ± 0.14	**4.71 ± 0.37***	2.62 ± 0.31	1 ± 0.03	9.73 ± 0.5	8.63 ± 0.35
Organic acids											
Citric acid	1 ± 0.04	**3.85 ± 0.2***	2.69 ± 0.09	1 ± 0.04	1.07 ± 0.04	1 ± 0.07	**1.75 ± 0.07**	1.79 ± 0.08	1 ± 0.07	**5.17 ± 0.31***	3.25 ± 0.15
Fumaric acid	1 ± 0.02	**1.56 ± 0.05***	1.33 ± 0.03	1 ± 0.02	1.02 ± 0.02	1 ± 0.02	**1.61 ± 0.03***	1.44 ± 0.03	1 ± 0.01	**1.74 ± 0.03***	1.35 ± 0.03
Glutaric acid, 2-oxo-	1 ± 0.03	**1.16 ± 0.03***	1.01 ± 0.03	1 ± 0.03	**0.87 ± 0.02**	1 ± 0.04	**1.81 ± 0.07***	1.55 ± 0.1	1 ± 0.04	**0.8 ± 0.03***	0.67 ± 0.03
Glyceric acid	1 ± 0.05	**2.28 ± 0.09***	1.67 ± 0.04	1 ± 0.05	**0.65 ± 0.02**	1 ± 0.07	**2.97 ± 0.18***	1.78 ± 0.09	1 ± 0.03	**1.58 ± 0.04***	0.86 ± 0.02
Malic acid	1 ± 0.03	**1.72 ± 0.07***	1.42 ± 0.02	1 ± 0.03	1 ± 0.04	1 ± 0.05	**1.93 ± 0.04***	2.07 ± 0.05	1 ± 0.02	**2.7 ± 0.04***	1.66 ± 0.02
Succinic acid	1 ± 0.02	**1.27 ± 0.04***	0.88 ± 0.02	1 ± 0.02	1.17 ± 0.08	1 ± 0.06	**2.13 ± 0.06***	1.55 ± 0.05	-	-	-
Sugars and Sugar alcohols											
Fructose	1 ± 0.01	**1.35 ± 0.06***	1.05 ± 0.02	1 ± 0.05	**1.56 ± 0.05**	1 ± 0.03	**2.93 ± 0.05***	2.16 ± 0.06	1 ± 0.02	**1.3 ± 0.04***	0.88 ± 0.02
Fructose-6-phosphate	1 ± 0.03	**0.39 ± 0.01**	0.39 ± 0.03	1 ± 0.04	1.09 ± 0.06	1 ± 0.05	**0.35 ± 0.02***	0.68 ± 0.03	-	-	-
Galactinol	1 ± 0.03	**49.6 ± 3.56***	13.43 ± 0.25	1 ± 0.21	2.43 ± 0.14	1 ± 0.05	**67.75 ± 2.54***	55.72 ± 1.63	1 ± 0.04	**73.59 ± 3.62***	7.17 ± 0.16
Glucose	1 ± 0.07	**1.26 ± 0.05***	1.02 ± 0.02	1 ± 0.09	0.96 ± 0.08	1 ± 0.05	**2.02 ± 0.04***	1.58 ± 0.09	1 ± 0.04	**1.22 ± 0.05***	0.91 ± 0.03
Glucose-6-phosphate	1 ± 0.03	**0.33 ± 0.01**	0.36 ± 0.03	1 ± 0.05	1.07 ± 0.05	1 ± 0.05	**0.32 ± 0.02***	0.65 ± 0.03	-	-	-
Glyceraldehyde-3-phosphate	1 ± 0.03	**0.55 ± 0.01***	0.62 ± 0.03	1 ± 0.03	1 ± 0.03	1 ± 0.05	**0.52 ± 0.04***	0.76 ± 0.02	1 ± 0.03	**0.84 ± 0.02**	0.58 ± 0.02
Sucrose	1 ± 0.01	1.07 ± 0.03*	0.96 ± 0.01	1 ± 0.02	1.08 ± 0.03	1 ± 0.01	**1.14 ± 0.02***	1.32 ± 0.02	1 ± 0.04	1.12 ± 0.04*	0.92 ± 0.03
Trehalose, alpha,alpha'	1 ± 0.02	**3.98 ± 0.15***	2.88 ± 0.07	1 ± 0.02	1.14 ± 0.05	1 ± 0.03	**4.47 ± 0.09***	2.89 ± 0.11	1 ± 0.02	**4.27 ± 0.09***	3.13 ± 0.09

In spite of rescuing root growth in *psp1.1psp1.1 HS:PSP1* (Figure 4.20) Ser was unable to completely restore the root metabolic profile (Table 4.6 and S6). 50% of the determined metabolites (27/56) still significantly differed compared to the WT (Table 4.4 and S6).

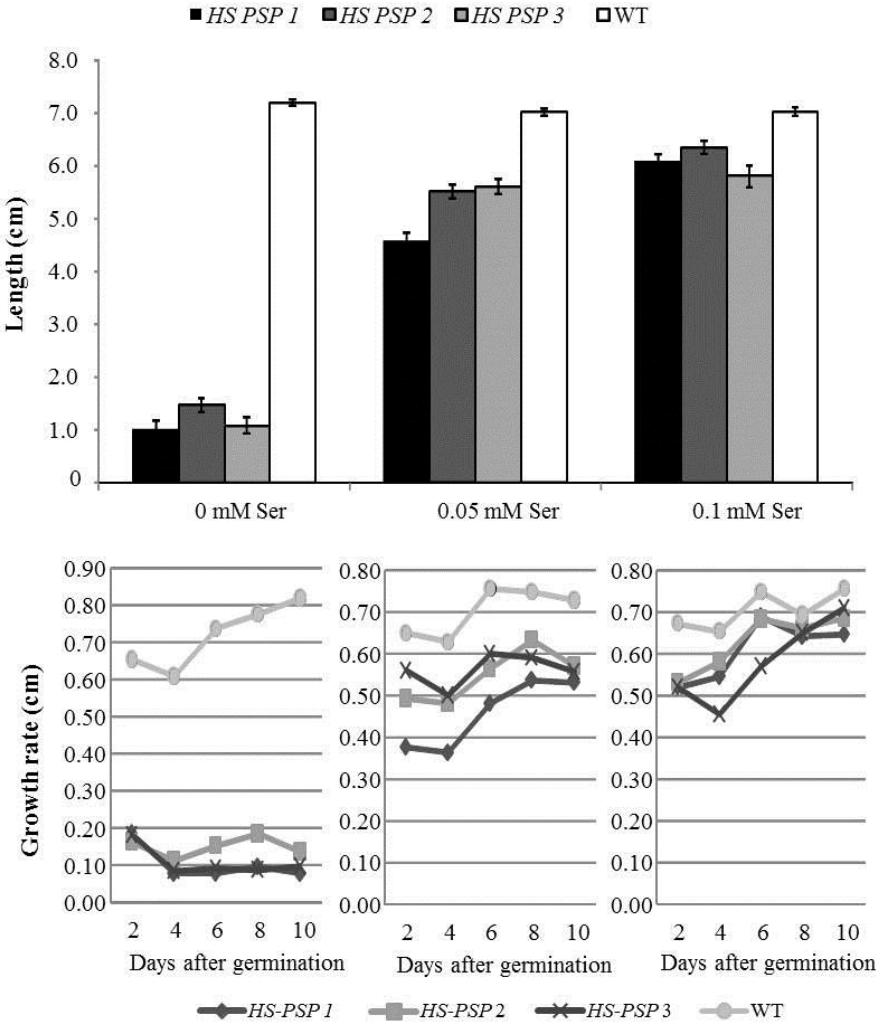

Figure 4.20. Root growth parameters of wild type (WT) and three different *psp1.1psp1.1 HS:PSP1* (*HS PSP)* lines in the presence of different concentrations of serine in the growing medium. A, root length. B, growth rate (n = 3).

However, metabolite variations were not as strong as in the absence of Ser (Table S6). Thus only three metabolites (glycerate, GABA and Galactinol) changed more than 50% compared to the WT (Table 4.4 and S6). In the *psp1.1psp1.1 HS:PSP1 g*rowth in the absence of Ser had more drastic consequences for the root metabolite profile. Under these conditions, 77% of metabolites were altered in the *psp1.1psp1.1 HS:PSP1* roots and most changed more than 50% compared to the WT (Table 4.4). In the *psp1.1psp1.1 HS:PSP1* roots, amino acids increased substantially and the most pronounced changes in quantitative terms (more than 2-fold) were those found in arginine, asparagine, glutamine, histidine and tryptophan (Table S6). For instance, argine increased more than 33 times or glutamine more than 7 times under the light contidions.

Unlike aerial parts, no similar trend was observed in under different conditions for the changes observed in the TCAC intermediates or sugars (Table S6). Regarding TCAC intermediates, citrate was the only metabolite whose contents increased significantly under all the tested conditions (not determined under the light conditions). There was no obvious change in major sugars like fructose, glucose or sucrose as there were in aerial parts. Only stress and/or signaling sugars, like galactinol or trehalose increased consistently under all the conditions (Table 4.6).

After PSP1 induction, the most important changes were related to the glutamine levels, which were significantly higher before induction under all the tested conditions and were significantly lower after induction as they approached the WT levels (Table S6). The same trends in glutamine levels were observed in aerial parts, but they only significantly reduced in the plants grown under high CO_2. Another amino acid related to glutamine

metabolism, GABA, also increased in both root and aerial parts before PSP1 induction, and significantly reduced after induction for all the conditions. No similar pattern after PSP1 induction in roots was found for the other analyzed metabolites. Only stress and/or signaling sugars galactinol or trehalose which increased consistently under all the conditions before induction, significantly lowered under the light and CO_2 conditions but not with darkness (Table 4.6).

Tabla 4.6. Summarized metabolomic profile in roots of wild-type (WT) and conditional mutant *psp1.1psp1.1 HS:PSP1 (HS PSP)* under three different conditions (light with or without serine in the medium, darkness and high levels of CO_2), with (+) or without (-) heat shock treatment. Data are normalised and related to the mean of WT for each condition. Each value represents mean ± SE (n = 6). Values in bold are significantly different from the WT and that significantly differed from the values of the heat shock treatment are followed by * (P > 0.05).

	Roots										
	Light					**Darkness**			**High CO_2**		
		-	+	**serine**			-	+		-	+
Amino acids	WT	*HS PSP*	*HS PSP*	WT	*HS PSP*	WT	*HS PSP*	*HS PSP*	WT	*HS PSP*	*HS PSP*
Arginine	1 ± 0.08	**8.34 ± 0.99***	4.97 ± 0.28	1 ± 0.05	0.76 ± 0.06	1 ± 0.03	**4.15 ± 0.09**	4.30 ± 0.22	1 ± 0.09	**2.24 ± 0.15**	1.94 ± 0.16
Asparagine	1 ± 0.08	**33.6 ± 1.02***	16.29 ± 0.93	1 ± 0.06	0.96 ± 0.10	1 ± 0.09	**12.62 ± 0.57***	19.23 ± 1.15	1 ± 0.13	**9.98 ± 0.68***	6.88 ± 0.64
GABA	1 ± 0.1	**2.91 ± 0.17***	1.84 ± 0.18	1 ± 0.12	1.69 ± 0.24	1 ± 0.03	**2.67 ± 0.04***	2.45 ± 0.04	1 ± 0.05	**1.49 ± 0.16***	0.95 ± 0.11
Glutamine	1 ± 0.1	**7.78 ± 0.26***	4.32 ± 0.35	1 ± 0.04	1.20 ± 0.06	1 ± 0.02	**2.9 ± 0.08***	2.52 ± 0.06	1 ± 0.04	**2.12 ± 0.08***	1.41 ± 0.06
Histidine	1 ± 0.07	**7.32 ± 1.64***	2.96 ± 0.40	1 ± 0.06	1.10 ± 0.08	1 ± 0.07	**3.52 ± 0.47***	7.25 ± 1.42	1 ± 0.16	**3.57 ± 0.48**	3.68 ± 0.81
Tryptophan	1 ± 0.09	**3.23 ± 0.38**	2.46 ± 0.24	1 ± 0.05	0.84 ± 0.06	1 ± 0.05	**2.23 ± 0.14***	3.22 ± 0.30	1 ± 0.05	**2.35 ± 0.10**	2.15 ± 0.21
Organic acids											
Citric acid	-	-	-	-	-	1 ± 0.05	**4.45 ± 0.11**	3.90 ± 0.11	1 ± 0.03	**3.08 ± 0.07***	2.39 ± 0.03
Glyceric acid	1 ± 0.07	**1.84 ± 0.03***	1.4 ± 0.04	1 ± 0.14	0.39 ± 0.02	1 ± 0.01	**0.62 ± 0.00***	1.79 ± 0.02	1 ± 0.01	**1.33 ± 0.09**	1.34 ± 0.10
Sugars and Sugar alcohols											
Fructose	1 ± 0.02	**2.38 ± 0.04**	2.07 ± 0.03	1 ± 0.05	0.63 ± 0.05	1 ± 0.01	**2.55 ± 0.02***	3.01 ± 0.03	1 ± 0.01	**0.91 ± 0.01***	1.25 ± 0.07
Galactinol	1 ± 0.05	**5.24 ± 0.19**	2.41 ± 0.10	1 ± 0.05	1.57 ± 0.08	1 ± 0.03	**7.51 ± 0.28**	7.76 ± 0.32	1 ± 0.03	**3.98 ± 0.18***	0.92 ± 0.08
Glucose	1 ± 0.05	1.07 ± 0.06	1.05 ± 0.04	1 ± 0.05	1 .00 ± 0.02	-	-	-	1 ± 0.07	0.97 ± 0.02*	0.85 ± 0.04
Sucrose	1 ± 0.05	0.98 ± 0.06	0.99 ± 0.03	-	-	1 ± 0.04	1.09 ± 0.03	0.97 ± 0.02	1 ± 0.05	0.99 ± 0.02*	0.85 ± 0.03
Trehalose, alpha,alpha'	1 ± 0.07	**5.25 ± 0.16**	3.51 ± 0.11	1 ± 0.04	1.35 ± 0.07	1 ± 0.02	**3.85 ± 0.08**	4.03 ± 0.12	1 ± 0.01	**3.48 ± 0.06***	2.07 ± 0.16

4.2.1.4.2.1 The special case of Ser

The whole Ser levels did not lower in the aerial part of *psp1.1psp1.1 HS:PSP1* compared to the WT. Only in roots and under high CO_2 conditions Ser levels were lower in *psp1.1psp1.1 HS:PSP1* than in the WT. However, as most of amino acids increased in *psp1.1psp1.1 HS:PSP1*, the percentage of Ser was significantly lower in the mutants under some conditions, especially in roots under darkness or high CO_2 conditions (Figure 4.21).

In WT aerial parts the percentage of Ser compared to the total amino acids was higher under light conditions than under darkness or CO_2 conditions (Figure 4.21A). In WT roots these differences between conditions were maintained, being the percentage of Ser in light conditions higher than in high CO_2 and darkness (Figure 4.21B).

In the aerial parts, the percentage of Ser in the *psp1.1psp1.1 HS:PSP1* was significantly lower than in WT under light (26%) and CO_2 (29%) conditions. In roots the differences in the percentage of Ser between WT and mutant were much higher than in the aerial parts under all conditions (38%, 43% and 60% reduction under light, darkness and high CO_2 conditions, respectively). Such differences disappeared when plants were grown in the presence of Ser.

No significant differences in the percentage of Ser were obtained in either aerial parts or roots in any of the conditions assayed when compared WT heat-shock treated and non-treated samples. However after the heat-shock treatment significant differences were found in the mutant. After PSP1 induction this percentage significantly increased in all conditions, especially in roots.

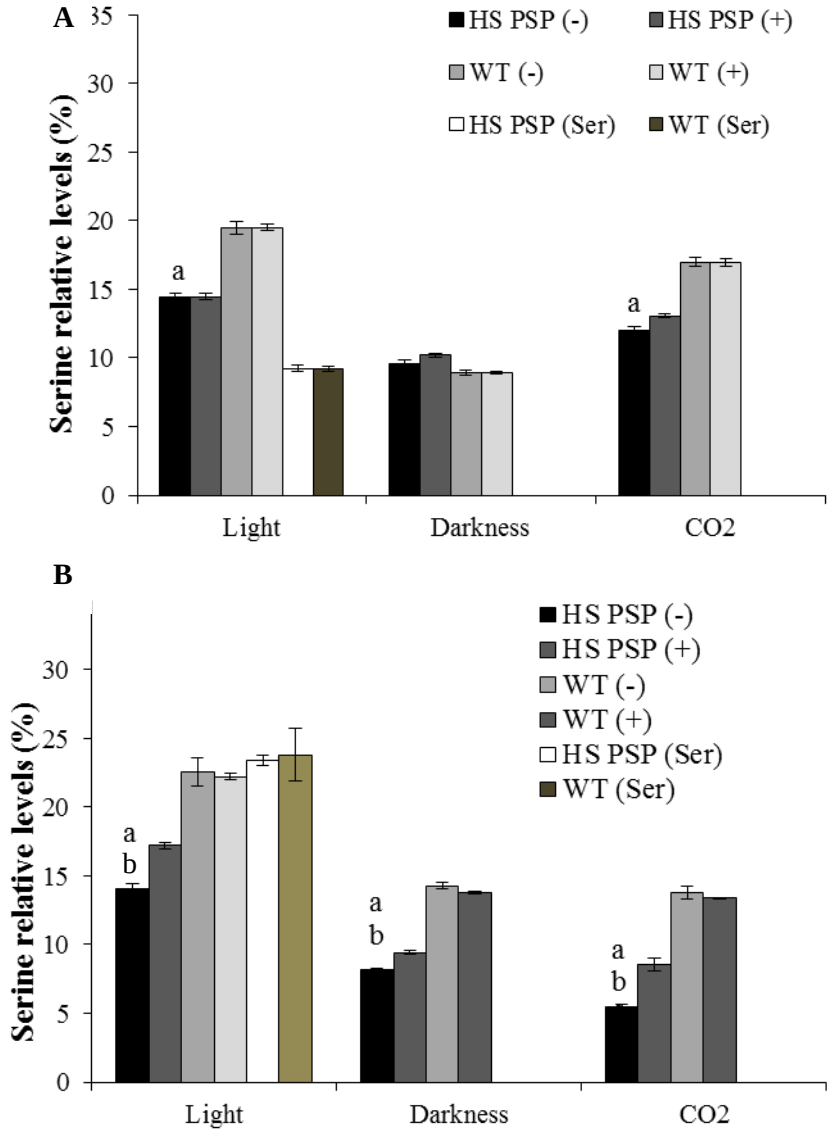

Figure 4.21. Percentage of Ser as compared to total amino acids in wild type (WT) and *psp1.1psp1.1 HS:PSP1* (*HS PSP*) aerial parts (A) and roots (B) grown under three different conditions (light with or without serine in the medium, darkness and high levels of CO_2), with (+) or without (-) heat shock treatment. n = 6. a, indicates a statistical difference from WT and b a statistical difference from the HS PSP (+), according to T-student test.

4.2.1.4.2.2 Determination of auxin content

Tryptophane levels were very high in both the roots and aerial parts of *psp1.1psp1.1 HS:PSP1* compared to the WT. Since this amino acid is the precursor of the phytohormone auxin, and we found that *psp1.1psp1.1 HS:PSP1* displayed cell division and elongation defects in roots, we measured auxin content in the roots and aerial parts of the mutant and WT lines (Table 4.7).

Table 4.7. Auxin content in roots and aerial parts of wild-type (WT) plants and *psp1.1psp1.1 HS:PSP1 (HS PSP)* lines. The values represent the mean ± SE (ng IAA / g dry weigth). n= three technical replicates of a pool of more than 50 plants.

Line	Aerial part	Roots
WT	554.00 ± 22.07	1,082.00 ± 48.62
HS PSP	328.00 ± 28.80	1,909.00 ± 28.78

As shown in Table 4.7, the auxin content in aerial parts was higher in the WT than in the *psp1.1psp1.1 HS:PSP1* lines. However, in roots the mutant lines presented an almost 2-fold auxin level compared to the WT. This result suggests that auxin levels could participate in the inhibition of the primary root growth of the *psp1.1psp1.1 HS:PSP1* lines by affecting both meristematic cell division and cell elongation. To confirm the higher auxin concentration in the PSP1-deficient lines, we crossed an artificial microRNA (*amiRNA*) *PSP1* silenced line with a line that carried an auxin fluorescent marker (*DR5:GFP*). As Figure 4.22 and Table 4.8 show, the fluorescence in the root meristem of the silenced line was much higher than in the WT lines.

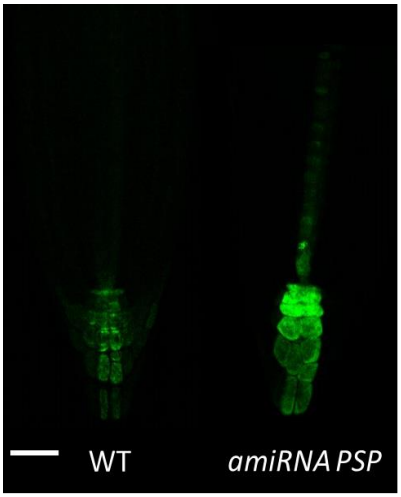

Figure 4.22. Auxin levels in WT *DR5:GFP* and *amiRNA* silenced *PSP* root tips visualised by GFP fluorescence. Scale bar: 50 μm.

Table 4.8. Auxin quantification in root tips of wild-type (WT) and PSP1 silenced lines (*amiRNA PSP*) measured as fluorescence intensity (GFP/ μm^2) of the *DR5::GFP* auxin marker. The values represent the mean ± SE; n = 11.

Line	Roots
WT	261.19 ± 38.37
amiRNA PSP	930.88 ± 104.80

4.2.1.4.2.3 Starch content

The starch is a metabolite that gives us an idea of the carbon metabolism dynamics. During the day, plants store the product of photosynthesis in their leaves in the form of starch granules in order to accumulate carbohydrates. However, this storage of carbohydrates is mobilized at night and used in several tasks, like respiration or growth.

In order to explore the content of such an important metabolite in the mutant lines, some samples were taken early in the morning before sunrise (6 am) and a second round of sampling was done late in the evening before sunset (8 pm). The results of the starch determination are presented in Table 4.9,

where we can see that starch storage is more pronounced in the mutant lines than in the WT plants for both conditions.

Table 4.9. Starch content (mg/g fresh weight) in aerial parts of wild-type (WT) and *psp1.1psp1.1 HS:PSP1 (HS PSP*) lines at the end of the night (am) and at the end of the light (pm) period. The results are the mean ± SE; n=4.

Line	am	pm
WT	0.86 ± 0.07	3.46 ± 0.09
HS PSP	6.57 ± 0.20	6.81 ± 0.40

These results indicate that the mutant lines are unable to mobilize starch from storage, so they tend to accumulate it. This could be a result of their dwarf phenotype compared to the WT plants, as we can see in Figure 4.23.

Figure 4.23. Phenotype of wild-type (WT) plants (left) compared with the *psp1.1psp1.1 HS:PSP1* plants (right) grown under green house conditions.

4.2.1.4.2.4 Activity of TCAC enzymes

After determining the metabolite profile of the mutant lines under different conditions, one of the general aspects to consider is the marked increase in the amount of some of the organic acids related to TCAC in both roots and AP. This is the case of citrate, succinate, fumarate and malate. In order to corroborate that TCAC was altered in the *psp1.1psp1.1 HS:PSP1* mutants, we determined the activities of some TCAC enzymes in roots and aerial parts. This was done at different time points before and after PSP1 induction in the conditional mutants. The assay results are summarized in Tables 4.10 and 4.11 and were used to perform a T-student statistical analysis.

Table 4.10. Citrate synthase (CS) and fumarase (F) activity (nmol NADH /g Fresh weigth · min) in aerial parts of wild type (WT) and *psp1.1psp1.1 HS:PSP1 (HS PSP)* lines at different time-points after *PSP* induction (0, 4 and 8 hours). Values represent the mean ± SE; n = 3. Values in bold are significantly different from WT ($p<0.05$).

Aerial Part						
	0		4		8	
Enzyme	WT	*HS PSP*	WT	*HS PSP*	WT	*HS PSP*
CS	30.49 ± 0.90	**57.17 ± 1.00**	30.66 ± 1.99	**59.86 ± 3.77**	49.56 ± 4.02	48.82 ± 1.91
F	241.71 ± 0.43	**371.26 ± 0.55**	311.47 ± 0.76	**398.22 ± 0.80**	356.57 ± 1.82	358.19 ± 0.41

Table 4.11. Citrate synthase (CS) and fumarase (F) activity (nmol NADH /g Fresh weigth · min) in roots of wild type (WT) and *psp1.1psp1.1 HS:PSP1 (HS PSP)* lines at different time-points after PSP induction (0, 4 and 8 hours). Values represent the mean ± SE; n = 3. Values in bold are significantly different from WT ($p<0.05$).

Roots						
	0		4		8	
Enzyme	WT	*HS PSP*	WT	*HS PSP*	WT	*HS PSP*
CS	12.55 ± 0.23	**24.61 ± 0.29**	23.54 ± 1.32	21.61 ± 0.82	28.26 ± 0.57	28.14 ± 1.55
F	5.63 ± 0.37	**12.75 ± 0.66**	10.37 ± 0.16	**14. 20 ± 0.11**	13.21 ± 0.24	12.13 ± 0.30

The activity of these enzymes was significantly higher in the roots and aerial parts of the mutants before PSP1 induction compared to the WT. However, some time after PSP1 induction the activity levels of these enzymes became similar to the WT levels and were not statistically different.

4.2.1.4.2.5 Ammonium measurements

Apart from organic acids, another interesting result in the metabolic profile of the mutant lines under all pre-induction conditions is the high level of glutamine compared to the WT. After induction the levels of this metabolite lowered considerably especially in roots. One of the reasons for the increment of this metabolite could be explained by the ammonium assimilation pathway. Plants assimilate ammonium in the form of glutamine through the activity of glutamine synthase (GS). In order to gain an idea of the concentration of ammonium inside the plant, we determine its content in aerial parts and roots (Table 4.12).

Table 4.12. Ammonium content (nmol/ mg FW) in aerial part and roots of wild-type (WT) and *psp1.1psp1.1HS:PSP1* (*HS PSP*) lines. The results represent the mean value ± SE; n = 3.

	Aerial part		Roots	
	WT	*HS PSP*	WT	*HS PSP*
[Ammonium]	2.48 ± 0.08	4.04 ± 0.12	6.45 ± 0.09	14.81 ± 1.38

As shown, the amount of ammonium in both plant parts in the mutant lines was 2-fold the amount found in the WT. This can be explained by lack of the PPSB function as follows: in mutants, inhibition of PSP1 activity affects the whole PPSB pathway, including the activity of the previous enzyme PSAT. This enzyme produces 2-oxoglutarate, the same as that needed for the Fd-GOGAT to synthesize glutamate in the plastid from glutamine (Figure 1.6). As PSAT is likely to be down regulated, there is not enough 2-oxoglutarate to form glutamate which, in turn, produces accumulation of glutamine and ammonium. This is probably why ammonium increased considerably in the mutant lines compared to the WT. Moreover, the

glutamate that cannot be used in ammonium assimilation could be used as a substrate by glutamate decarboxylase (GAD) to form GABA. Since the GABA levels were significantly high in the *psp1.1psp1.1 HS:PSP1* mutants for all the assayed conditions, and as they reduced after induction, we measured the *GAD* gene expression. The gene At5g17330 which codes for an isoform of GAD was induced in the *psp1.1psp1.1 HS:PSP1* lines as compared to WT (Table 4.13), especially in the aerial parts and was accordingly reduced to WT levels after PSP1 induction.

Table 4.13. Relative expression levels of *GAD* in *psp1.1psp1.1 HS:PSP1 (HS PSP)*.

	Aerial part		**Roots**	
Gene	*HS PSP (-)*	*HS PSP (+)*	*HS PSP (-)*	*HS PSP (+)*
At5g17330	1.73 ± 0.19	1.01 ± 0.05	1.31 ± 0.08	0.92 ± 0.12

As it has been shown that high ammonium levels inhibit root growth (Qin et al., 2008; Li et al., 2014) we tested the effect of the cation in the *psp1.1psp1.1 HS:PSP1* root growth. As shown in Figure 4.24 the mutant root grew better in a medium with nitrate as the sole nitrogen source, than in a medium with a mixture of both nitrate and ammonium. Contrary to the mutant, the WT root length was similar in both media, although there was a trend to a decrease in a medium with ammonium as sole source of nitrogen.

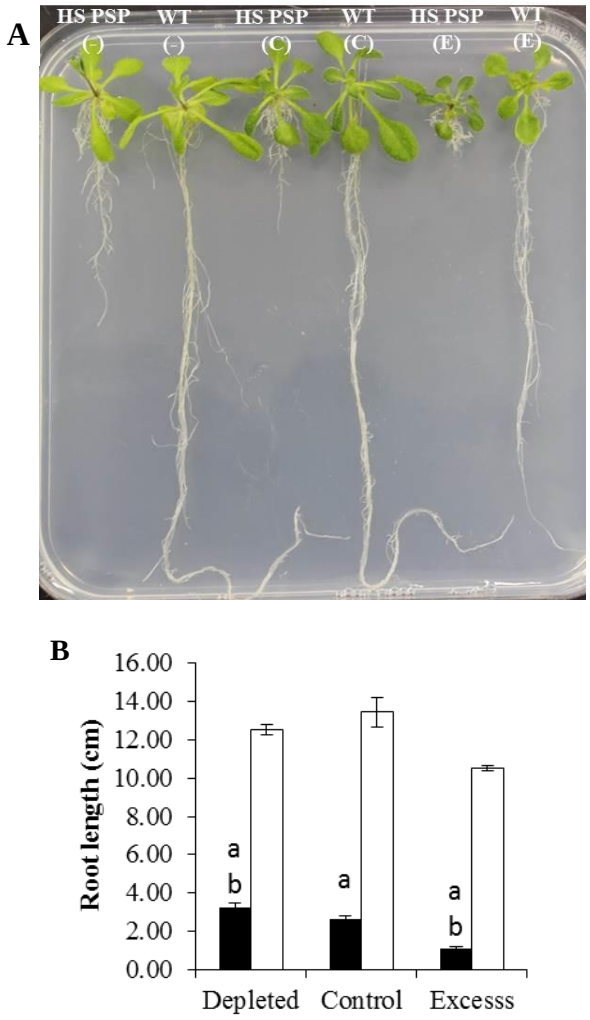

Figure 4.24. Ammonium assay. A, phenotype of the *psp1.1psp1.1 HS:PSP1* (*HS PSP*) compared to the WT in ammonium depleted medium (-), control (C) and excess of ammonium (E). Values of the root length (B), root fresh weight (C) and rosette fresh weight (D) in the three different medium. (n=30).a, significantly different from WT. b, significantly different from control, according to T-student test.

4.2.1.4.3 RNA-seq data analysis

In order to explore not only the differences in gene expression between the *psp1.1psp1.1 HS:PSP1* and WT lines, but to also identify the primary gene targets of PSP1 activity, an RNA-Seq analysis was performed. After taking into account the major role assigned to PPSB under dark conditions, and the results obtained in the PCA analysis of the metabolite data, we decided to perform a transcriptomic analysis in samples collected at the end of the dark period. Before starting the analysis of the data obtained by this method, a previous validation of the results was performed by qRT-PCR. For this purpose, several genes that presented a change in expression between the *psp1.1psp1.1 HS:PSP1* lines before and after induction were tested **(**Figure 4.25).

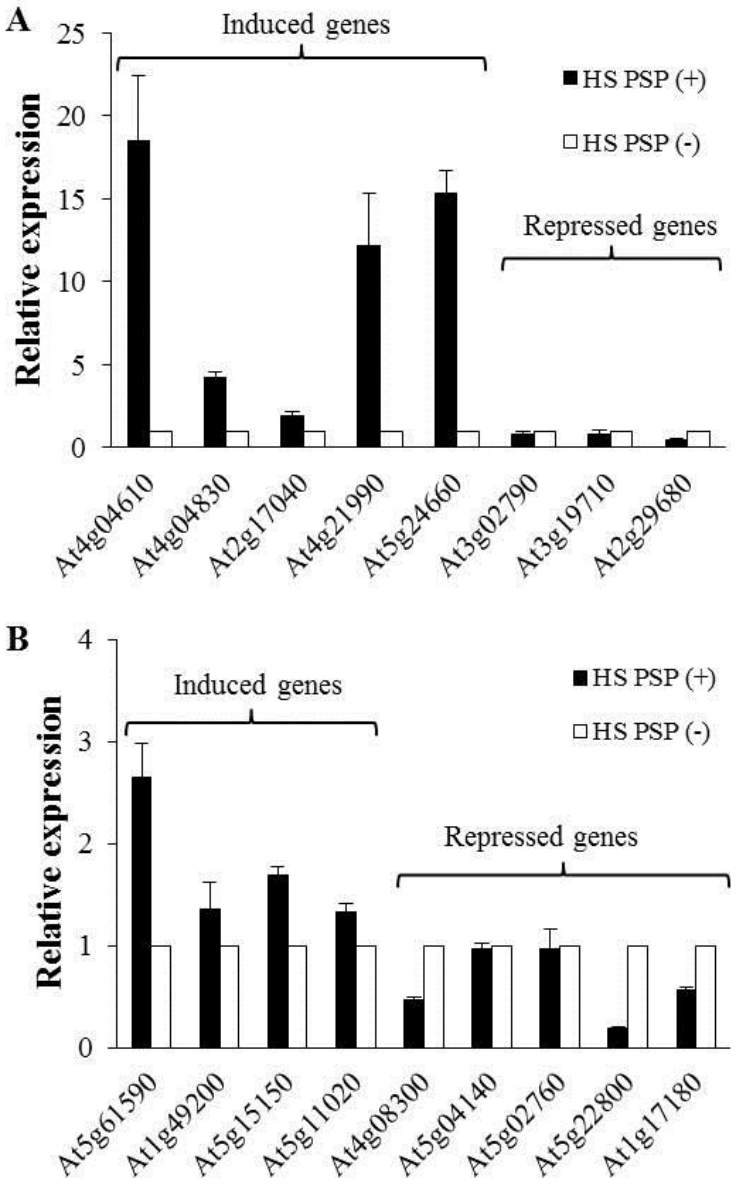

Figure 4.25. Validation of RNA-Seq by qRT-PCR of selected genes in aerial parts (A) and roots (B) of *psp1.1psp1.1 HS:PSP1* (*HS PSP*) lines with (+) and without (-) heat-shock induction. The values of the non-induced lines (HS PSP(-)) were used as reference (n = 3).

The change in expression of the other genes in the *psp1.1psp1.1 HS:PSP1* lines *vs.* the WT lines was also analyzed. As a whole, 80% of the tested genes followed the same expression pattern in the qRT-PCR and RNA-Seq experiments, which validates the data obtained by this latter method.

In a first step of the transcriptomic analysis of the *psp1.1psp1.1 HS:PSP1* lines, a comparison was made between the WT plants and mutant lines with no heat-shock treatment. All those genes whose difference in expression between these lines was statistically significant according to the adjusted P-value ($P < 0.05$) were selected. Afterward, a list of repressed and induced genes was obtained and a functional enrichment analysis was performed using the web "VirtualPlant v1.3" (http://virtualplant.bio.nyu.edu/cgi-bin/vpweb/).

In aerial parts, 224 genes were differentially expressed in the *psp1.1psp1.1 HS:PSP1* mutants compared to the WT plants. Among these genes, 72 were repressed and 152 were induced. A functional enrichment analysis distributed these genes into several general categories, as depicted in Figure 4.26. The same procedure was followed for roots, where 2,871 genes were differentially expressed compared to the WT and 1,562 were repressed and 1,271 induced.

The results obtained in the functional enrichment provided the first evidences for the possible categories that could be further explored.

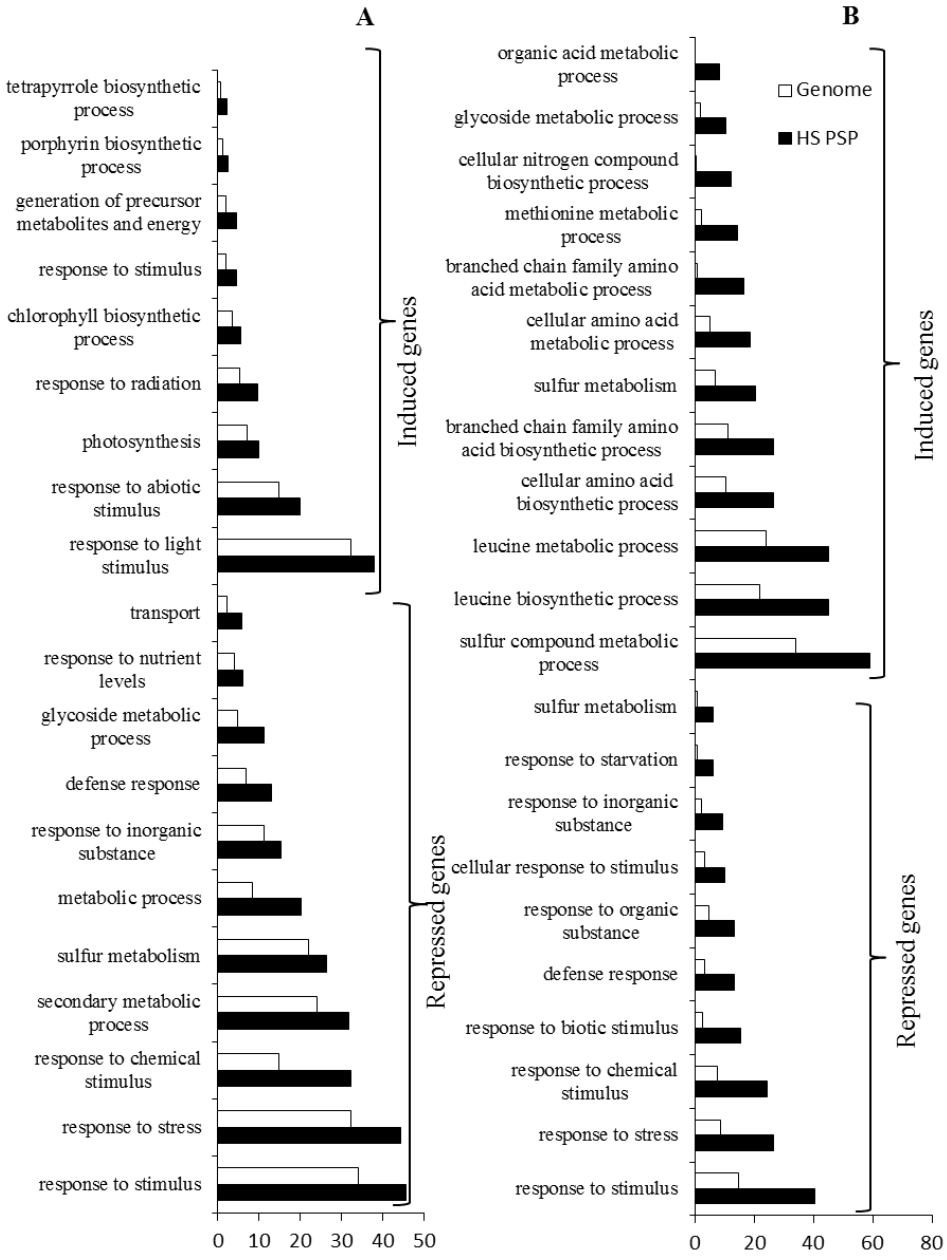

Figure 4.26. Functional categories significantly enriched ($p<0.05$) in *psp1.1psp1.1 HS:PSP1* (HS PSP) roots (A) and aerial parts (B) as compared to wild-type plants (n =3).

When comparing the transcriptomic data with the phenotypes observed in *psp1.1psp1.1 HS:PSP1* and with their metabolite profile, e.g. the arrested root phenotype of the *psp1.1psp1.1 HS:PSP1* mutant lines, the high auxin levels in them, the marked presence of tryptophan in these lines and the relationship between Ser production and sulfur and ammonium assimilation, we decided to concentrate on the functional categories that were related to auxin and tryptophan metabolism, and on those related to sulfur and ammonium assimilation.

For this purpose, we identified those genes related with the aforementioned categories, whose expression levels altered in the mutant compared with the WT, and changed significantly after PSP1 induction. In this way, it was possible to classify the genes into two different groups, depending on the fact whether the differences between genes after treatment significantly differed from the WT levels (Table 4.14) or not (Table 4.15).

Table 4.14. List of genes related to auxin, sulfur and ammonium metabolism in the *psp1.1psp1.1HS:PSP1 (HS PSP)* aerial parts and roots whose expression is statistically different from wild-type (WT) before PSP1 induction [WT *vs HS PSP* (-)] and whose expression is significantly reverted to WT levels after PSP induction [WT *vs HS PSP* (+)] .Values describe the $\log_2$(fold change); $p < 0.05$.

AERIAL PART

Gene	WT *vs HS PSP* (-)	WT *vs HS PSP* (+)	Description
Auxin metabolism			
At1g05470	-0.97	0.00	CVP2, DNAse I-like superfamily protein
At1g44350	-1.32	-0.63	ILL6, IAA-leucine resistant (ILR)-like gene 6
At2g22240	0.82	0.09	ATMIPS2, myo-inositol-1-phosphate synthase 2
Ammonium assimilation		No genes in this category	
Sulfur metabolism			
At3g12520	2.32	1.11	SULTR4;2, sulfate transporter 4;2
At4g39940	-1.10	-0.19	AKN2, APK2, APS-kinase 2
At5g24660	4.12	2.18	LSU2, response to low sulfur 2

ROOTS

Gene	WT *vs HS PSP* (-)	WT *vs HS PSP* (+)	Description
Auxin metabolism			
At1g23160	-4.12	-0.94	Auxin-responsive GH3 family protein
At1g24100	0.68	0.50	UGT74B1, UDP-glucosyl transferase 74B1
At1g48850	0.72	0.29	Enolpyruvylshikimate-3-phosphate phospholyase
At1g55320	1.25	0.33	AAE18, acyl-activating enzyme 18
At2g01950	-0.67	-0.49	BRL2, VH1, BRI1-like 2
At2g06850	-1.15	-0.56	EXT, XTH4, xyloglucan endotransglucosylase 4
At2g33310	-0.91	-0.16	IAA13, auxin-induced protein 13
At2g33860	-0.85	-0.61	ARF3, auxin-responsive factor
At2g44490	0.67	-0.08	PEN2, Glycosyl hydrolase superfamily protein
At2g45210	-1.36	-0.35	SAUR-like auxin-responsive protein family

At3g05290	-1.00	0.09	PNC1, peroxisomal adenine nucleotide carrier 1
At3g44310	0.76	-0.11	ATNIT1, NIT1, NITI, nitrilase 1
At3g44320	1.16	0.53	AtNIT3, nitrilase 3
At4g02610	-2.11	-0.80	Aldolase-type TIM protein
At4g14560	1.08	0.93	AXR5, IAA1, indole-3-acetic acid inducible
At4g18710	-0.87	-0.24	ATSK21, BIN2, Protein kinase superfamily
At4g31990	-1.08	-0.15	AAT3, ASP5, aspartate aminotransferase 5
At4g34800	-1.82	-1.13	SAUR-like auxin-responsive protein family
At4g37390	0.93	-0.01	AUR3, GH3-2, GH3.2, Auxin-responsive GH3
At5g01490	2.15	0.00	ATCAX4, CAX4, cation exchanger 4
At5g13320	3.16	0.21	GDG1, GH3.12, WIN3, Auxin-responsive GH3
At5g13360	1.08	0.26	Auxin-responsive GH3 family protein
At5g13370	1.07	0.14	Auxin-responsive GH3 family protein
At5g17990	0.89	0.04	Pat1, TRP1, tryptophan biosynthesis 1
At5g19550	0.97	0.50	AAT2, ASP2, aspartate aminotransferase 2
At5g54510	1.03	0.77	DFL1, GH3.6, Auxin-responsive GH3 family
At5g66120	0.85	0.46	3-dehydroquinate synthase, putative
Ammonium assimilation			
At2g05990	-0.72	0.21	ENR1, MOD1, NAD(P)-bindingsuperfamily
At4g31990	-1.08	-0.15	AAT3, ASP5, aspartate aminotransferase 5
At5g19550	0.97	0.50	AAT2, ASP2, aspartate aminotransferase 2
At5g35630	0.77	0.42	ATGSL1, GLN2, GS2, glutamine synthetase 2
At5g37600	1.19	0.25	ATGSR1, GLN1;1, GSR 1, glutamine synthase
At5g53460	0.78	0.34	GLT1, NADH-dependent glutamate synthase 1
Sulfur metabolism			
At3g45070	0.90	0.68	P-loop containing triphosphate hydrolases protein
At4g26970	0.76	0.06	ACO2, aconitase 2
At5g13550	1.08	0.75	SULTR4;1, sulfate transporter 4.1
At5g63990	0.97	0.27	Inositol monophosphatase family
At5g64000	1.40	0.68	ATSAL2, Inositol monophosphatase family

Table 4.14 presents those genes whose expression altered in the mutant, but did not significantly differ from WT after PSP1 induction. Several genes were identified that could be included in auxin metabolism, ammonium assimilation or sulfur metabolism category in both roots and aerial parts. The number of genes whose expression level accomplished this criterion was larger in roots than in aerial parts.

When we consider roots, the "auxin metabolism" category contained many genes whose expression was elevated and became down-regulated after heat-shock treatment. Some good examples of them are: At5g13370, At5g13320, At4g37390 and At5g13360, which encode auxin-responsive GH3 family proteins; At2g33310 or At4g14560, which encode auxin-induced proteins; and At3g44320, which encodes for a nitrilase that catalyzes the hydrolysis of indole-3-acetonitrile to indole-3-acetic acid. This last gene is the only one of the four Arabidopsis nitrilases whose mRNA levels were strongly induced when plants underwent sulfur deprivation.

When we explored other categories, many genes related with ammonium and sulfur metabolism assimilation were down-regulated after heat-shock treatment, which could indicate an alteration to these pathways in the mutant lines. In ammonium assimilation, genes like At5g37600 (GLN1), At5g35630 (GLN2), At5g53460 (GLT1) that encode for glutamine synthetases and glutamate synthase, respectively, or At5g19550 (AAT2), the gene encoding a cytosolic aspartate aminotransferase, are induced in the mutant but down-regulated after PSP1 induction. However the gene coding for the plastidial isoform of aspartate aminotransferare (AAT1, At4g31990) was represed in the mutant and reverted to WT levels after PSP1 induction. Several genes involved in the sulfur metabolism were also deregulated, and

of them, At4g26970, that encodes an aconitase or At5g13550, encoding a sulfate transporter, reach similar levels of expression compared to the WT after the heat shock treatment.

In aerial parts, very few genes of auxin metabolism were altered. With sulfur metabolism, it is worth mentioning At5g24660, which encodes for LSU2 in response to low sulfur levels.

A second group of genes involved in auxin, ammonium or sulfur metabolism whose expression was altered in the mutant, but did not revert to the WT levels upon PSP1 induction, was also found (Table 4.15). These genes could be considered genes lately responding to PSP1 activity or simply secondary response genes. Only two genes classified in this group (At5g04140 and At2g03760) completely reverted their expression pattern (induced before and repressed after PSP1 induction or *vice versa*) and could be considered as primary response genes. As indicated in Table 4.15, the mutant roots presented more altered genes than the aerial parts. Many genes included in the auxin metabolism category were identified: genes that encode for auxin-responsive GH3 family protein (At2g23170 or At1g28130); genes that encode a transcription factor that binds to auxin responsive elements (At1g19850), or encodes a phospholipase D required for auxin transport and distribution (At3g05630). Regarding ammonium assimilation in roots, five genes were up-regulated in *psp1.1psp1.1 HS:PSP1*. Two of them were particularly interesting. One gene coded for an isoform of GS (At1g66200, ATGSR2), which was induced in the mutant and its expression lowered from 2.4- to a 1.4-fold increase after PSP1 induction. Another gene coded for Fd-GOGAT (At5g04140), whose

expression was induced before and repressed after PSP1 induction in the mutant compared to the WT.

TABLE 4.15. List of genes related to auxin, sulfur and ammonium metabolism in the *psp1.1psp1.1 HS:PSP1* (*HS PSP*) aerial parts and roots whose expression is statistically different from wild-type (WT) before and after PSP1 induction .Values describe the $\log_2$(fold change); $p < 0.05$.

AERIAL PART

Gene	WT *vs* *HS* *PSP* (-)	WT *vs* *HS* *PSP* (+)	Description
Auxin metabolism			
At3g53480	1.16	1.02	ATPDR9, pleiotropic drug resistance 9
At3g05630	2.14	1.48	PLDZETA2, phospholipase D P2
Ammonium assimilation			No genes in this category
Sulfur metabolism			
At5g10180	-0.94	-1.04	SULTR2;1, slufate transporter 2;1
At4g21990	2.02	1.41	APR3,APS reductase 3
At4g04610	2.13	1.56	APR1, APS reductase 1
At1g62180	0.83	0.67	5'adenylylphosphosulfate reductase 2

ROOTS

Gene	WT *vs* *HS* *PSP* (-)	WT *vs* *HS* *PSP* (+)	Description
Auxin metabolism			
At5g02840	-1.13	-1.25	LCL1, LHY/CCA1-like 1
At3g48360	-1.16	-1.61	ATBT2, BT2, BTB and TAZ domain
At2g23170	2.71	1.56	GH3.3, Auxin-responsive GH3 family
At5g17300	-0.79	-0.93	RVE1, Homeodomain-like superfamily
At5g12330	1.90	1.74	LRP1, Lateral root primordium protein-
At1g22410	0.90	0.82	Class-II DAHP synthetase family protein
At4g37610	-0.64	-0.68	BTB and TAZ domain protein 5

At2g20340	-1.40	-1.26	Pyridoxal phosphate transferases family
At3g28910	1.42	1.83	ATMYB30, MYB30,
At1g28130	0.94	0.70	GH3.17, Auxin-responsive GH3 family
At5g37770	1.24	1.16	CML24, EF hand calcium-binding protein
At2g22330	-1.23	-1.09	CYP79B3, cytochrome P450
At4g11280	0.98	1.41	ATACS6, 1-aminocyclopropane synthase 6
At3g04730	-0.70	-0.78	IAA16, indoleacetic acid-induced protein 16
At4g34240	-0.94	-1.03	ALDH3, aldehyde dehydrogenase 3I1
At4g36250	1.08	0.67	ALDH3F1, aldehyde dehydrogenase 3F1
At1g19850	1.00	0.79	IAA24, auxin-responsive factor
At3g05630	2.35	1.82	PDLZ2, PLDZETA2, phospholipase D P2
Ammonium assimilation			
At4g34710	0.68	0.61	ATADC2, SPE2, arginine decarboxylase 2
At2g39800	0.71	1.13	delta1-pyrroline-5-carboxylate synthase 1
At1g66200	2.38	1.43	ATGSR2, GSR2, glutamine synthase
At4g24830	0.97	1.09	arginosuccinate synthase family
At5g04140	0.87	-0.95	FD-GOGAT, GLS1, glutamate synthase 1
Sulfur metabolism			
At5g10180	1.39	1.64	SULTR2;1, slufate transporter 2;1
At4g35640	3.61	1.93	ATSERAT3;2, serine acetyltransferase 3;2
At4g33030	1.02	0.87	SQD1, sulfoquinovosyldiacylglycerol 1
At1g62180	1.73	1.24	5'adenylylphosphosulfate reductase 2
At1g13420	1.43	0.84	ATST4B, ST4B, sulfotransferase 4B
At2g03760	0.95	-0.89	AtSOT1, ST, ST1, sulphotransferase 12
At2g14750	1.13	1.13	AKN1, APK, APK1, ATAKN1, APS kinase
At3g15990	0.89	1.34	SULTR3;4, sulfate transporter 3;4
At3g12520	1.10	1.33	SULTR4;2, sulfate transporter 4;2
At1g78000	1.98	1.36	SULTR1;2, sulfate transporter 1;2
At4g21990	0.94	0.66	APR3, PRH-26, PRH26, APS reductase 3
At3g02870	1.04	0.89	VTC4, Inositol monophosphatase family.
At4g04610	2.35	1.69	APR, PRH19, APS reductase 1
At1g18590	0.99	0.74	ATSOT17, SOT17, sulfotransferase 17
At1g22150	5.06	8.14	SULTR1;3, sulfate transporter 1;3

With sulfur metabolism, 15 genes were up-regulated in *psp1.1psp1.1 HS:PSP1* compared to the WT before PSP1 induction. This category included genes like: At4g33030, which encodes a protein involved in sulfolipid biosynthesis; genes At1g62180, At4g21990 or At4g04610, whose translated proteins are APS reductases and play a key role in sulfate assimilation; At4g35640, which encodes a serine acetyltransferase. Many of the genes involved in sulfate transport, like SULTR1;2 (At1g78000), SULTR2;1 (At1g78000), SULTR3;4(At3g15990), SULTR4;2 (At3g12520) or SULTR1;3 (At1g22150), that encode the sulfate transporters induced under sulfate limitation were up-regulated in *psp1.1psp1.1 HS:PSP1*. A reduced expression trend was observed for most of them after PSP1 induction, but their levels were still higher when compared to the WT. This was the case of APS reductase 1 (At4g04610) and serine acetyltransferase (At4g35640), whose induction levels dropped from 2.4 to 1.7 and 2.6 to 1.9 compared to the WT, respectively. There was the case of the Ser acetyltransferase enzyme, which is involved in sulfur assimilation and cysteine biosynthesis and whose expression is induced in both roots and shoots under sulfur-starved conditions. This enzyme could be the key that connects the PPSB with sulfur metabolism. Finally, the expression of gene At2g03760, which codes for a sulfotransferase AtSOT1, reverted and also induced in the mutant line before and repressed after PSP1 expression compared to the WT.

In aerial parts, very few genes related to auxin and sulfur metabolism were found in *psp1.1psp1.1 HS:PSP1* compared to the WT. *APS reductases 1, 2* and *3* (At4g04610, At1g62180 and At4g21990, respectively) were all up-regulated in the mutant, and they all showed the reduced expression

tendency upon PSP1 induction. Interestingly, the gene that codes for sulfate transporter SULTR2;1 (At5g10180) was repressed before and after PSP1 induction.

4.2.2 DISCUSSION

4.2.2.1 The homozygous *psp1* mutation is embryo lethal

The existence of the PPSB in plants has been known since the 1950s. However, the quantitative contribution and physiological significance of this pathway had not been defined in plants, mainly due to the coexistence of two other pathways with the same metabolic function. We found that PSP1 activity is essential for embryo development. Homozygous *psp1.1psp1.1* mutants show a delay in embryo development starting at the globular stage, which finally led to abortion. At early stages of embryogenesis, many nutrients are supplied to the embryo by the endosperm and/or maternal tissues, while, at later stages, most metabolites are synthesized autonomously by the embryo itself. At the globular-heart transition stage, many metabolic pathways are established in the embryo. Specifically, the first step of differentiation of proplastids, where PSP1 is localized, occurs at the globular-to heart transition phase (Devic, 2008). The delay in *psp1.1psp1.1* mutant embryo development at the globular stage is probably related to the establishment of the PPSB in the embryo.

4.2.2.2 A crucial role of the PSP1 activity in pollen and tapetum development in Arabidopsis thaliana.

Microsporogenesis is linked directly to normal tapetum development. It has been shown that the specific mutations that disrupt the normal development of tapetal cells affect, in turn, microsporogenesis (Kawanabe et al., 2006; Vizcay-Barrena et al., 2006; Yang et al., 2007). Both microspore and tapetal cell development involve the activity of precise metabolic programmes that are tightly regulated in time and space. Thus any blockage of a metabolic pathway can result in male gametophyte lethality (Suzuki et al., 2009). With the PPSB, lack of function of PSP1 leads to abnormal pollen and tapetum development. In this case, one possible explanation is that lack of PSP1 compromises the supply of Ser to these cells, which could lead to a male sterile condition (Cascales-Miñana et al., 2013). It has been demonstrated that PSP1 is expressed in both microspore and tapetal cells in crucial pollen development steps (Cascales-Miñana et al., 2013). Our results support the notion that both sporophytic (tapetal cells) and gametophytic (microspores) cells are affected by lack of PSP1 activity, which induces both sporophytic and gametophytic structural alterations. Since it has been demonstrated that tapetal cells are important for microspore development as they provide metabolites, enzymes, nutrients and sporopollenin precursors, lack of PSP1 activity in these cells impairs pollen development. So the final male sterility phenotype observed in the *psp1.1psp1.1 35S:PSP1* lines should be the consequence of both sporophytic and gametophytic defects. Nevertheless, we were unable to quantify the contribution of each cell type to the final microspore aberrations.

Although no obvious differences were observed in the microspore or tapetum between the WT and *psp1.1psp1.1 35S:PSP1* in early development stages (the tetrad stage), a thicker primexine layer was observed in *psp1.1psp1.1 35S:PSP1* as compared to the WT. This could be explained by an earlier delivery of sporopollenin from tapetal cells to the *psp1.1psp1.1 35S:PSP1* microspores. Whatever the case, the final exine layer appeared normal in both the WT and *psp1.1psp1.1 35S:PSP1* microspores. Differences began to appear after the ring-vacuolated stage. In the microspore, one of the main features was that the nucleus of the mutant microspore did not undergo mitosis. Many studies have related the role of Ser in the regulation of the cell cycle and oncogenesis in mammals (Bachelor et al., 2011; Locasale et al., 2011; Pollari et al., 2011; Possemato, 2011). In both mammals and plants, it has been confirmed that Ser provides one-carbon units to the tretrahydrofolate metabolism, which is essential to DNA and RNA metabolism (Hanson et al., 2001; Hanson et al., 2011; Kalhan et al., 2012). In mitogenically stimulated lymphocytes, a correlation between the increase in Ser utilisation and demands for increasing nucleotide biosynthesis for DNA replication during cellular proliferation has been established (Eichler et al., 1981). Therefore, Ser can connect the primary metabolism with cell cycle progression regulation. Given the evidence for the one-carbon metabolism taking place in *Arabidopsis* plastids (Zhang et al., 2010), the arrested microspore development in the ring-vacuolated stage in *psp1.1psp1.1 35S:PSP1* suggests that the PPSB could be required to supply Ser towards the proper functioning of the one-carbon metabolism in some non-photosynthetic cells.

After the ring-vacuolated development stage, *psp1.1psp1.1 35S:PSP1* contained no oil bodies in the tapetosomes of tapetal cells. In the WT tapetal layer, tapetosomes are composed of oleosin-coated oil droplets sequestered in numerous membranous vesicles, both of which assemble in and then detach from the ER (Hsieh et al., 2007; Hsieh et al., 2005). The proper development of an intine layer in the microspore and of the tapetosomes in the tapetum relies on correct endomembrane formation. Sphingolipids are major components of endomembranes (Dietrich et al., 2008). The first step in sphingolipid synthesis is the condensation of Ser and palmitoyl CoA in a reaction catalysed by Serine palmitoyltransferase (SPT) (Dietrich et al., 2008). Ultrastructural analyses have revealed that mutant *spt* pollen grains shrink, stop their development in the ring-vacuolated stage and no first mitotic division occurs (Dietrich et al., 2008), as in the *psp1.1psp1.1 35S:PSP1* microspores. We hypothesised that the Ser needed for SPT activity in tapetal cells and pollen is provided by the PPSB. Since this pathway was blocked in the *psp1.1psp1.1 35S:PSP1*, it was not possible to supply Ser to these cell types for proper sphingolipid synthesis. As a result, no normal membranes were formed in tapetosomes. Since these oil bodies need membranous vesicles and are closely related with the ER, an alteration in their normal formation may explain their absence in the *psp1.1psp1.1 35S:PSP1*.

Tapetosome oil bodies are surrounded by a coat of proteins named oleosins. There are nine genes in *Arabidopsis* that encode tapetum oleosins, and one of them, GRP17 (At5g07530), is a glycine-rich protein (Suzuki et al., 2013). GRP17 is highly expressed to produce an oleosin of 53 kDa, which represents about 70% of all the oleosins in the tapetum (Hsieh et al., 2004).

This oleosin possesses numerous repeats of short peptides with several Ser, and most predominantly glycine, residues at its C-terminus (Hsieh et al., 2004). Ser, which is the precursor of the glycine needed for GRP17 biosynthesis, could be provided by the PPSB in tapetal cells. A study on the compositions of lipid bodies (Hernandez-Pinzon et al., 1999) has shown that the major lipid-bound proteins present in the pollen coat are precisely the C-terminal domains of oleosin proteins. Therefore, the oil bodies of the visible tapetosomes in the WT tapetal cells, which were absent in the *psp1.1psp1.1 35S:PSP1*, could be important for the formation of pollen coat components, and could be responsible for the absence of a pollen coat in the *psp1.1psp1.1 35S:PSP1* pollen grains. After considering all these facts, underlining the importance of the PPSB for providing Ser for proper microspore development in the anthers of *Arabidopsis thaliana* is certainly not unreasonable.

Cells from the tapetum and microspores develop as "communicating" neighbors. Early in development, tapetum cells are involved in the secretion of molecules into the locule for microspore maturation. We propose that the absence of PSP1 activity affects the proper development of both cell types, which in turn affects pollen maturation. The developmental modifications observed in the *psp1.1psp1.1 35S:PSP1-GFP* tapetum along with the specific *PSP1* expression in this cell layer during the critical stages of pollen maturation suggest that an essential step in microspore development is PSP1 expression during the post-tetrad stages in the tapetum and not in the microspore itself.

4.2.2.3 Ser homeostasis is altered in *psp1.1psp1.1 HS:PSP1*

We studied the metabolic profile of conditional mutants under different conditions. Light and high CO_2 conditions were chosen to study if the Ser obtained through photorespiration was enough to sustain a normal metabolic profile. It was also interesting to study how compromised the metabolism of the *psp1.1psp1.1 HS:PSP1* mutants was under dark conditions.

In spite of the drastic growth defects associated with the *psp1* mutation, the relative levels of Ser in *psp1.1psp1.1 HS:PSP1* were not significantly lower than in the WT under most assayed conditions, and were even higher in some (in aerial parts with high CO_2 or in the darkness). Only in roots under high CO_2 conditions was a significant reduction in Ser relative content found in *psp1.1psp1.1 HS:PSP1* compared to the WT. Since PSP1 deficiency limits *Arabidopsis* growth under not only high CO_2 conditions, relative Ser content is not a good indicator of the PPSB contribution to plant growth and development, probably because it does not reflect the Ser levels in different cellular types. So other parameters should be taken into account.

When studying the percentage of Ser compared to the total amino acid measured, some interesting conclusions were drawn. In the WT aerial parts, the Ser percentage was higher with light at ambient CO_2 than under high CO_2 or darkness conditions. These data suggest that Ser biosynthesis is greater under light conditions at ambient CO_2 levels, which would agree with current knowledge indicating that most Ser in aerial parts is synthesized through the glycolate pathway. Thus under conditions in which

photorespiration diminishes or is eliminated (high CO_2 or darkness), plants have a lower percentage of Ser than when photorespiration is active.

The data obtained with *psp1.1psp1.1 HS:PSP1* support the notion that the PPSB could contribute to Ser homeostasis in aerial parts since the percentage of Ser clearly lowered in the mutant under light conditions not only at high but also at ambient CO_2 as compared to the WT. The PPSB contribution in Ser biosynthesis in aerial parts could be more important than that observed since glycolate pathway activation in the mutant as a compensatory mechanism can not be ruled out. No differences in the percentage of Ser between the WT and the mutant were found under the dark conditions, which were unexpected results. We could speculate that under dark conditions, Ser is less required or that the non-photorespiratory glycerate pathway, which synthesizes Ser through three reverse reactions of part of the photorespiratory cycle, is more active at night and can compensate for lack of the PPSB in aerial parts.

The percentage of Ser lowered under all the assayed conditions in mutant roots compared to the WT and, to a greater extent, compared to aerial parts, especially in the darkness and under high CO_2 conditions. These results, along with the severe root developmental arrest phenotype, support the PPSB being the most important pathway for Ser supply in roots. The much higher percentage of Ser in the roots of both the WT and mutants under light conditions, compared to the darkness or high CO_2, indicates that the Ser synthesized in aerial parts by glycolate pathways can reach roots and can partly compensate for lack of PPSB activity. Thus, the lower percentages of Ser found in mutant aerial parts could be, at least in part, the result from transport of the amino acid to roots. Accordingly, one relevant question that

needs to be answered is why glycerate or glycolate pathways cannot compensate for lack of PPSB activity in roots and reproductive organs. We previously proposed that Ser biosynthetic pathways participate differently in amino acid homeostasis in accordance with cell type. Perhaps some cells (i.e., tapetum cells) are devoid of Ser transporters, or others (i.e., meristematic cells) are not conveniently connected to the vasculature. Since Ser supply to the growing medium rescues root growth in *psp1.1psp1.1 HS:PSP1,* the most plausible hypothesis, at least in root meristematic cells, is that the Ser supplied through the phloem does not reach them. Hence the only supplies of this amino acid for these cells originate from intracellular biosynthesis. In these circumstances, our data support that bulk relative Ser content probably does not reflect the amino acid level in such cells. In all these scenarios, our results suggest that other Ser biosynthetic pathways, such as the glycerate pathway, or the activity of the Gly decarboxylase complex:Ser hydroxymethyltransferase coupled reactions, are of little biological relevance in cells from the tapetum, embryo or root meristems, and that only the PPSB is responsible for Ser supply to the cells involved in specific developmental events.

4.2.2.4 Metabolic pathways affected by/responding to PPSB

Although Ser was able to complement normal mutant growth and restored primary root growth, the absence of total metabolite profile complementation in the presence of Ser in both aerial parts and roots suggested additional functions for the PPSB, or interactions between the intermediates of the pathway with other metabolites and metabolic pathways. Our results indicated that some of PPSB metabolic interactions

could be common to all the assayed conditions, while others could be more organ- or condition- specific. Both central carbon (TCAC, glycolysis, sugar metabolism) and nitrogen metabolism (amino acid metabolism) were altered in aerial parts. In roots PPSB deficiency affected mainly amino acid metabolism, especially ammonium assimilation related processes.

In aerial parts, the TCAC was particularly affected in the presence of light. Measured levels of TCAC intermediates and the activity the TCAC enzymes were higher in *psp1.1psp1.1 HS:PSP1* than in the WT. Both TCAC activities and metabolite levels were reverted or approached WT levels after PSP1 induction. We believe that after inducting the PPSB by heat-shock treatment, most of the 3-PGA pool is used as a substrate for the PPSB instead of being diverted downstream of the glycolytic pathway, and then to the TCAC. Under high CO_2 conditions, the increases observed in the mutant TCAC metabolites (citrate, fumarate, malate) were more marked than under light conditions, which may indicate that the PPSB flux is more important when the glycolate pathway is inhibited.

The amino acid levels in the mutant were drastically modified under the different conditions, and in both aerial parts and roots. The most important changes noted in roots were related to amino acids glutamine and GABA. Both metabolites increased in the mutant under all the assayed conditions, especially under light conditions, and clearly reduced after PSP1 induction. In aerial parts, glutamine and GABA also increased under all the assayed conditions. Once again glutamine particularly increased under light conditions, but only the GABA levels lowered after PSP1 induction. Other nitrogen-rich amino acids, such as asparagine, drastically increased in the

mutant, especially in roots. These results indicate that ammonium assimilation could be altered in *psp1.1psp1.1 HS:PSP1* (Benstein et al., 2013) found that silencing PGDH, the enzyme that catalyze the first reaction of the PPSB, increased the glutamine and ammonium levels in *Arabidopsis* aerial parts, which suggests that PSAT activity is required to provide 2-oxoglutarate for ammonium fixation. The PSAT, the second enzyme of the PPSB, catalyzes the conversion of 3-phosphohydroxypyruvate into 3-phosphoserine by using one molecule of glutamate, and by producing one molecule of 2-oxoglutarate. This 2-oxoglutarate is required for ammonium assimilation via the GS/GOGAT cycle; concretely the reaction catalyzed by GOGAT uses one molecule of 2-oxoglutarate and one of glutamine to synthesize two molecules of glutamate.

Here we provide further evidence that the PPSB is required for proper GS/GOGAT pathway functioning. The high ammonium levels found in *psp1.1psp1.1 HS:PSP1,* along with the mutant root growth hypersensitivity phenotype to the cation, indicates that the GS/GOGAT pathway was blocked during one of the reactions, which would lead to the accumulation of precursors such as glutamine and ammonium. A relationship between the ammonium concentration and the up-regulation of glutamine synthetase isoenzymes has been described (Ishiyama et al., 2004)**.** We found that many genes which code for isoforms of GS and GOGAT were induced in the mutant. In particular, two GOGAT isoforms (*GLT1* and *GLU1*) were induced in mutant roots. After PSP1 induction, *GLT1* expression did not significantly differ from the WT, while *GLU1* expression lowered to below WT levels. These results support the idea that despite the enzymes involved

in the GS/GOGAT pathway in the mutant having high expressions, the final product was not obtained, probably because one of the precursors was missing. We postulate that PSP1 inactivation in *psp1.1psp1.1 HS:PSP1* also affects PSAT activity, which reduce the availability of 2-oxoglutarate in the plastid and led to the accumulation of ammonium, glutamine and GABA. This, would affect normal plant development, especially roots. The metabolite analysis indicated that 2-oxoglutarate levels rose under light and darkness conditions in mutant aerial parts, but lowered under CO_2 conditions. Changes in the 2-oxoglutarate levels are difficult to interpret since this metabolite can be synthesized by different pathways and in different compartments, such as photorespiration in the peroxisome, the TCAC in mitochondria and the PPSB in the chloroplast. Differences in the 2-oxoglutarate levels in the mutant, compared to the WT (higher than in the WT under ambient CO_2 and lower under high CO_2 conditions) suggested that an important part of the 2-oxoglutarate measured under ambient CO_2 in the mutant would result from an increased photorespiration rate in peroxisomes, probably as a compensatory mechanism for lack of PPSB activity. Several reports have shown that increased photorespiration is associated with rising levels of 2-oxoglutarate, day respiration and nitrogen assimilation (Bloom et al., 2010; Tcherkez et al., 2012; Rachmilevitch et al., 2004)**.** The increase in TCAC intermediates and activities in *psp1.1psp1.1 HS:PSP1* supports such evidence. The high 2-oxoglutarate levels measured in the mutant under dark conditions, compared to the WT, could be attributed to a greater respiration activity at night. If our hypothesis is correct, under both ambient CO_2 and darkness conditions, the higher 2-oxoglutarate levels measured in the mutant would be restricted to

peroxisomes and mitochondria, respectively. Thus mutant plastids could lack 2-oxoglutarate, as measured under high CO_2 conditions. GABA could also play an essential role as a sink of glutamate when GS/GOGAT is restricted. Glutamate can be converted into GABA by a reaction catalyzed by glutamate decarboxylase (GAD). The higher GAD expression in aerial parts of *psp1.1psp1.1 HS:PSP1* before PSP1 induction, and its lower expression after PSP1 induction support this idea.

Our results of the transcriptomic profile of mutants showed an increase in not only the expression levels of the genes that encode sulfate transporter isoforms but also of sulfate assimilation enzymes, e.g adenosine 5'-phosphosulfate reductase (APR1-3) and serine acetyltransferase, which could support the idea that the mutant behaves as if it were under sulfur starvation conditions. O-Acetyl Ser (OAS) also substantially increased in both roots and aerial parts of mutants compared to the WT under all the conditions. It is known that OAS concentrations in leaves and roots increase in sulfur-starved Arabidopsis, and that this metabolite induces the expression of the genes involved in sulfate uptake and assimilation (Hirai et al., 2003). All these data suggest that *psp1.1psp1.1 HS:PSP1* suffers sulfur deficiency. Ser is required for sulfur assimilation. Enzyme Ser-acetyltransferase requires Ser to synthesize OAS, which is the substrate into which reduced hydrogen sulfide is incorporated to produce cysteine in a reaction catalyzed by OAS thiol-lyase. Accordingly, Ser deficiency in the plastid of certain cells could provoke sulfur starvation and induce expression of sulfur related genes.

Since OAS is the product of Ser-acetyltransferase, the higher OAS levels in the mutant compared to the WT cannot be understood unless they are restricted to certain cell types or are compartmentalized within the cell. In the first scenario, perhaps the OAS levels are an indication of the metabolite levels in those cell types where Ser would not be deficient. If this were the case, the sulfur starvation of the mutant could only result from root inhibition, which would indirectly affect sulfate uptake from the medium. In the second scenario, high levels of OAS could be found in a compartment but low levels could be found in others, such as plastids. Ser acetyltransferases are not only present in mitochondria and cytosol. It has been found that some cytosolic isoforms suc as *ATSERAT3;*2 are induced in both roots and shoots under sulfur-starved conditions (Kawashima et al., 2005). We found that the expression of the cytosolic ATSERAT3;2 isoform was highly induced in the mutant and could account for the high levels of OAS measured. According to this, we believe that this high levels of OAS are either not found in the right cell or in the right compartment.

4.2.2.5 Role of the PPSB in root development

The *psp1.1psp1.1 HS:PSP1* line presents a drastic phenotype not only at level of embryo lethality or pollen development, but also at root development. The results indicate that *psp1.1psp1.1 HS:PSP1* primary roots have a shorter meristem with a lower number of cells than the WT, but also the cell length at the elongation zone is significantly shorter than in the WT. This result suggests that PSP1 is required for cell division and the elongation of the primary root meristem. This PSP1 activity requirement

could be related with the Ser deficit in meristematic cells. As discussed earlier, Ser from the glycolate pathway in aerial parts could reach root cells, but may not reach the meristematic cells that are not connected to the other cells by the vasculature. As we discussed before the PPSB could be the sole source of Ser for the meristematic cells involved in root growth and development. In mammals, there is evidence to indicate that the PPSB plays a pivotal role in the cell proliferation control having been implicated in cancer progression (Locasale et al., 2011; Possemato, 2011). In mammals and yeast it has been shown that L-Ser also plays an indispensable role in several cellular processes; for example, the metabolism of one-carbon units, where it is the main source of these molecules for methylation reactions of nucleic acids and proteins via S-adenosylmethionine generation (Maddocks et al., 2016; Labuschagne et al., 2014; Li et al., 2015). The participation of Ser in plant cell proliferation has not been proved. Our results indicate that Ser and PPSB could well play a role in the control of this process, which could be required for proper one-carbon metabolism function in highly active dividing cells.

As we have seen, lack of PSP1 activity has drastic effects on several metabolic pathways. These alterations could also affect plant developmental processes. It has been demonstrated that high ammonium levels in root tissue inhibit primary root growth by reducing the length of the meristem and elongation zone in Arabidopsis (Liu et al., 2013b). Both a reduction in root meristem length and elongation zone were found in *psp1.1psp1.1 HS:PSP1*. The mutant root also grew better in ammonium-free medium as an N source. These results indicate that at least ammonium toxicity as a

result of impairmed PPSB activity could negatively alter root growth in the mutant.

Another factor that could participate in root growth inhibition is the high auxin concentration found in the mutant. Auxin levels lowered in aerial parts, but increased in the roots of the mutant compared to the WT. Many genes related to auxin metabolism were deregulated in the mutant. These results suggest that the high auxin level in roots may participate in their growth inhibition.

According to these results, the primary root inhibition phenotype found in *psp1.1psp1.1 HS:PSP1* could be the result of several factors: lack of Ser for one-carbon metabolism in the meristem, ammonium toxicity and high auxin levels. Since *psp1.1psp1.1 HS:PSP1* growth in ammonium-free medium has a limited effect on root growth, the role of Ser itself and/or auxin could prove more relevant. Further studies will be needed to unravel this specific contribution of auxin and Ser on primary root growth.

5. CONCLUSIONS

In this thesis we have unraveled the functions of the PPSB in *Arabidopsis*, the source of the precursor of this pathway and its connections with plant metabolism and development. From our results we can conclude that:

1) The main source of 3-PGA for the PPSB comes from the plastidial glycolytic pathway, especially in heterotrophic cells. Our results indicate that 3-PGA pools may be equilibrated by the cytosol-plastid interconnections in photosynthetic, but not in heterotrophic cells.

2) Although the PPSB is expressed in photosynthetic and non-photosynthetic tissues, it plays an essential role in specific heterotrophic cells, which could be poorly connected to the vasculature and in which the main, if not the only, source of Ser is the PPSB.

3) In this sense, PSP1 is essential for embryo and mature pollen development. Lack of PSP1 activity delayed embryo development and led to aborted embryos, classified as early curled cotyledons. It also arrested microspore development at the polarized stage. Finally, PSP1 affects primary root development, by reducing cell division in the meristem and cell length in the elongation zone. Ser could then be the link connecting primary metabolism with cell cycle progression as has been shown in animal systems.

4) PPSB affects the TCAC, the ammonium assimilation pathway and probably the sulfate assimilation pathway. Our data indicate that this pathway could be an important switch between carbon and nitrogen metabolism in plants

6. REFERENCES

Literature Cited

Aharoni A, Galili G (2011) Metabolic engineering of the plant primary-secondary metabolism interface. Curr Opin Biotechnol **22:** 239-244

Andre C, Benning C (2007) Arabidopsis seedlings deficient in a plastidic pyruvate kinase are unable to utilize seed storage compounds for germination and establishment. Plant Physiol **145:** 1670-1680

Andriotis VM, Krüger NJ, Pike MJ, Smith AM (2010) Plastidial glycolysis in developing Arabidopsis embryos. New Phytol **185:** 649-662

Anoman AD, Muñoz-Bertomeu J, Rosa-Tellez S, Flores-Tornero M, Serrano R, Bueso E, Fernie AR, Segura J, Ros R (2015) Plastidial Glycolytic Glyceraldehyde-3-Phosphate Dehydrogenase Is an Important Determinant in the Carbon and Nitrogen Metabolism of Heterotrophic Cells in Arabidopsis. Plant Physiol **169:** 1619-1637

Arabidopsis Genome Initiative (2000) Analysis of the genome sequence of the flowering plant Arabidopsis thaliana. Nature **408:** 796-815

Ariizumi T, Hatakeyama K, Hinata K, Inatsugi R, Nishida I, Sato S, Kato T, Tabata S, Toriyama K (2004) Disruption of the novel plant protein NEF1 affects lipid accumulation in the plastids of the tapetum and exine formation of pollen, resulting in male sterility in Arabidopsis thaliana. Plant J **39:** 170-181

Aharoni A, Vorst O (2001) DNA microarrays for functional plant genomics. Plant Molecular Biology **48:** 99-118

Bachelor MA, Lu Y, Owens DM (2011) L-3-Phosphoserine phosphatase (PSPH) regulates cutaneous squamous cell carcinoma proliferation independent of L-serine biosynthesis. J Dermatol Sci **63:** 164-172

Backues SK, Korasick DA, Heese A, Bednarek SY (2010) The Arabidopsis dynamin-related protein2 family is essential for gametophyte development. Plant Cell **22:** 3218-3231

Li B, Li G (2014) Ammonium stress in Arabidopsis:signaling, genetic loci, and physiological targets. Trends Plant Sci **19:** 107-114

Baud S, Wuilleme S, Dubreucq B, de Almeida A, Vuagnat C, Lepiniec L, Miquel M, Rochat C (2007) Function of plastidial pyruvate kinases in seeds of Arabidopsis thaliana. Plant J **52:** 405-419

Bauwe H, Hagemann M, Fernie AR (2010) Photorespiration: players, partners and origin Trends Plant Sci **15:** 330-336

Bedinger P (1992) The remarkable biology of pollen. Plant Cell **4:** 879-887

Benstein RM, Ludewig K, Wulfert S, Wittek S, Gigolashvili T, Frerigmann H, Gierth M, Flügge UI, Krüger S (2013) Arabidopsis phosphoglycerate dehydrogenase1 of the phosphoserine pathway is essential for development and required for ammonium assimilation and tryptophan biosynthesis. Plant Cell **25:** 5011-5029

Bertani G (1951) Studies on lysogenesis. I. The mode of phage liberation by lysogenic Escherichia coli. J Bacteriol **62:** 293-300

Bloom AJ, Burger M, Rubio Asensio JS, Cousins AB (2010) Carbon dioxide enrichment inhibits nitrate assimilation in wheat and Arabidopsis. Science **328:** 899-903

Borevitz JO, Ecker JR (2004) Plant genomics: the third wave. Annu Rev Genomics Hum Genet **5:** 443-477

Brautigam A, Weber AP (2009) Proteomic analysis of the proplastid envelope membrane provides novel insights into small molecule and protein transport across proplastid membranes. Mol Plant **2:** 1247-1261

Cascales-Miñana B, Muñoz-Bertomeu J, Flores-Tornero M, Anoman AD, Pertusa J, Alaiz M, Osorio S, Fernie AR, Segura J, Ros R (2013) The phosphorylated pathway of serine biosynthesis is essential both for male gametophyte and embryo development and for root growth in Arabidopsis. Plant Cell **25:** 2084-2101

Chen M, Thelen JJ (2010) The plastid isoform of triose phosphate isomerase is required for the postgerminative transition from heterotrophic to autotrophic growth in Arabidopsis. Plant Cell **22:** 77-90

Clough SJ, Bent AF (1998) Floral dip: a simplified method forAgrobacterium-mediated transformation ofArabidopsis thaliana. The Plant Journal **16:** 735-743

Curtis MD, Grossniklaus U (2003) A gateway cloning vector set for high-throughput functional analysis of genes in planta. Plant Physiol **133:** 462-469

Czechowski T, Stitt M, Altmann T, Udvardi MK, Scheible WR (2005) Genome-wide identification and testing of superior reference genes for transcript normalization in Arabidopsis. Plant Physiol **139:** 5-17

Devic M (2008) The importance of being essential: EMBRYO-DEFECTIVE genes in Arabidopsis. C R Biol **331:** 726-736

Dietrich CR, Han G, Chen M, Berg RH, Dunn TM, Cahoon EB (2008) Loss-of-function mutations and inducible RNAi suppression of Arabidopsis LCB2 genes reveal the critical role of sphingolipids in gametophytic and sporophytic cell viability. Plant J **54:** 284-298

Dong X, Hong Z, Sivaramakrishnan M, Mahfouz M, Verma DP (2005) Callose synthase (CalS5) is required for exine formation during microgametogenesis and for pollen viability in Arabidopsis. Plant J **42:** 315-328

Douce R, Bourguignon J, Neuburger M, Rebeille F (2001) The glycine decarboxylase system: a fascinating complex. Trends Plant Sci **6:** 167-176

Droux M (2004) Sulfur assimilation and the role of sulfur in plant metabolism: a survey. Photosynth Res **79:** 331-348

Echeverria E, Boyer CD, Thomas PA, Liu KC, Shannon JC (1988) Enzyme activities associated with maize kernel amyloplasts. Plant Physiol **86:** 786-792

Eichler HG, Hubbard R, Snell K (1981) The role of serine hydroxymethyltransferase in cell proliferation: DNA synthesis from serine following mitogenic stimulation of lymphocytes. Biosci Rep **1:** 101-106

Eicks M, Maurino V, Knappe S, Flugge UI, Fischer K (2002) The plastidic pentose phosphate translocator represents a link between the cytosolic and the plastidic pentose phosphate pathways in plants. Plant Physiol **128:** 512-522

Facchinelli F, Weber AP (2011) The metabolite transporters of the plastid envelope: an update. Front Plant Sci **2:** 50

Feng X, Dickinson HG (2010) Tapetal cell fate, lineage and proliferation in the Arabidopsis anther. Development **137:** 2409-2416

Fernie AR, Carrari F, Sweetlove LJ (2004) Respiratory metabolism: glycolysis, the TCA cycle and mitochondrial electron transport. Curr Opin Plant Biol **7:** 254-261

Fischer K (2011) The import and export business in plastids: transport processes across the inner envelope membrane. Plant Physiol **155:** 1511-1519

Fischer K, Kammerer B, Gutensohn M, Arbinger B, Weber A, Hausler RE, Flugge UI (1997) A new class of plastidic phosphate translocators: a putative link between primary and secondary metabolism by the phosphoenolpyruvate/phosphate antiporter. Plant Cell **9:** 453-462

Fischer K, Weber A (2002) Transport of carbon in non-green plastids. Trends Plant Sci **7:** 345-351

Flügge UI (1999) Phosphate Translocators in Plastids. Annu Rev Plant Physiol Plant Mol Biol **50:** 27-45

Flügge UI, Fischer K, Gross A, Sebald W, Lottspeich F, Eckerskorn C (1989) The triose phosphate-3-phosphoglycerate-phosphate translocator from spinach chloroplasts: nucleotide sequence of a full-length cDNA clone and import of the in vitro synthesized precursor protein into chloroplasts. EMBO J **8:** 39-46

Flügge UI, Weber A (1994) A rapid method for measuring organelle-specific substrate transport in homogenates from plant tissues. Planta **194:** 181-185

Focks N BC (1998) wrinkled1: A novel, low-seed-oil mutant of Arabidopsis with a deficiency in the seed-specific regulation of carbohydrate metabolism. Plant Physiol **118:** 91-101

Givan CV (2007) Evolving concepts in plant glycolysis: two centuries of progress Biological Reviews **74:** 277 <last_page> 309

Grienenberger E, Besseau S, Geoffroy P, Debayle D, Heintz D, Lapierre C, Pollet B, Heitz T, Legrand M (2009) A BAHD acyltransferase is expressed in the tapetum of Arabidopsis anthers and is involved in the synthesis of hydroxycinnamoyl spermidines. Plant J **58:** 246-259

Guan YF, Huang XY, Zhu J, Gao JF, Zhang HX, Yang ZN (2008) RUPTURED POLLEN GRAIN1, a member of the MtN3/saliva gene family, is crucial for exine pattern formation and cell integrity of microspores in Arabidopsis. Plant Physiol **147:** 852-863

Guo L, Devaiah SP, Narasimhan R, Pan X, Zhang Y, Zhang W, Wang X (2012) Cytosolic glyceraldehyde-3-phosphate dehydrogenases interact with phospholipase Ddelta to transduce hydrogen peroxide signals in the Arabidopsis response to stress. Plant Cell **24:** 2200-2212

Hajirezaei MR, Biemelt S, Peisker M, Lytovchenko A, Fernie AR, Sonnewald U (2006) The influence of cytosolic phosphorylating glyceraldehyde 3-phosphate dehydrogenase (GAPC) on potato tuber metabolism. J Exp Bot **57:** 2363-2377

Handford J, Davies DD (1958) Formation of phosphoserine from 3-phopho-glycerate in higher plants. Nature **182:** 532-533

Hanson AD, Gregory JF, (2011) Folate biosynthesis, turnover, and transport in plants. Annu Rev Plant Biol **62:** 105-125

Hanson AD, Roje S (2001) One-Carbon Metabolism in Higher Plants. Annu Rev Plant Physiol Plant Mol Biol **52:** 119-137

Hellens RP, Edwards EA, Leyland NR, Bean S, Mullineaux PM (2000) pGreen: a versatile and flexible binary Ti vector for Agrobacterium-mediated plant transformation. Plant Mol Biol **42:** 819-832

Hernandez-Pinzon I, Ross JH, Barnes KA, Damant AP, Murphy DJ (1999) Composition and role of tapetal lipid bodies in the biogenesis of the pollen coat of Brassica napus. Planta **208:** 588-598

Hirai MY, Fujiwara T, Awazuhara M, Kimura T, Noji M, Saito K (2003) Global expression profiling of sulfur-starved Arabidopsis by DNA macroarray reveals the role of O-acetyl-l-serine as a general regulator of gene expression in response to sulfur nutrition. Plant J **33:** 651-663

Ho CL, Noji M, Saito K (1999a) Plastidic pathway of serine biosynthesis. Molecular cloning and expression of 3-phosphoserine phosphatase from Arabidopsis thaliana. J Biol Chem **274:** 11007-11012

Ho CL, Noji M, Saito M, Saito K (1999b) Regulation of serine biosynthesis in Arabidopsis. Crucial role of plastidic 3-phosphoglycerate dehydrogenase in non-photosynthetic tissues. J Biol Chem **274:** 397-402

Ho CL, Noji M, Saito M, Yamazaki M, Saito K (1998) Molecular characterization of plastidic phosphoserine aminotransferase in serine biosynthesis from Arabidopsis. Plant J **16:** 443-452

Ho CL, Saito K (2001) Molecular biology of the plastidic phosphorylated serine biosynthetic pathway in Arabidopsis thaliana. Amino Acids **20:** 243-259

Holsters M, de Waele D, Depicker A, Messens E, van Montagu M, Schell J (1978) Transfection and transformation of Agrobacterium tumefaciens Molecular and General Genetics MGG **163:** 181-187

Hsieh K, Huang AH (2007) Tapetosomes in Brassica tapetum accumulate endoplasmic reticulum-derived flavonoids and alkanes for delivery to the pollen surface. Plant Cell **19:** 582-596

Hsieh K, Huang AH (2005) Lipid-rich tapetosomes in Brassica tapetum are composed of oleosin-coated oil droplets and vesicles, both assembled in and then detached from the endoplasmic reticulum. Plant J **43:** 889-899

Hsieh K, Huang AH (2004) Endoplasmic reticulum, oleosins, and oils in seeds and tapetum cells. Plant Physiol **136:** 3427-3434

Innis MA, Gelfand DH (1990) Optimization of PCRs. In MA Innis, DH Gelfand, JJ Sninsky, TJ White., ed, PCR Protocols: A Guide to Methods and Applications., Ed Academic PressNew York, pp 3-12

ISAA (2010) Agricultural Biotechnology (A Lot More than Just GM Crops).https://www.isaaa.org/resources/publications/agricultural_biotechnology/do wnload/Agricultural_Biotechnology.pdf.

Ishiguro S, Nishimori Y, Yamada M, Saito H, Suzuki T, Nakagawa T, Miyake H, Okada K, Nakamura K (2010) The Arabidopsis FLAKY POLLEN1 gene encodes a 3-hydroxy-3-methylglutaryl-coenzyme A synthase required for development of tapetum-specific organelles and fertility of pollen grains. Plant Cell Physiol **51:** 896-911

Ishiyama K, Inoue E, Watanabe-Takahashi A, Obara M, Yamaya T, Takahashi H (2004) Kinetic properties and ammonium-dependent regulation of cytosolic isoenzymes of glutamine synthetase in Arabidopsis. J Biol Chem **279:** 16598-16605

Ito T, Nagata N, Yoshiba Y, Ohme-Takagi M, Ma H, Shinozaki K (2007) Arabidopsis MALE STERILITY1 encodes a PHD-type transcription factor and regulates pollen and tapetum development. Plant Cell **19:** 3549-3562

Jessen D, Olbrich A, Knufer J, Kruger A, Hoppert M, Polle A, Fulda M (2011) Combined activity of LACS1 and LACS4 is required for proper pollen coat formation in Arabidopsis. Plant J **68:** 715-726

Jiang J, Zhang Z, Cao J (2013) Pollen wall development: the associated enzymes and metabolic pathways. Plant Biol (Stuttg) **15:** 249-263

Journet EP, Douce R (1985) Enzymic capacities of purified cauliflower bud plastids for lipid synthesis and carbohydrate metabolism. Plant Physiol **79:** 458-467

Kalhan SC, Hanson RW (2012) Resurgence of serine: an often neglected but indispensable amino Acid. J Biol Chem **287:** 19786-19791

Kammerer B (1998) Molecular Characterization of a Carbon Transporter in Plastids from Heterotrophic Tissues: The Glucose 6-Phosphate/Phosphate Antiporter THE PLANT CELL ONLINE **10:** 105-118

Kawanabe T, Ariizumi T, Kawai-Yamada M, Uchimiya H, Toriyama K (2006) Abolition of the tapetum suicide program ruins microsporogenesis. Plant Cell Physiol **47:** 784-787

Kawashima CG, Berkowitz O, Hell R, Noji M, Saito K (2005) Characterization and expression analysis of a serine acetyltransferase gene family involved in a key step of the sulfur assimilation pathway in Arabidopsis. Plant Physiol **137:** 220-230

Kehoe DM, Villand P, Somerville S (1999) DNA microarrays for studies of higher plants and other photosynthetic organisms. Trends Plant Sci **4:** 38-41

Kleczkowski LA, Givan CV (1988) Serine Formation in Leaves by Mechanisms other than the Glycolate Pathway. J Plant Physiol **132:** 641-652

Knappe S, Flugge UI, Fischer K (2003) Analysis of the plastidic phosphate translocator gene family in Arabidopsis and identification of new phosphate translocator-homologous transporters, classified by their putative substrate-binding site. Plant Physiol **131:** 1178-1190

Koncz C SJ (1986) The promoter of TL-DNA gene 5 controls the tissue-specific expression of chimaeric genes carried by a novel type of Agrobacterium binary vector. MGG Molecular & General Genetics **204:** 383-396

Koornneef M, Meinke D (2010) The development of Arabidopsis as a model plant. Plant J **61:** 909-921

Labuschagne CF, van den Broek NJ, Mackay GM, Vousden KH, Maddocks OD (2014) Serine, but not glycine, supports one-carbon metabolism and proliferation of cancer cells. Cell Rep **7:** 1248-1258

Lam HM, Coschigano KT, Oliveira IC, Melo-Oliveira R, Coruzzi GM (1996) The Molecular-Genetics of Nitrogen Assimilation into Amino Acids in Higher Plants Annu Rev Plant Physiol Plant Mol Biol **47:** 569-593

Lancien M, Gadal P, Hodges M (2000) Enzyme redundancy and the importance of 2-oxoglutarate in higher plant ammonium assimilation. Plant Physiol **123:** 817-824

Leustek T, Saito K (1999) Sulfate transport and assimilation in plants. Plant Physiol **120:** 637-644

Li S, Swanson SK, Gogol M, Florens L, Washburn MP, Workman JL, Suganuma T (2015) Serine and SAM Responsive Complex SESAME Regulates Histone Modification Crosstalk by Sensing Cellular Metabolism. Mol Cell **60:** 408-421

Lisec J, Schauer N, Kopka J, Willmitzer L, Fernie AR (2006) Gas chromatography mass spectrometry-based metabolite profiling in plants. Nat Protoc **1:** 387-396

Liu L, Fan XD (2013a) Tapetum: regulation and role in sporopollenin biosynthesis in Arabidopsis. Plant Mol Biol **83:** 165-175

Liu Y, Lai N, Gao K, Chen F, Yuan L, Mi G (2013b) Ammonium inhibits primary root growth by reducing the length of meristem and elongation zone and decreasing elemental expansion rate in the root apex in Arabidopsis thaliana. PLoS One **8:** e61031

Locasale JW, Grassian AR, Melman T, Lyssiotis CA, Mattaini KR, Bass AJ, Heffron G, Metallo CM, Muranen T, Sharfi H, Sasaki AT, Anastasiou D, Mullarky E, Vokes NI, Sasaki M, Beroukhim R, Stephanopoulos G, Ligon AH, Meyerson M, Richardson AL, Chin L, Wagner G, Asara JM, Brugge JS, Cantley LC, Vander Heiden MG (2011) Phosphoglycerate dehydrogenase diverts glycolytic flux and contributes to oncogenesis. Nat Genet **43:** 869-874

López-Juez E (2007) Plastid biogenesis, between light and shadows. J Exp Bot **58:** 11-26

Maddocks OD, Labuschagne CF, Adams PD, Vousden KH (2016) Serine Metabolism Supports the Methionine Cycle and DNA/RNA Methylation through De Novo ATP Synthesis in Cancer Cells. Mol Cell **61:** 210-221

Mandel M, Higa A (1992) Calcium-dependent bacteriophage DNA infection. 1970. Biotechnology **24:** 198-201

Masclaux-Daubresse C, Reisdorf-Cren M, Pageau K, Lelandais M, Grandjean O, Kronenberger J, Valadier MH, Feraud M, Jouglet T, Suzuki A (2006) Glutamine synthetase-glutamate synthase pathway and glutamate dehydrogenase play distinct roles in the sink-source nitrogen cycle in tobacco. Plant Physiol **140:** 444-456

Matsuhara S, Jingu F, Takahashi T, Komeda Y (2000) Heat-shock tagging: a simple method for expression and isolation of plant genome DNA flanked by T-DNA insertions. Plant J **22:** 79-86

Maurino VG, Peterhansel C. (2010) Photorespiration: Current status and approaches for metabolic engineering. Curr Opin Plant Biol **13:** 249-256

Meinke DW, Cherry JM, Dean C, Rounsley SD, Koornneef M (1998) Arabidopsis thaliana: a model plant for genome analysis. Science **282:** 662, 679-82

Meyerowitz EM (2001) Prehistory and history of Arabidopsis research. Plant Physiol **125:** 15-19

Michard E, Lima PT, Borges F, Silva AC, Portes MT, Carvalho JE, Gilliham M, Liu LH, Obermeyer G, Feijo JA (2011) Glutamate receptor-like genes form Ca2+ channels in pollen tubes and are regulated by pistil D-serine. Science **332:** 434-437

Miernyk JA, Dennis DT (1992) A Developmental Analysis of the Enolase Isozymes from Ricinus communis. Plant Physiol **99:** 748-750

Mothet J, Parent AT, Wolosker H, Brady RO, Linden DJ, Ferris CD, Rogawski MA, Snyder SH (2000) D-Serine is an endogenous ligand for the glycine site of the N-methyl-D-aspartate receptor Proceedings of the National Academy of Sciences **97:** 4926-4931

Muñoz-Bertomeu J, Cascales-Miñana B, Irles-Segura A, Mateu I, Nunes-Nesi A, Fernie AR, Segura J, Ros R (2010) The plastidial glyceraldehyde-3-phosphate dehydrogenase is critical for viable pollen development in Arabidopsis. Plant Physiol **152:** 1830-1841

Muñoz-Bertomeu J, Cascales-Miñana B, Mulet JM, Baroja-Fernandez E, Pozueta-Romero J, Kuhn JM, Segura J, Ros R (2009) Plastidial glyceraldehyde-3-phosphate dehydrogenase deficiency leads to altered root development and affects the sugar and amino acid balance in Arabidopsis. Plant Physiol

Neuhaus HE, Emes MJ (2000a) Nonphotosynthetic Metabolism in Plastids. Annu Rev Plant Physiol Plant Mol Biol **51:** 111-140

Neuhaus HE, Wagner R (2000b) Solute pores, ion channels, and metabolite transporters in the outer and inner envelope membranes of higher plant plastids. Biochim Biophys Acta **1465:** 307-323

Paxson-Sowders DM, Dodrill CH, Owen HA, Makaroff CA (2001) DEX1, a novel plant protein, is required for exine pattern formation during pollen development in Arabidopsis. Plant Physiol **127:** 1739-1749

Pfaffl MW (2001) A new mathematical model for relative quantification in real-time RT-PCR. Nucleic Acids Res **29:** e45

Plaxton WC (1996) The Organization and Regulation of Plant Glycolysis. Annu Rev Plant Physiol Plant Mol Biol **47:** 185-214

Pollari S, Kakonen SM, Edgren H, Wolf M, Kohonen P, Sara H, Guise T, Nees M, Kallioniemi O (2011) Enhanced serine production by bone metastatic breast cancer cells stimulates osteoclastogenesis. Breast Cancer Res Treat **125:** 421-430

Possemato R, et al. (2011) Functional genomics reveal that the serine synthesis pathway is essential in breast cancer. Nature **476:** 346-350

Prabhakar V, Lottgert T, Geimer S, Dormann P, Kruger S, Vijayakumar V, Schreiber L, Gobel C, Feussner K, Feussner I, Marin K, Staehr P, Bell K, Flugge UI, Hausler RE (2010) Phosphoenolpyruvate provision to plastids is essential for gametophyte and sporophyte development in Arabidopsis thaliana. Plant Cell **22:** 2594-2617

Pyke KA (2010) Plastid division. AoB Plants **2010:** plq016

Qin C, Qian W, Wang W, Wu Y, Yu C, Jiang X, Wang D, Wu P (2008) GDP-mannose pyrophosphorylase is a genetic determinant of ammonium sensitivity in Arabidopsis thaliana. Proc Natl Acad Sci U S A **105:** 18308-18313

Quilichini TD, Douglas CJ, Samuels AL (2014) New views of tapetum ultrastructure and pollen exine development in Arabidopsis thaliana. Ann Bot

Rachmilevitch S, Cousins AB, Bloom AJ (2004) Nitrate assimilation in plant shoots depends on photorespiration. Proc Natl Acad Sci U S A **101:** 11506-11510

Raines CA (2003) The Calvin cycle revisited. Photosynth Res **75:** 1-10

Regan SM, Moffatt BA (1990) Cytochemical Analysis of Pollen Development in Wild-Type Arabidopsis and a Male-Sterile Mutant. Plant Cell **2:** 877-889

Reiser J, Linka N, Lemke L, Jeblick W, Neuhaus HE (2004) Molecular physiological analysis of the two plastidic ATP/ADP transporters from Arabidopsis. Plant Physiol **136:** 3524-3536

Riens B, Lohaus G, Heineke D, Heldt HW (1991) Amino Acid and sucrose content determined in the cytosolic, chloroplastic, and vacuolar compartments and in the Phloem sap of spinach leaves. Plant Physiol **97:** 227-233

Scholl RL, May ST, Ware DH (2000) Seed and molecular resources for Arabidopsis. Plant Physiol **124:** 1477-1480

Schwender J, Ohlrogge JB, Shachar-Hill Y (2003) A flux model of glycolysis and the oxidative pentosephosphate pathway in developing Brassica napus embryos J Biol Chem **278:** 29442-29453

Slaughter JC, Davies DD (1968) The isolation and characterization of 3-phosphoglycerate dehydrogenase from peas. Biochem J **109:** 743-748

Smyth DR, Bowman JL, Meyerowitz EM (1990) Early flower development in Arabidopsis. Plant Cell **2:** 755-767

Stitt M, Lilley RM, Gerhardt R, Heldt HW (1989) [32] Metabolite levels in specific cells and subcellular compartments of plant leaves. Meth Enzymol **174:** 518-552

Suzuki M, Nakagawa S, Kamide Y, Kobayashi K, Ohyama K, Hashinokuchi H, Kiuchi R, Saito K, Muranaka T, Nagata N (2009) Complete blockage of the mevalonate pathway results in male gametophyte lethality. J Exp Bot **60:** 2055-2064

Suzuki T, Masaoka K, Nishi M, Nakamura K, Ishiguro S (2008) Identification of kaonashi mutants showing abnormal pollen exine structure in Arabidopsis thaliana. Plant Cell Physiol **49:** 1465-1477

Suzuki T, Tsunekawa S, Koizuka C, Yamamoto K, Imamura J, Nakamura K, Ishiguro S (2013) Development and disintegration of tapetum-specific lipid-accumulating organelles, elaioplasts and tapetosomes, in Arabidopsis thaliana and Brassica napus. Plant Sci **207:** 25-36

Takahashi H (2010) Regulation of sulfate transport and assimilation in plants. Int Rev Cell Mol Biol **281:** 129-159

Tcherkez G, Mahe A, Guerard F, Boex-Fontvieille ER, Gout E, Lamothe M, Barbour MM, Bligny R (2012) Short-term effects of CO(2) and O(2) on citrate metabolism in illuminated leaves. Plant Cell Environ **35:** 2208-2220

ten Hove CA, Lu KJ, Weijers D (2015) Building a plant: cell fate specification in the early Arabidopsis embryo. Development **142:** 420-430

Ting JT, Wu SS, Ratnayake C, Huang AH (1998) Constituents of the tapetosomes and elaioplasts in Brassica campestris tapetum and their degradation and retention during microsporogenesis. Plant J **16:** 541-551

Tolbert NE (1997) The C2 oxidative photosynthetic carbon cycle. Annu Rev Plant Physiol Plant Mol Biol **48:** 1-25

Tolbert NE (1980) Photorespiration. In: The biochemistry of plants, 488-525

Toujani W, Muñoz-Bertomeu J, Flores-Tornero M, Rosa-Tellez S, Anoman AD, Alseekh S, Fernie AR, Ros R (2013) Functional characterization of the plastidial 3-phosphoglycerate dehydrogenase family in Arabidopsis. Plant Physiol **163:** 1164-1178

Tzafrir I, Pena-Muralla R, Dickerman A, Berg M, Rogers R, Hutchens S, Sweeney TC, McElver J, Aux G, Patton D, Meinke D (2004) Identification of genes required for embryo development in Arabidopsis. Plant Physiol **135:** 1206-1220

Van der Straeten D, Rodrigues-Pousada RA, Goodman HM, Van Montagu M (1991) Plant enolase: gene structure, expression, and evolution. Plant Cell **3:** 719-735

Vizcay-Barrena G, Wilson ZA (2006) Altered tapetal PCD and pollen wall development in the Arabidopsis ms1 mutant. J Exp Bot **57:** 2709-2717

Wang Z, Gerstein M, Snyder M (2009) RNA-Seq: a revolutionary tool for transcriptomics. Nat Rev Genet **10:** 57-63

Weber AP, Fischer K (2007) Making the connections--the crucial role of metabolite transporters at the interface between chloroplast and cytosol. FEBS Lett **581:** 2215-2222

Weber AP, Schwacke R, Flugge UI (2005) Solute transporters of the plastid envelope membrane. Annu Rev Plant Biol **56:** 133-164

Winter D, Vinegar B, Nahal H, Ammar R, Wilson GV, Provart NJ (2007) An "Electronic Fluorescent Pictograph" browser for exploring and analyzing large-scale biological data sets. PLoS One **2:** e718

Wise RR (2006) The Diversity of Plastid Form and Function. In: The Structure and Function of Plastids. Springer, The Netherlands, 3-26

Weckwerth W (2007) Metabolomics: Methods and Protocols, Ed Wolfram Weckwerth. Humana Press, Totowa, NJ

Wu S, Ramonell K, Gollub J, Somerville S (2001) Plant gene expression profiling with DNA microarrays. Plant Physiology and Biochemistry **39:** 917-926

Yamamoto Y, Nishimura M, Hara-Nishimura I, Noguchi T (2003) Behavior of vacuoles during microspore and pollen development in Arabidopsis thaliana. Plant Cell Physiol **44:** 1192-1201

Yang C, Vizcay-Barrena G, Conner K, Wilson ZA (2007) MALE STERILITY1 is required for tapetal development and pollen wall biosynthesis. Plant Cell **19:** 3530-3548

Yoshida K, Furuya S, Osuka S, Mitoma J, Shinoda Y, Watanabe M, Azuma N, Tanaka H, Hashikawa T, Itohara S, Hirabayashi Y (2004) Targeted disruption of the mouse 3-phosphoglycerate dehydrogenase gene causes severe neurodevelopmental defects and results in embryonic lethality. J Biol Chem **279:** 3573-3577

Zhang W, Sun Y, Timofejeva L, Chen C, Grossniklaus U, Ma H (2006) Regulation of Arabidopsis tapetum development and function by DYSFUNCTIONAL TAPETUM1 (DYT1) encoding a putative bHLH transcription factor. Development **133:** 3085-3095

Zhang Y, Sun K, Sandoval FJ, Santiago K, Roje S (2010) One-carbon metabolism in plants: characterization of a plastid serine hydroxymethyltransferase. Biochem J **430:** 97-105

7. APPENDIX

Table S1. List of primers used in this thesis for genotyping, cloning and qRT-PCR.

Gene	Name	Sequence
Primers for mutants genotyping		
At1g79530 (GAPCp1)	LP390_G10	TTCGTTTCTGATTCTCTTGCG
	LB1_SAIL	GCCTTTTCAGAAATGGATAAATAGCCTTGCTTCC
	RP390_G10	TCATCCCTTGATGTTGCAATG
At1g16300 (GAPCp2)	LP137288	TCTTCCAATTCGACCAAAACC
	LBa1	TGGTTCACGTAGTGGGCCATCG
	RP137288.D	TCCTCGTGTCGAGCTTTATCC
At1g18640 (PSP1)	PSP_RP	CTCGACAAGAGACCCCCAAG
	PSP-LP	CCGCCAAGATTGATTAGTCTG
	LBb1.3	ATTTTGCCGATTTCGGAAC
Primers for cloning		
At5g46110 (TPT)	At5g46110RepCR8	TGCTTTCTTTCCTTGCCGTTTC
	At5g46110FopCR8	ATGGAGTCACGCGTGCTGTTACG
	At5g46110XbaIRe3	GCTCTAGACTATGCTTTCTTTCCTTGCCGTTTC
	At5g46110XhoIFo	CCGCTCGAGATGGAGTCACGCGTGCTGTTACG
	At5g46100Fcentral	GCTACCAATACCTTGGAGGGG
Primers for qRT-PCR		
At5g46110 (TPT)	At5g46110.4RTRev	TGCAACTCCAGCAATGGCTAT
	At5g46110.4RTFor	TGAAACGTGTGTTCGTGATCG
At1g18640 (PSP1)	PSP 2 RTRev	CTCGACAAGAGACCCCCAAG
	PSP 2 RT For	GATGCCAAGAATCGATGCTAC

Table S2. List of primers used in this thesis for RNAseq validation.

Gene	Name	Sequence
Primers for RNAseq Validation		
In aerial part		
At4g04610	At4g04610F	GAAATACGGGAACGATATCGC
	At4g04610R	ATGGCCTCCCAGTCAAATGA
At4g04830	At4g04830F	ACTCCCTGGTGCCATAAACC
	At4g04830R	GGTTGGATTACCGTAACCTTCTC
At2g17040	At2g17040F	GACTGATTGGGTGATGAACGAG
	At2g17040R	TCTGCCCTTTGCTCCAATAC
At4g21990	At4g21990F	ATGAGCATACTCAATCAGAGCAAC
	At4g21990R	CCTCTTGAGATCATGGATAAAGC
At5g24660	AT5G24660 for	GCTTGAAGCAGAATCTTTAGACCAG
	AT5G24660 rev	CAGAGTCTGAAGAAAGACGAGAGAG
At3g02790	At3g02790F	CGAAGGAGATTCAAGCGAAGA
	At3g02790R	CGTGGCCTCCTTTCTCTTT
At3g19710	At3g19710F	GACCCGTCTGGATATCACTTAAC
	At3g19710R	TGACTAGTATTGCATCCGTAACCT
At2g29680	At2g29680F	TAGTCTTGCTCGAGACGATAAACTA
	At2g29680R	TCATAGAAGACAGTTGCGGAAGA
In roots		
At5g61590	At5g61590F	CTGCTTCCATTTGCAGAATCTC
	At5g61590R	CTGGTCTCTAGAACCCTTTAACCC
At1g49200	At1g49200F	CAACCCATTTGACCACAACAC
	At1g49200R	AGGACTGAGAGAAGCATCAGAACA
At5g15150	At5g15150F	GCTTCTGCGAATTCTCTCTTGA
	At5g15150R	ATTCTCTTCTTGCCCACAACAA
At5g11020	At5g11020F	AGGATCTATGACGCTTGGTAACTT
	At5g11020R	CCTGTGGAGAAACTAGCTCCC
At4g08300	AT4G08300 for	TTACCAGTGAAGTAAACGAAGGTG
	AT4G08300 rev	GGGTTACACTTGGGTATTGTTAGTC
At5g04140	At5g04140F	TGCAGCTGAAGAGCTTAATTGA
	At5g04140R	GCCAGAAGAGAGGTAGATACTTTTC
At5g02760	At5g02760F	TGGGAGCATCTTAGCAACCA
	At5g02760R	TCTTTGCTGCTTCCTTCAATG
At5g22800	At5g22800F	TGAGTCAGCATCGGTGTCATC
	At5g22800R	AAGCAGCTGTCTATAAAGCATCTGT
At1g17180	At1g17180R	CCACTTCTTCCTTCTGATCCTTAC
	At1g17180R	CCTCATGCTCTTCGCCTTTA

Table S3 Metabolite levels in the aerial parts of wild-type (WT), *gapcp1gapcp2* (*g1g2*) and *g1g2 35S:TPT-His* (35S:TPT-His) lines. Data are relative values normalized to the mean response calculated for the WT. Values represent the mean ± SE of 5-6 independent determinations for WT and *g1g2* and 11-12 determinations for the 35S:TPT-His lines (two different lines). Values that are significantly different to WT are shown in bold, and those that significantly differed from *g1g2* are followed by *, ($P < 0.05$).

	WT	*g1g2*	35S:TPT
Amino acids			
Alanine, D, L	1 ± 0.05	0.90 ± 0.04	1.02 ± 0.04
Alanine, β	1 ± 0.03	**1.71 ± 0.05**	0.92 ± 0.02*
Arginine	1 ± 0.09	1.06 ± 0.04	0.95 ± 0.06
Asparagine	1 ± 0.16	**3.30 ± 0.26**	1.27 ± 0.16*
Aspartate	1 ± 0.02	**1.47 ± 0.03**	0.98 ± 0.06*
Cysteine	1 ± 0.07	**1.56 ± 0.03**	1.16 ± 0.10*
GABA	1 ± 0.06	**1.27 ± 0.04**	**1.36 ± 0.04**
Glutamate	1 ± 0.04	**1.48 ± 0.04**	1.01 ± 0.04*
Glutamine	1 ± 0.05	**1.74 ± 0.09**	1.06 ± 0.10*
Glycine	1 ± 0.03	**0.75 ± 0.02**	**0.82 ± 0.02**
Isoleucine	1 ± 0.03	0.96 ± 0.01	**0.80 ± 0.01***
Lysine	1 ± 0.12	1.08 ± 0.03	0.81 ± 0.05*
Methionine	1 ± 0.15	**1.69 ± 0.05**	0.96 ± 0.09*
Ornithine	1 ± 0.20	1.20 ± 0.15	1.35 ± 0.21
Phenylalanine	1 ± 0.05	**1.63 ± 0.07**	**0.88 ± 0.03***
Proline	1 ± 0.03	**1.90 ± 0.03**	**1.20 ± 0.05***
Serine	1 ± 0.03	**0.88 ± 0.02**	**0.93 ± 0.01***
Serine, O-acetyl	1 ± 0.14	**0.53 ± 0.03**	0.96 ± 0.11*
Serine, Homo-	1 ± 0.09	1.36 ± 0.20	2.93 ± 0.60
Threonine	1 ± 0.03	1.04 ± 0.02	**0.94 ± 0.01***
Tryptophane	1 ± 0.23	**2.34 ± 0.39**	0.80 ± 0.12*
Valine	1 ± 0.05	1.08 ± 0.02	**0.81 ± 0.01***
Organic acids			
Ascorbic acid	1 ± 0.11	**1.68 ± 0.22**	0.82 ± 0.05*
Benzoic acid	1 ± 0.12	0.84 ± 0.02	0.86 ± 0.08
Citrate	1 ± 0.15	**2.02 ± 0.07**	0.93 ± 0.05*
Fumarate	1 ± 0.01	**1.83 ± 0.02**	**1.28 ± 0.05***
Galacturonic acid	1 ± 0.04	**1.59 ± 0.04**	1.04 ± 0.02*
Glycerate	1 ± 0.08	**3.09 ± 0.38**	**1.25 ± 0.05***
Glycolic acid	1 ± 0.06	**1.25 ± 0.04**	0.87 ± 0.05*
Glutaric acid, 2-oxo-	1 ± 0.23	**1.68 ± 0.11**	0.88 ± 0.06*
Isocitric acid	1 ± 0.14	**2.05 ± 0.10**	0.84 ± 0.10*
Malate	1 ± 0.02	**1.36 ± 0.03**	1.06 ± 0.02*
Nicotinic acid	1 ± 0.03	**1.36 ± 0.02**	1.10 ± 0.03*
Phosphoric acid	1 ± 0.07	**0.22 ± 0.02**	0.91 ± 0.05*
Pyroglutamic acid	1 ± 0.03	**1.44 ± 0.04**	1.02 ± 0.05*
Pyruvate	1 ± 0.07	**1.53 ± 0.13**	**0.87 ± 0.03***
Threonic acid	1 ± 0.14	0.88 ± 0.05	0.99 ± 0.06

Table S3. Continuation.

	WT	*g1g2*	35S:TPT
Sugars and sugar alcohols			
Fructose	1 ± 0.02	**2.01 ± 0.04**	1.05 ± 0.11*
Fructose-6-P	1 ± 0.02	**0.72 ± 0.02**	0.85 ± 0.06
Fucose	1 ± 0.09	1.27 ± 0.10	0.88 ± 0.03*
Galactinol	1 ± 0.06	**2.72 ± 0.10**	0.92 ± 0.05*
Glyceraldehyde-3-phosphate	1 ± 0.04	0.94 ± 0.03	1.03 ± 0.04
Glycerol	1 ± 0.17	0.72 ± 0.14	0.83 ± 0.10
Glycerol-3-P	1 ± 0.05	0.92 ± 0.03	1.05 ± 0.05
Glucose	1 ± 0.03	**1.61 ± 0.11**	0.93 ± 0.10*
Glucose-6-P	1 ± 0.02	**0.73 ± 0.03**	0.97 ± 0.07*
Maltose	1 ± 0.04	**1.77 ± 0.03**	0.99 ± 0.06*
Myo-inositol	1 ± 0.02	**2.14 ± 0.03**	1.24 ± 0.07*
Raffinose	1 ± 0.09	**2.52 ± 0.06**	1.03 ± 0.07*
Rhamnose	1 ± 0.03	**1.08 ± 0.02**	0.96 ± 0.02*
Ribose	1 ± 0.04	**1.71 ± 0.05**	1.10 ± 0.06*
Sucrose	1 ± 0.02	**1.15 ± 0.02**	**0.87 ± 0.03***
Threitol	1 ± 0.01	**0.72 ± 0.01**	0.91 ± 0.03*
Trehalose	1 ± 0.02	**2.66 ± 0.05**	1.10 ± 0.03*
Xylose	1 ± 0.02	**1.62 ± 0.03**	1.02 ± 0.03*
Miscellaneous			
Putrescine	1 ± 0.07	**1.65 ± 0.15**	0.89 ± 0.07*
Spermidine	1 ± 0.15	**2.46 ± 0.24**	0.99 ± 0.18*
Uracil	1 ± 0.02	**0.80 ± 0.03**	**0.84 ± 0.03**
Urea	1 ± 0.07	0.90 ± 0.03	0.93 ± 0.14

Table S4. Metabolite levels in the roots of wild-type (WT), *gapcp1gapcp2* (*g1g2*) and *g1g2 35S:TPT-His* (35S:TPT-His) lines. Data are relative values normalized to the mean response calculated for the WT. Values represent the mean ± SE of 5-6 independent determinations for WT and *g1g2* and 11-12 determinations for the 35S:TPT-His lines (two different lines). Values that are significantly different to WT are shown in bold, and those that significantly differed from *g1g2* are followed by *, ($P < 0.05$).

	WT	*g1g2*	35S:TPT
Amino acids			
Alanine, D, L	1 ± 0.23	**3.41 ± 0.66**	1.74 ± 0.23*
Alanine, β	1 ± 0.07	**1.75 ± 0.05**	1.08 ± 0.06*
Arginine	1 ± 0.04	**2.59 ± 0.11**	1.12 ± 0.06*
Asparagine	1 ± 0.12	1.11 ± 0.05	0.92 ± 0.05*
Aspartate	1 ± 0.12	**1.37 ± 0.11**	1.20 ± 0.09
Cysteine	1 ± 0.10	**2.99 ± 0.18**	1.26 ± 0.09*
GABA	1 ± 0.15	**2.93 ± 0.42**	**1.74 ± 0.20***
Glutamate	1 ± 0.05	**1.60 ± 0.02**	1.00 ± 0.07*
Glutamine	1 ± 0.11	**2.34 ± 0.24**	0.99 ± 0.08*
Glycine	1 ± 0.05	**1.76 ± 0.13**	0.96 ± 0.07*
Isoleucine	1 ± 0.06	**1.46 ± 0.09**	1.09 ± 0.05*
Lysine	1 ± 0.06	1.10 ± 0.05	**0.84 ± 0.03***
Methionine	1 ± 0.08	**2.94 ± 0.24**	1.51 ± 0.17*
Ornithine	1 ± 0.06	1.49 ± 0.28	1.21 ± 0.07
Phenylalanine	1 ± 0.04	**1.50 ± 0.03**	1.04 ± 0.04*
Proline	1 ± 0.04	**2.58 ± 0.13**	1.18 ± 0.07*
Serine	1 ± 0.04	**0.86 ± 0.04**	1.18 ± 0.06*
Serine, O-acetyl	1 ± 0.12	**1.51 ± 0.14**	**1.48 ± 0.11**
Threonine	1 ± 0.06	**1.34 ± 0.06**	1.15 ± 0.06*
Tryptophane	1 ± 0.19	**1.69 ± 0.12**	1.28 ± 0.12*
Tyrosine	1 ± 0.26	1.53 ± 0.15	0.99 ± 0.10*
Valine	1 ± 0.07	**1.42 ± 0.06**	1.05 ± 0.06*
Organic acids			
Ascorbic acid	1 ± 0.10	**6.40 ± 0.23**	**2.13 ± 0.28***
Benzoic acid	1 ± 0.08	**1.87 ± 0.17**	**1.35 ± 0.09***
Citrate	1 ± 0.04	**4.78 ± 0.10**	**1.61 ± 0.07***
Fumarate	1 ± 0.06	**1.40 ± 0.05**	**1.63 ± 0.09**
Glycerate	1 ± 0.05	**5.53 ± 0.26**	**1.65 ± 0.06***
Glycolic acid	1 ± 0.08	1.13 ± 0.07	**1.95 ± 0.11***
Glutaric acid, 2-oxo-	1 ± 0.26	**3.45 ± 0.63**	1.49 ± 0.21*
Nicotinic acid	1 ± 0.07	1.13 ± 0.04	1.02 ± 0.04
Phosphoric acid	1 ± 0.07	**0.52 ± 0.04**	**0.78 ± 0.04***
Pyroglutamic acid	1 ± 0.08	**2.76 ± 0.08**	**1.32 ± 0.07***
Pyruvate	1 ± 0.06	**2.31 ± 0.13**	1.33 ± 0.10*
Succinate	1 ± 0.06	**1.71 ± 0.07**	1.15 ± 0.06*
Threonic acid	1 ± 0.05	**1.45 ± 0.06**	**0.84 ± 0.04***

Table S4. Continuation.

	WT	*g1g2*	35S:TPT
Sugars and sugar alcohols			
Fructose	1 ± 0.04	**4.44 ± 0.09**	1.00 ± 0.05*
Fructose-6-P	1 ± 0.04	**0.78 ± 0.02**	**0.77 ± 0.02**
Fucose	1 ± 0.03	**2.86 ± 0.14**	**1.73 ± 0.16***
Galactinol	1 ± 0.06	**1.71 ± 0.03**	1.25 ± 0.10*
Glyceraldehyde-3-phosphate	1 ± 0.05	**1.43 ± 0.02**	**1.30 ± 0.06**
Glucose	1 ± 0.17	**2.00 ± 0.03**	1.06 ± 0.09*
Maltose	1 ± 0.05	**1.95 ± 0.11**	**1.22 ± 0.04***
Mannitol	1 ± 0.05	**4.25 ± 0.10**	0.99 ± 0.05*
Myo-inositol	1 ± 0.05	**3.86 ± 0.10**	**1.38 ± 0.09***
Raffinose	1 ± 0.25	**2.20 ± 0.19**	1.42 ± 0.14*
Sucrose	1 ± 0.18	1.11 ± 0.11	0.94 ± 0.10
Trehalose	1 ± 0.10	**2.87 ± 0.06**	1.11 ± 0.04*
Miscellaneous			
Urea	1 ± 0.18	0.61 ± 0.10	0.88 ± 0.06

Table S5. Levels of metabolites in aerial parts of wild-type (WT) and conditional mutant *psp1.1psp1.1 HS:PSP1 (HS PSP)* under three different conditions (light with or without serine in the medium, darkness and high levels of CO_2), with (+) or without (-) heat shock treatment. Data are normalised and related to the mean of the WT for each condition. Each value represents the mean ± SE (n = 6). Values in bold are significantly different from the WT and that significantly differed from the values of the heat shock treatment are followed by * (P > 0.05).

	Aerial part										
	Light					**Darkness**			**High CO_2**		
		-	+	**serine**			-	+		-	+
Amino acids	WT	*HS PSP*	*HS PSP*	WT	*HS PSP*	WT	*HS PSP*	*HS PSP*	WT	*HS PSP*	*HS PSP*
Alanine	1 ± 0.17	0.79 ± 0.10*	0.69 ± 0.08	1 ± 0.13	0.95 ± 0.09	1 ± 0.07	**0.66 ± 0.04**	0.61 ± 0.03	1 ± 0.09	0.88 ± 0.05	0.87 ± 0.06
Alanine, beta	1 ± 0.03	**1.59 ± 0.06***	1.36 ± 0.04	1 ± 0.04	**0.82 ± 0.03**	1 ± 0.05	**1.22 ± 0.04***	1.03 ± 0.03	1 ± 0.04	**1.37 ± 0.03***	1.18 ± 0.05
Arginine	1 ± 0.05	**2.48 ± 0.07**	2.63 ± 0.07	1 ± 0.03	0.96 ± 0.04	1 ± 0.04	**2.32 ± 0.08***	2.96 ± 0.12	1 ± 0.02	**2.32 ± 0.09***	2.02 ± 0.06
Asparagine	1 ± 0.20	**3.22 ± 0.28**	3.07 ± 0.29	1 ± 0.19	0.87 ± 0.10	1 ± 0.11	**2.32 ± 0.12***	2.81 ± 0.14	1 ± 0.16	**3.82 ± 0.13***	1.98 ± 0.07
Aspartic acid	1 ± 0.02	**1.31 ± 0.03**	1.25 ± 0.01	1 ± 0.02	0.98 ± 0.02	1 ± 0.01	**1.23 ± 0.01***	1.12 ± 0.02	1 ± 0.03	**1.87 ± 0.02***	1.55 ± 0.02
Cysteine	1 ± 0.10	1.24 ± 0.08	1.15 ± 0.08	1 ± 0.06	0.93 ± 0.05	1 ± 0.05	1.08 ± 0.05	1.15 ± 0.05	1 ± 0.07	**2.70 ± 0.17***	1.65 ± 0.06
GABA	1 ± 0.08	**2.25 ± 0.14***	1.59 ± 0.13	1 ± 0.06	0.91 ± 0.07	1 ± 0.04	**2.27 ± 0.06***	1.73 ± 0.10	1 ± 0.06	**2.54 ± 0.13***	2.09 ± 0.16
Glutamic acid	1 ± 0.07	**1.47 ± 0.06**	1.33 ± 0.04	1 ± 0.07	1.02 ± 0.05	1 ± 0.03	**1.42 ± 0.02***	1.3 ± 0.03	1 ± 0.03	**1.25 ± 0.04***	1.04 ± 0.03
Glutamine	1 ± 0.16	**2.74 ± 0.23**	2.37 ± 0.14	1 ± 0.09	0.98 ± 0.07	1 ± 0.06	**1.44 ± 0.05***	1.42 ± 0.05	1 ± 0.04	**1.27 ± 0.05**	1.12 ± 0.06
Glycine	1 ± 0.04	**0.83 ± 0.03***	1.00 ± 0.04	1 ± 0.03	**1.28 ± 0.03**	1 ± 0.09	**3.5 ± 0.08***	4.22 ± 0.30	1 ± 0.02	**2.30 ± 0.04***	1.2 ± 0.02
Histidine	1 ± 0.34	**6.02 ± 0.40**	14.12 ± 0.98	1 ± 0.19	0.84 ± 0.16	1 ± 0.26	**3.28 ± 0.14***	4.45 ± 0.22	1 ± 0.04	**5.42 ± 0.13***	3.49 ± 0.07
Homoserine	1 ± 0.04	**2.06 ± 0.12**	1.84 ± 0.09	1 ± 0.04	0.98 ± 0.05	-	-	-	1 ± 0.05	1.09 ± 0.05	1 ± 0.04
Isoleucine	1 ± 0.02	**1.33 ± 0.02***	1.17 ± 0.03	1 ± 0.02	**0.88 ± 0.01**	1 ± 0.05	**1.14 ± 0.04***	0.86 ± 0.02	1 ± 0.02	**1.60 ± 0.02***	1.49 ± 0.03
Leucine	1 ± 0.12	0.97 ± 0.07	0.94 ± 0.05	1 ± 0.07	1.2 0± 0.07	-	-	-	1 ± 0.1	**1.20 ± 0.06***	1.04 ± 0.05
Lysine	1 ± 0.05	**2.18 ± 0.07***	2.23 ± 0.07	1 ± 0.03	**0.91 ± 0.02**	1 ± 0.05	**1.84 ± 0.09**	1.86 ± 0.08	1 ± 0.02	**2.42 ± 0.13**	2.32 ± 0.12
Methionine	1 ± 0.02	**1.2 ± 0.05**	1.22 ± 0.05	1 ± 0.03	0.91 ± 0.03	1 ± 0.04	**1.17 ± 0.06**	1.22 ± 0.03	1 ± 0.03	1.09 ± 0.04*	0.92 ± 0.03
Ornithine	1 ± 0.02	**1.96 ± 0.05***	2.17 ± 0.07	1 ± 0.04	0.9 0± 0.03	1 ± 0.06	**1.86 ± 0.06***	2.54 ± 0.10	1 ± 0.06	**2.39 ± 0.09**	2.18 ± 0.06
Phenylalanine	1 ± 0.01	**2.38 ± 0.04**	2.35 ± 0.04	1 ± 0.03	**0.93 ± 0.01**	1 ± 0.05	**1.93 ± 0.04**	1.93 ± 0.04	1 ± 0.05	**2.68 ± 0.07**	2.09 ± 0.04
Proline	1 ± 0.03	**1.37 ± 0.05***	1.20 ± 0.03	1 ± 0.03	1.03 ± 0.02	1 ± 0.09	**0.73 ± 0.06**	0.74 ± 0.05	1 ± 0.03	**5.11 ± 0.16***	2.52 ± 0.07
Proline, 4-hydroxy	1 ± 0.03	**1.59 ± 0.05**	1.45 ± 0.05	1 ± 0.03	1.01 ± 0.03	-	-	-	-	-	-
Serine	1 ± 0.01	**1.11 ± 0.02**	1.10 ± 0.02	1 ± 0.02	0.98 ± 0.01	1 ± 0.02	**1.64 ± 0.03**	1.64 ± 0.05	1 ± 0.02	**1.20 ± 0.03***	1.03 ± 0.03
Serine, O-acetyl-	1 ± 0.02	**2.72 ± 0.09***	2.12 ± 0.04	1 ± 0.03	0.98 ± 0.03	1 ± 0.04	**2.67 ± 0.06**	2.52 ± 0.07	1 ± 0.03	**4.13 ± 0.08***	3.14 ± 0.10
Threonine	1 ± 0.02	**1.38 ± 0.03***	1.25 ± 0.02	1 ± 0.02	1.01 ± 0.01	1 ± 0.04	**1.26 ± 0.03**	1.32 ± 0.04	1 ± 0.01	**1.65 ± 0.03***	1.32 ± 0.03
Tryptophan	1 ± 0.07	**5.53 ± 0.43**	5.53 ± 0.30	1 ± 0.11	0.85 ± 0.04	1 ± 0.06	**4.21 ± 0.14**	3.88 ± 0.15	1 ± 0.05	**12.98 ± 0.72***	7.62 ± 0.31
Tyrosine	1 ± 0.15	**5.56 ± 0.48**	5.1 0± 0.44	1 ± 0.04	0.92 ± 0.06	1 ± 0.14	**4.71 ± 0.37***	2.62 ± 0.31	1 ± 0.03	**9.73 ± 0.50**	8.63 ± 0.35
Valine	1 ± 0.01	**1.35 ± 0.02***	1.22 ± 0.02	1 ± 0.02	**0.92 ± 0.01**	1 ± 0.04	**1.23 ± 0.03***	1 .00± 0.02	1 ± 0.02	**1.75 ± 0.02***	1.41 ± 0.02

Table S5. Continuation

	Aerial part										
	Light					Darkness			High CO_2		
		- serine	+ serine				- serine	+ serine		- serine	+ serine
Organic acids	WT	*HS PSP*	*HS PSP*	WT	*HS PSP*	WT	*HS PSP*	*HS PSP*	WT	*HS PSP*	*HS PSP*
Ascorbic acid	1 ± 0.04	**0.43 ± 0.12**	0.41 ± 0.1	1 ± 0.04	**0.82 ± 0.05**	1 ± 0.12	**0.46 ± 0.13***	0.07 ± 0.04	1 ± 0.14	0.79 ± 0.29	1.09 ± 0.28
Benzoic acid	1 ± 0.05	**1.30 ± 0.08**	1.21 ± 0.08	1 ± 0.05	1.02 ± 0.08	1 ± 0.17	**1.31 ± 0.04***	0.95 ± 0.09	1 ± 0.09	**1.64 ± 0.06***	1.21 ± 0.04
Citric acid	1 ± 0.04	**3.85 ± 0.20***	2.69 ± 0.09	1 ± 0.04	1.07 ± 0.04	1 ± 0.07	**1.75 ± 0.07**	1.79 ± 0.08	1 ± 0.07	**5.17 ± 0.31***	3.25 ± 0.15
Dehydroascorbic acid dimer	1 ± 0.03	**1.97 ± 0.13***	1.45 ± 0.07	1 ± 0.03	0.99 ± 0.05	1 ± 0.09	**2.51 ± 0.14***	1.79 ± 0.12	-	-	-
Fumaric acid	1 ± 0.02	**1.56 ± 0.05***	1.33 ± 0.03	1 ± 0.02	1.02 ± 0.02	1 ± 0.02	**1.61 ± 0.03***	1.44 ± 0.03	1 ± 0.01	**1.74 ± 0.03***	1.35 ± 0.03
Glucuronic acid	1 ± 0.03	**1.66 ± 0.04***	1.33 ± 0.06	1 ± 0.03	0.96 ± 0.02	-	-	-	-	-	-
Glutaric acid, 2-oxo-	1 ± 0.03	**1.16 ± 0.03***	1.01 ± 0.03	1 ± 0.03	**0.87 ± 0.02**	1 ± 0.04	**1.81 ± 0.07***	1.55 ± 0.10	1 ± 0.04	**0.80 ± 0.03***	0.67 ± 0.03
Glyceric acid	1 ± 0.05	**2.28 ± 0.09***	1.67 ± 0.04	1 ± 0.05	**0.65 ± 0.02**	1 ± 0.07	**2.97 ± 0.18***	1.78 ± 0.09	1 ± 0.03	**1.58 ± 0.04***	0.86 ± 0.02
Malic acid	1 ± 0.03	**1.72 ± 0.07***	1.42 ± 0.02	1 ± 0.03	1 .00± 0.04	1 ± 0.05	**1.93 ± 0.04***	2.07 ± 0.05	1 ± 0.02	**2.70 ± 0.04***	1.66 ± 0.02
Nicotinic acid	1 ± 0.03	**2.82 ± 0.10***	2.47 ± 0.09	1 ± 0.03	0.95 ± 0.02	1 ± 0.05	**3.45 ± 0.12***	2.82 ± 0.13	1 ± 0.03	**2.91 ± 0.08***	2.20 ± 0.06
Phosphoric acid	1 ± 0.02	**0.17 ± 0.02**	0.20 ± 0.02	1 ± 0.02	**0.90 ± 0.01**	1 ± 0.03	**0.22 ± 0.02***	0.29 ± 0.02	1 ± 0.27	**0.23 ± 0.01***	0.38 ± 0.02
Pyroglutamic acid	1 ± 0.02	**1.20 ± 0.03**	1.19 ± 0.02	1 ± 0.02	1 .00± 0.03	-	-	-	-	-	-
Pyruvic acid	1 ± 0.04	1.10 ± 0.04	0.85 ± 0.03	1 ± 0.04	0.97 ± 0.03	1 ± 0.04	**1.39 ± 0.05***	1.19 ± 0.05	1 ± 0.03	**0.97 ± 0.04***	0.77 ± 0.04
Succinic acid	1 ± 0.02	**1.27 ± 0.04***	0.88 ± 0.02	1 ± 0.02	1.17 ± 0.08	1 ± 0.06	**2.13 ± 0.06***	1.55 ± 0.05	-	-	-
Threonic acid	1 ± 0.06	**2.20 ± 0.16**	1.94 ± 0.08	1 ± 0.06	1.04 ± 0.05	-	-	-	-	-	-
Sugars and Sugar alcohols											
Fructose	1 ± 0.01	**1.35 ± 0.06***	1.05 ± 0.02	1 ± 0.05	**1.56 ± 0.05**	1 ± 0.03	**2.93 ± 0.05***	2.16 ± 0.06	1 ± 0.02	**1.3 ± 0.04***	0.88 ± 0.02
Fructose-6-phosphate	1 ± 0.03	**0.39 ± 0.01**	0.39 ± 0.03	1 ± 0.04	1.09 ± 0.06	1 ± 0.05	**0.35 ± 0.02***	0.68 ± 0.03	-	-	-
Galactinol	1 ± 0.03	**49.60 ± 3.56***	13.43 ± 0.25	1 ± 0.21	2.43 ± 0.14	1 ± 0.05	**67.75 ± 2.54***	55.72 ± 1.63	1 ± 0.04	**73.59 ± 3.62***	7.17 ± 0.16
Gentiobiose	1 ± 0.14	**0.46 ± 0.06***	0.46 ± 0.05	1 ± 0.10	0.84 ± 0.07	1 ± 0.06	**0.41 ± 0.05**	0.43 ± 0.04	1 ± 0.01	**5.20 ± 0.18***	4.11 ± 0.13
Glucose	1 ± 0.07	**1.26 ± 0.05***	1.02 ± 0.02	1 ± 0.09	0.96 ± 0.08	1 ± 0.05	**2.02 ± 0.04***	1.58 ± 0.09	1 ± 0.04	**1.22 ± 0.05***	0.91 ± 0.03
Glucose-6-phosphate	1 ± 0.03	**0.33 ± 0.01**	0.36 ± 0.03	1 ± 0.05	1.07 ± 0.05	1 ± 0.05	**0.32 ± 0.02***	0.65 ± 0.03	-	-	-
Glyceraldehyde-3-phosphate	1 ± 0.03	**0.55 ± 0.01***	0.62 ± 0.03	1 ± 0.03	1.00 ± 0.03	1 ± 0.05	**0.52 ± 0.04***	0.76 ± 0.02	1 ± 0.03	**0.84 ± 0.02***	0.58 ± 0.02
Glycerol	1 ± 0.06	1.15 ± 0.07	1.04 ± 0.09	1 ± 0.06	1.01 ± 0.09	1 ± 0.12	**0.83 ± 0.08***	1.21 ± 0.10	1 ± 0.02	**1.44 ± 0.08***	1.25 ± 0.06
Inositol, myo	1 ± 0.01	**2.29 ± 0.06***	1.79 ± 0.02	1 ± 0.02	**1.07 ± 0.02**	1 ± 0.03	**1.99 ± 0.02***	1.71 ± 0.03	1 ± 0.01	**2.64 ± 0.07***	1.52 ± 0.03
Sucrose	1 ± 0.01	**1.07 ± 0.03**	0.96 ± 0.01	1 ± 0.02	1.08 ± 0.03	1 ± 0.01	**1.14 ± 0.02***	1.32 ± 0.02	1 ± 0.04	1.12 ± 0.04*	0.92 ± 0.03
Threitol	1 ± 0.02	**0.54 ± 0.01**	0.5 ± 0.01	1 ± 0.03	**0.85 ± 0.01**	1 ± 0.05	**0.53 ± 0.02**	0.54 ± 0.02	1 ± 0.01	**0.86 ± 0.02***	0.8 ± 0.02
Trehalose, alpha,alpha'	1 ± 0.02	**3.98 ± 0.15***	2.88 ± 0.07	1 ± 0.02	1.14 ± 0.05	1 ± 0.03	**4.47 ± 0.09***	2.89 ± 0.11	1 ± 0.02	**4.27 ± 0.09***	3.13 ± 0.09
Xylose	1 ± 0.01	**1.37 ± 0.02***	1.11 ± 0.02	1 ± 0.04	**0.88 ± 0.03**	1 ± 0.04	**1.42 ± 0.03***	1.07 ± 0.03	1 ± 0.02	**1.73 ± 0.05***	1.28 ± 0.06
Miscellaneous											
Putrescine	1 ± 0.04	**3.70 ± 0.08***	3.09 ± 0.09	1 ± 0.06	0.92 ± 0.03	1 ± 0.05	0.92 ± 0.05	1.00 ± 0.05	1 ± 0.01	**4.45 ± 0.09***	5.12 ± 0.16
Uracil	1 ± 0.04	**0.59 ± 0.02**	0.67 ± 0.03	1 ± 0.03	**0.84 ± 0.02**	-	-	-	1 ± 0.15	0.98 ± 0.12	0.96 ± 0.11
Urea	1 ± 0.03	**1.27 ± 0.06***	1.11 ± 0.04	1 ± 0.03	**0.88 ± 0.02**	1 ± 0.07	1.23 ± 0.06	1.22 ± 0.07	1 ± 0.04	**1.47 ± 0.06***	1.12 ± 0.03

Tabla S6. Levels of metabolites in roots of wild-type (WT) and conditional mutant *psp1.1psp1.1 HS:PSP1 (HS PSP)* under three different conditions (light with or without serine in the medium, darkness and high levels of CO_2), with (+) or without (-) heat shock treatment. Data are normalised and related to the mean of the WT for each condition. Each value represents the mean ± SE (n = 6). Values in bold are significantly different from the WT and that significantly differed from the values of the heat shock treatment are followed by * (P > 0.05).

	Roots											
	Light					**Darkness**			**High CO_2**			
		-	+	**serine**			-	+		-	+	
Amino acids	WT	*HS PSP*	*HS PSP*	WT	*HS PSP*	WT	*HS PSP*	*HS PSP*	WT	*HS PSP*	*HS PSP*	
Alanine	1 ± 0.10	**1.84 ± 0.10***	1.30 ± 0.05	1 ± 0.15	0.91 ± 0.08	1 ± 0.03	**1.83 ± 0.07**	1.79 ± 0.05	1 ± 0.05	**0.67 ± 0.04***	0.54 ± 0.04	
Alanine, beta	1 ± 0.09	**3.06 ± 0.10***	1.44 ± 0.03	1 ± 0.18	1.04 ± 0.06	1 ± 0.06	**1.62 ± 0.05***	1.40 ± 0.03	1 ± 0.02	1.09 ± 0.07*	0.75 ± 0.07	
Arginine	1 ± 0.08	**8.34 ± 0.99***	4.97 ± 0.28	1 ± 0.05	0.76 ± 0.06	1 ± 0.03	**4.15 ± 0.09**	4.30 ± 0.22	1 ± 0.09	**2.24 ± 0.15**	1.94 ± 0.16	
Asparagine	1 ± 0.08	**33.6 ± 1.02***	16.29 ± 0.93	1 ± 0.06	0.96 ± 0.10	1 ± 0.09	**12.62 ± 0.57***	19.23 ± 1.15	1 ± 0.13	**9.98 ± 0.68***	6.88 ± 0.64	
Aspartic acid	1 ± 0.04	**1.96 ± 0.04***	1.19 ± 0.05	1 ± 0.05	0.79 ± 0.04	1 ± 0.02	**1.16 ± 0.02***	1.29 ± 0.02	1 ± 0.03	**0.79 ± 0.03**	0.77 ± 0.08	
Cysteine	1 ± 0.03	**2.22 ± 0.07***	1.43 ± 0.03	1 ± 0.05	1.03 ± 0.05	1 ± 0.05	**1.93 ± 0.03***	2.01 ± 0.03	1 ± 0.02	**1.17 ± 0.04***	0.96 ± 0.05	
GABA	1 ± 0.10	**2.91 ± 0.17***	1.84 ± 0.18	1 ± 0.12	1.69 ± 0.24	1 ± 0.03	**2.67 ± 0.04***	2.45 ± 0.04	1 ± 0.05	**1.49 ± 0.16***	0.95 ± 0.11	
Glutamic acid	1 ± 0.03	**2.22 ± 0.04***	1.61 ± 0.03	1 ± 0.02	0.78 ± 0.03	1 ± 0.01	**1.69 ± 0.02**	1.61 ± 0.04	1 ± 0.02	**1.46 ± 0.04***	1.29 ± 0.06	
Glutamine	1 ± 0.10	**7.78 ± 0.26***	4.32 ± 0.35	1 ± 0.04	1.20 ± 0.06	1 ± 0.02	**2.90 ± 0.08***	2.52 ± 0.06	1 ± 0.04	**2.12 ± 0.08***	1.41 ± 0.06	
Glycine	1 ± 0.06	**2.03 ± 0.07***	1.75 ± 0.06	1 ± 0.08	1.01 ± 0.05	1 ± 0.04	**1.65 ± 0.04**	1.84 ± 0.11	1 ± 0.12	0.90 ± 0.03	1.19 ± 0.36	
Histidine	1 ± 0.07	**7.32 ± 1.64***	2.96 ± 0.40	1 ± 0.06	1.10 ± 0.08	1 ± 0.07	**3.52 ± 0.47***	7.25 ± 1.42	1 ± 0.16	**3.57 ± 0.48**	3.68 ± 0.81	
Homoserine	1 ± 0.08	**2.21 ± 0.06***	1.56 ± 0.04	1 ± 0.21	0.62 ± 0.04	-	**-**	-	1 ± 0.07	**1.00 ± 0.03***	0.84 ± 0.03	
Isoleucine	1 ± 0.09	**1.61 ± 0.06***	1.22 ± 0.04	1 ± 0.12	1.06 ± 0.06	1 ± 0.01	**1.09 ± 0.02***	1.21 ± 0.04	1 ± 0.03	**1.24 ± 0.04***	0.90 ± 0.12	
Leucine	1 ± 0.07	0.91 ± 0.08	1.07 ± 0.08	1 ± 0.19	0.96 ± 0.09	-	**-**	-	1 ± 0.07	0.98 ± 0.03	1.03 ± 0.04	
Lysine	1 ± 0.03	**1.43 ± 0.09***	0.90 ± 0.03	1 ± 0.03	0.73 ± 0.03	1 ± 0.01	**0.75 ± 0.02***	0.91 ± 0.04	1 ± 0.09	**0.72 ± 0.04**	0.93 ± 0.16	
Methionine	1 ± 0.06	**1.3 ± 0.03***	0.77 ± 0.03	1 ± 0.06	0.71 ± 0.05	1 ± 0.02	0.97 ± 0.02*	0.92 ± 0.02	1 ± 0.03	**0.65 ± 0.02***	0.49 ± 0.06	
Ornithine	1 ± 0.05	**7.22 ± 0.26***	4.91 ± 0.23	1 ± 0.04	0.66 ± 0.05	1 ± 0.02	**3.70 ± 0.10**	3.96 ± 0.26	-	-	-	
Phenylalanine	1 ± 0.06	**2.76 ± 0.04***	2.15 ± 0.08	1 ± 0.06	0.87 ± 0.05	1 ± 0.02	**1.34 ± 0.01**	1.33 ± 0.02	1 ± 0.07	**1.64 ± 0.06**	1.33 ± 0.23	
Proline	1 ± 0.08	**3.99 ± 0.17***	2.54 ± 0.06	1 ± 0.11	1.34 ± 0.05	1 ± 0.09	**1.55 ± 0.11**	1.42 ± 0.09	1 ± 0.02	**4.79 ± 0.25***	2.73 ± 0.3	
Proline, 4-hydroxy	1 ± 0.04	**2.36 ± 0.08***	1.76 ± 0.03	1 ± 0.10	0.87 ± 0.03	-	-	-	-	-	-	
Serine	1 ± 0.09	1.01 ± 0.03*	0.94 ± 0.02	1 ± 0.15	1.02 ± 0.04	1 ± 0.02	1.02 ± 0.01*	1.24 ± 0.03	1 ± 0.04	**0.63 ± 0.03**	0.80 ± 0.09	
Serine, O-acetyl-	1 ± 0.09	**4.15 ± 0.18***	2.50 ± 0.07	1 ± 0.19	1.39 ± 0.08	1 ± 0.02	**1.28 ± 0.02***	1.59 ± 0.10	1 ± 0.01	**1.62 ± 0.01***	1.39 ± 0.08	
Threonine	1 ± 0.08	**1.51 ± 0.03***	1.22 ± 0.02	1 ± 0.15	1.30 ± 0.04	1 ± 0.02	**1.23 ± 0.01**	1.26 ± 0.03	1 ± 0.02	1.08 ± 0.05	0.91 ± 0.09	
Tryptophan	1 ± 0.09	**3.23 ± 0.38**	2.46 ± 0.24	1 ± 0.05	0.84 ± 0.06	1 ± 0.05	**2.23 ± 0.14***	3.22 ± 0.30	1 ± 0.05	**2.35 ± 0.1**	2.15 ± 0.21	
Tyrosine	1 ± 0.10	**2.48 ± 0.33**	1.77 ± 0.21	1 ± 0.09	1.02 ± 0.09	1 ± 0.11	**1.50 ± 0.15***	2.50 ± 0.28	1 ± 0.17	1.08 ± 0.12	1.57 ± 0.29	
Valine	1 ± 0.06	**1.92 ± 0.08***	1.34 ± 0.03	1 ± 0.08	1.08 ± 0.04	1 ± 0.02	**1.42 ± 0.02**	1.35 ± 0.03	1 ± 0.02	**1.57 ± 0.04***	1.04 ± 0.11	

Table S6. Continuation

	Roots											
	Light					Darkness			High CO_2			
		-	+	serine			-	+		-	+	
Organic acids	WT	*HS PSP*	*HS PSP*	WT	*HS PSP*	WT	*HS PSP*	*HS PSP*	WT	*HS PSP*	*HS PSP*	
Ascorbic acid	1 ± 0.14	**0.27 ± 0.05+**	0.1 ± 0.04	1 ± 0.06	0.7 ± 0.09	1 ± 0.05	**0.80 ± 0.10***	0.18 ± 0.05	1 ± 0.07	**0.04 ± 0.00***	0.19 ± 0.02	
Benzoic acid	1 ± 0.04	1.14 ± 0.06*	0.87 ± 0.03	1 ± 0.07	1.04 ± 0.07	1 ± 0.02	**1.12 ± 0.02**	1.12 ± 0.03	1 ± 0.06	1.01 ± 0.06*	0.72 ± 0.06	
Citric acid	-	-	-	-	-	1 ± 0.05	**4.45 ± 0.11**	3.9 ± 0.11	1 ± 0.03	**3.08 ± 0.07***	2.39 ± 0.03	
Dehydroascorbic acid dimer	1 ± 0.09	1.04 ± 0.07*	0.76 ± 0.02	1 ± 0.05	1.37 ± 0.07	1 ± 0.02	**0.67 ± 0.06***	0.95 ± 0.03	-	-	-	
Fumaric acid	1 ± 0.08	**1.40 ± 0.07***	0.97 ± 0.01	1 ± 0.19	1.39 ± 0.05	1 ± 0.04	1.06 ± 0.05*	1.34 ± 0.04	1 ± 0.02	1.07 ± 0.04	0.9 ± 0.09	
Glyceric acid	1 ± 0.07	**1.84 ± 0.03***	1.4 ± 0.04	1 ± 0.14	0.39 ± 0.02	1 ± 0.01	**0.62 ± 0.00***	1.79 ± 0.02	1 ± 0.01	**1.33 ± 0.09**	1.34 ± 0.1	
Malic acid	1 ± 0.04	**1.44 ± 0.03***	0.84 ± 0.02	1 ± 0.11	0.7 ± 0.03	1 ± 0.01	**0.97 ± 0.01***	1.22 ± 0.03	1 ± 0.01	0.93 ± 0.04	0.95 ± 0.03	
Nicotinic acid	1 ± 0.06	1.13 ± 0.08*	0.93 ± 0.04	1 ± 0.15	0.91 ± 0.02	1 ± 0.02	**0.76 ± 0.02**	0.82 ± 0.02	1 ± 0.02	**0.70 ± 0.02**	0.61 ± 0.05	
Phosphoric acid	1 ± 0.12	**0.49 ± 0.03***	0.35 ± 0.02	1 ± 0.23	1.1 ± 0.07	1 ± 0.03	**0.45 ± 0.01***	0.41 ± 0.01	1 ± 0.02	**0.47 ± 0.03**	0.38 ± 0.04	
Pyruvic acid	1 ± 0.04	**1.61 ± 0.06***	1.08 ± 0.03	1 ± 0.03	0.9 ± 0.03	1 ± 0.01	**1.28 ± 0.05***	1.47 ± 0.03	1 ± 0.01	**0.74 ± 0.02**	0.71 ± 0.04	
Succinic acid	1 ± 0.11	1.07 ± 0.04*	0.73 ± 0.01	1 ± 0.19	0.84 ± 0.04	1 ± 0.02	**0.66 ± 0.01***	1.15 ± 0.03	-	-	-	
Sugars and Sugar alcohols												
Fructose	1 ± 0.02	**2.38 ± 0.04**	2.07 ± 0.03	1 ± 0.05	0.63 ± 0.05	1 ± 0.01	**2.55 ± 0.02***	3.01 ± 0.03	1 ± 0.01	**0.91 ± 0.01***	1.25 ± 0.07	
Fructose-6-phosphate	1 ± 0.09	0.85 ± 0.03	0.6 ± 0.09	1 ± 0.06	0.62 ± 0.04	1 ± 0.04	**0.62 ± 0.03***	0.52 ± 0.01	-	-	-	
Galactinol	1 ± 0.05	**5.24 ± 0.19***	2.41 ± 0.1	1 ± 0.05	1.57 ± 0.08	1 ± 0.03	**7.51 ± 0.28**	7.76 ± 0.32	1 ± 0.03	**3.98 ± 0.18***	0.92 ± 0.08	
Gentiobiose	1 ± 0.07	1.39 ± 0.13	1.2 ± 0.02	1 ± 0.05	1 ± 0.01	-	-	-	1 ± 0.02	**1.52 ± 0.06***	1.27 ± 0.1	
Glucose	1 ± 0.05	1.07 ± 0.06	1.05 ± 0.04	1 ± 0.05	1 ± 0.02	-	-	-	1 ± 0.07	0.97 ± 0.02*	0.85 ± 0.04	
Glucose-6-phosphate	1 ± 0.07	**0.78 ± 0.03**	0.43 ± 0.03	1 ± 0.04	0.58 ± 0.03	1 ± 0.05	**0.61 ± 0.02***	0.5 ± 0.01	-	-	-	
Glyceraldehyde-3-phosphate	1 ± 0.04	**0.72 ± 0.04**	0.57 ± 0.03	1 ± 0.03	1.05 ± 0.06	1 ± 0.03	**0.7 ± 0.03***	0.58 ± 0.04	1 ± 0.04	**0.64 ± 0.04***	0.38 ± 0.03	
Glycerol	1 ± 0.08	**1.41 ± 0.06***	1.05 ± 0.04	1 ± 0.15	1.2 ± 0.05	1 ± 0.05	1.29 ± 0.10	1.23 ± 0.11	1 ± 0.04	**0.89 ± 0.03**	0.85 ± 0.1	
Inositol, myo	1 ± 0.01	**1.78 ± 0.05**	1.43 ± 0.02	1 ± 0.01	0.83 ± 0.01	1 ± 0.02	**1.49 ± 0.03**	1.48 ± 0.02	1 ± 0.03	**1.19 ± 0.02***	0.98 ± 0.05	
Sucrose	1 ± 0.05	0.98 ± 0.06	0.99 ± 0.03	-	-	1 ± 0.04	1.09 ± 0.03	0.97 ± 0.02	1 ± 0.05	0.99 ± 0.02*	0.85 ± 0.03	
Threitol	1 ± 0.08	**0.28 ± 0.01**	0.25 ± 0.01	1 ± 0.18	0.59 ± 0.02	1 ± 0.01	**0.27 ± 0.00**	0.27 ± 0.01	1 ± 0.01	**0.34 ± 0.01**	-	
Trehalose, alpha,alpha'	1 ± 0.07	**5.25 ± 0.16**	3.51 ± 0.11	1 ± 0.04	1.35 ± 0.07	1 ± 0.02	**3.85 ± 0.08**	4.03 ± 0.12	1 ± 0.01	**3.48 ± 0.06***	2.07 ± 0.16	
Xylose	1 ± 0.07	**4.2 ± 0.1**	3.2 ± 0.08	1 ± 0.06	0.67 ± 0.04	1 ± 0.02	**2.07 ± 0.05***	2.29 ± 0.05	1 ± 0.02	1.11 ± 0.04*	1.44 ± 0.12	
Miscellaneous												
Putrescine	1 ± 0.07	**3.21 ± 0.16**	2.24 ± 0.18	1 ± 0.09	0.8 ± 0.17	1 ± 0.03	**1.87 ± 0.02**	1.89 ± 0.02	1 ± 0.04	1.10 ± 0.11*	1.9 ± 0.13	
Uracil	1 ± 0.05	**1.26 ± 0.06**	1.43 ± 0.08	1 ± 0.16	1.17 ± 0.05	-	-	-	1 ± 0.15	1.53 ± 0.29	1.01 ± 0.1	
Urea	1 ± 0.09	0.96 ± 0.03	0.85 ± 0.03	1 ± 0.20	0.79 ± 0.04	1 ± 0.06	**0.75 ± 0.04**	0.81 ± 0.04	1 ± 0.11	**0.62 ± 0.04**	0.71 ± 0.1	